

---

# **INTERACTIONS BETWEEN PROTEINS AND IDENTIFICATION OF HIGH AFFINITY ANTAGONISTS**

---

**Laura Tornatore**

Dottorato in Scienze Biotecnologiche – XXI ciclo  
Indirizzo Biotecnologie molecolari  
Università di Napoli Federico II







*A Zia Lena . . .*

## INDEX

<b>A.1 Riassunto: Interazione tra proteine ed identificazione di antagonisti ad alta affinità</b>	<b>pag. 1</b>
<b>A.2 Summary: Interactions between proteins and identification of high affinity antagonists</b>	<b>pag. 6</b>
<b>1. INTRODUCTION</b>	
<b>1.1 Drug discovery and protein-protein interactions</b>	<b>pag. 8</b>
<b>1.2 Protein kinases in drug discovery and development</b>	<b>pag. 10</b>
<b>1.3 Gadd45 Family : key proteins of cell signalling</b>	<b>pag. 11</b>
<b>1.4 Gadd45<math>\beta</math> in the cell system: functional - structural characterization</b>	<b>pag. 11</b>
<b>1.5 Gadd45<math>\beta</math> and MKK7: a potential target for therapies anti-cancer and anti – inflammatory</b>	<b>pag. 13</b>
<b>1.6 Bio-molecular Engineering and Combinatorial Design: two alternative approaches in drug discovery</b>	<b>pag. 16</b>
<b>1.7 Therapeutic peptides: interesting prospective of Medicinal chemistry</b>	<b>pag. 16</b>
<b>1.8 Aim of the project</b>	<b>pag. 17</b>
<b>2. MATERIAL AND METHODS</b>	
<b>2.1 Cloning expression and purification of recombinant protein</b>	<b>pag. 20</b>
<b>2.1.1 Cloning</b>	<b>pag. 20</b>
<b>2.1.2 Expression</b>	<b>pag. 21</b>
<b>2.2 Peptides synthesis and purification</b>	<b>pag. 23</b>
<b>2.3 Digestion with trypsin and peptide fractionation</b>	<b>pag. 24</b>
<b>2.4 Spectroscopic characterization of hGadd45<math>\beta</math> and hMKK7</b>	<b>pag. 25</b>
<b>2.4.1 CD analysis of native proteins spectra</b>	<b>pag. 25</b>
<b>2.4.2 Gadd45<math>\beta</math> stability against chemical denaturants</b>	<b>pag. 25</b>
<b>2.5 Characterization of Gadd45<math>\beta</math> structure by hydrodynamic methods and LC-MS</b>	<b>pag. 26</b>

<b>2.5.1 Native gels</b>	<b>pag. 26</b>
<b>2.5.2 Gel-filtration chromatography</b>	<b>pag. 26</b>
<b>2.5.3 LC-MS</b>	<b>pag. 26</b>
<b>2.5.4 Protein alkylation assays</b>	<b>pag. 27</b>
<b>2.6 Combinatorial tetrapeptides library: synthesis and iterative deconvolution</b>	<b>pag. 27</b>
<b>2.7 Binding and competitive Enzyme-Linked Immunosorbent Assay (ELISA)</b>	<b>pag. 32</b>
<b>2.7.1 Biotinylation of Gadd45<math>\beta</math></b>	<b>pag. 32</b>
<b>2.7.2 Gadd45<math>\beta</math> -MKK7 association and competition ELISA assays</b>	<b>pag. 33</b>
<b>2.7.3 Dose dependent competition assay</b>	<b>pag. 33</b>
<b>2.7.4 Gadd45<math>\beta</math> self-association and competition ELISA assays</b>	<b>pag. 34</b>
<b>2.8 Tissue culture and transfection assays</b>	<b>pag. 34</b>
<b>2.9 Cell lyses and western blot analysis</b>	<b>pag. 35</b>
<b>2.10 Activation of MKK7 immunoprecipitation and kinase assays</b>	<b>pag. 35</b>
<b>2.11 Binding and competition assay by combined Immunoprecipitation, kinase assay and western blotting</b>	<b>pag. 36</b>
<b>3. RESULTS AND DISCUSSION</b>	
<b>3.1 Gadd45<math>\beta</math> cloning, expression and purification</b>	<b>pag. 38</b>
<b>3.2 MKK7 cloning, expression and purification</b>	<b>pag. 42</b>
<b>3.3 Investigation of Gadd45<math>\beta</math> oligomerization by size exclusion chromatography analysis.</b>	<b>pag. 45</b>
<b>3.4 Spectroscopic characterization of Gadd45 <math>\beta</math></b>	<b>pag. 48</b>
<b>3.5 Identification of regions of Gadd45<math>\beta</math> involved in auto-association</b>	<b>pag. 50</b>
<b>3.5.1 The rationale of the strategy</b>	<b>pag. 50</b>
<b>3.5.2 Characterization of regions of Gadd45<math>\beta</math> involved in auto-association</b>	<b>pag. 51</b>

<b>3.5.4 Gadd45<math>\beta</math> eHelices characterization by CD</b>	<b>pag. 57</b>
<b>3.5.5 Gadd45<math>\beta</math> forms a homodimeric complex that binds tightly to MKK7</b>	<b>pag. 59</b>
<b>3.6 Biomolecular engineering by combinatorial chemistry and high-throughput screening</b>	<b>pag. 62</b>
<b>3.6.1 Design of combinatorial tetra peptides library</b>	<b>pag. 62</b>
<b>3.6.2 First generation of simplified peptide libraries</b>	<b>pag. 63</b>
<b>3.6.3 Focused library: tetrapeptides of second generation</b>	<b>pag. 67</b>
<b>3.6.4 Validation of the combinatorial approach</b>	<b>pag. 69</b>
<b>3.6.5 Lead peptides engineering</b>	<b>pag. 69</b>
<b>3.7 From combinatorial chemistry to validated hit: defining the mechanism of inhibition</b>	<b>pag. 70</b>
<b>3.7.1 Investigation of inhibition mechanism</b>	<b>pag. 70</b>
<b>4. CONCLUSIONS AND PERSPECTIVES</b>	
<b>4.1 Antagonists of Gadd45<math>\beta</math> – Mkk7: from combinatorial approach to new therapeutic components</b>	<b>pag. 76</b>
<b>5. REFERENCES</b>	<b>pag. 81</b>
<b>6. ABBREVIATION INDEX</b>	<b>pag. 86</b>
<b>7. SCIENTIFIC PRESENTATIONS</b>	<b>pag. 87</b>
<b>8. PUBLICATION</b>	<b>pag. 88</b>

## **A.1 Riassunto: Interazione tra proteine ed identificazione di antagonisti ad alta affinità**

Negli ultimi anni la comunità scientifica ed il mondo imprenditoriale stanno sinergicamente tentando d'individuare nuove strategie terapeutiche che possono riscontrare concrete applicazioni in campo bio-medico e biotecnologico. In questa era post genetica, la proteomica sta offrendo una serie interessanti prospettive che inevitabilmente si riflettono nello sviluppo del *Drug Discovery - Delivery*. Infatti, al fine d'identificare nuovi farmaci risulta indispensabile individuare inizialmente dei promettenti pathways cellulari ed in seguito condurre un'analisi strutturale e funzionale dei fattori proteici coinvolti.

Patologie come l'infiammazione cronica e la carcinogenesi sono state da sempre oggetto di studio ma solo recentemente Michael Karin ha confermato l'ipotesi che i fattori trascrizionali NF- $\kappa$ B possano rappresentare il vero e proprio legame molecolare tra processo infiammatorio e tumorigenesi. Infatti, oltre a coordinare la risposta immunitaria, NF  $\kappa$ B riveste un ruolo cruciale nella carcinogenesi; in particolare la sua azione promotrice o inibitrice dello sviluppo e della progressione tumorale risulta essere cellula -specifico. Considerando l'importanza di NF- $\kappa$ B nella risposta immunitaria innata ed adattativa, la sua diretta inattivazione può determinare una grave immunodeficienza. Di conseguenza nella definizione di terapie anti- cancro non è possibile optare per né un' inibizione prolungata e sostanziale di NF $\kappa$ B, né per un'efficace prevenzione verso le cause che ne determinano la cronica attivazione. Infatti un uso prolungato di medicinali antinfiammatori, atti a neutralizzare sia infiammazioni croniche che infezioni microbiche e virali, potrebbe determinare una serie di effetti collaterali difficilmente controllabili. Per questo motivo, recentemente le vie trasduzionali regolate NF- $\kappa$ B sono state indicate come potenziali ed alternativi obiettivi terapeutici per la prevenzione ed il trattamento dei tumori.

Questo progetto di ricerca s'inserisce perfettamente in questa prospettiva, infatti il suo obiettivo principale consiste nella selezione di molecole in grado di bloccare l'azione anti-apoptotica e pro-oncogenica indotta dal fattore trascrizionale NF- $\kappa$ B interferendo nell'interazione tra le proteine Gadd45 $\beta$  ed MKK7 .

L'interesse biotecnologico del progetto è strettamente correlato all'identificazione di molecole- antagoniste che possano essere utilizzate come agenti terapeutici nei processi infiammatori inducenti la crescita e progressione delle cellule tumorali.

Infatti, è noto dalla letteratura che l'interazione tra la proteina Gadd45 $\beta$  e la MAP kinasi MKK7 risulta essere cruciale oltre che nei processi infiammatori anche nella chemio-resistenza del cancro. Gadd45 $\beta$  (Growth Arrest and DNA-Damage-inducible) è una proteina acida di circa 18 KDa espressa in risposta ad un ampio spettro di agenti genotossici fattori inducenti stress ossidativi e radiazioni ionizzanti. Inoltre è stato dimostrato che l'espressione di Gadd45 $\beta$  essendo regolata dal fattore trascrizionale NF- $\kappa$ B, risulta essere correlata ad una serie di insulti citotossici quali la sovra-produzione di TNF $\alpha$  e di altre citochine. In letteratura è ampiamente descritto il meccanismo molecolare mediante il quale Gadd45 $\beta$  promuove e sostiene la fisiologica reazione antiapoptotica mediata da NF- $\kappa$ B- in risposta a diversi stimoli di morte cellulare. Precisamente Gadd45 $\beta$  esplica la sua azione citoprotettiva

interagendo fisicamente con alcuni componenti essenziali della famiglia delle MAPKs quali MKK4 e MKK7. Queste due chinasi sono conosciute come i diretti attivatori di JNK che è uno dei più importanti ed efficaci mediatori della morte cellulare programmata. Recentemente è stato descritto come l'interazione tra Gadd45 $\beta$  e MKK7 sia mediata dai domini 60-86 e 103-114 di Gadd45 $\beta$ , contenenti molti residui acidi, e dal dominio 132-156 di MKK7, ricco in aminoacidi basici, costituenti il sito attivo dell'enzima. L'interazione di Gadd45 $\beta$  con la chinasi comporta un mascheramento del residuo di Lys<sup>149</sup> presente nel dominio catalitico di MKK7. Il legame tra le due proteine genera una incompatibilità sterica tra Gadd45 $\beta$  ed l'ATP che si concretizza nell'inibizione dell'attività chinasi di MKK7. La conseguente soppressione della cascata di JNK comporta uno spostamento dell'omeostasi cellulare verso un ciclo di sopravvivenza che risulta essere un aspetto cruciale sia nell'oncogenesi che nell'infiammazione. Sulla base di queste osservazioni si può facilmente delineare il ruolo chiave svolto da Gadd45 $\beta$  nel delicato equilibrio tra azione pro-apoptotica del TNF $\alpha$  (ed altre citochine) ed effetti anti-apoptotici del fattore di trascrizione NF- $\kappa$ B. Per tali ragioni l'interazione Gadd45 $\beta$ -MKK7 risulta essere un obiettivo di enorme rilevanza terapeutica per lo sviluppo di molecole anti-infiammatorie ed anti-tumorali basate sul miglioramento dell'attività endogena del TNF $\alpha$ .

Dal momento che il binomio struttura-funzione risulta essere essenziale per comprendere a livello molecolare i meccanismi cellulari, la prima parte del progetto è stata incentrata sulla caratterizzazione di Gadd45 $\beta$  ed MKK7 utilizzando tecniche bio-molecolari spettroscopiche e bio-chimiche. Inizialmente sono state ottimizzate le condizioni di clonaggio, espressione in *E. Coli* e purificazione delle due proteine in forma ricombinante.

Una preliminare caratterizzazione strutturale di MKK7, impiegando tecniche di dicroismo circolare, ha confermato che la chinasi mostra una conformazione prevalentemente ad  $\alpha$  elica con un discreto contributo di  $\beta$  sheet. Inoltre le successive analisi mediante cromatografia ad esclusione molecolare, hanno permesso di constatare che MKK7 tende a presentarsi prevalentemente in forma dimerica. I risultati sperimentali ottenuti sono in accordo con i dati riportati in letteratura per MKK7 e per chinasi omologhe.

Per quanto concerne Gadd45 $\beta$  e' stata condotta una dettagliata analisi strutturale mirata alla caratterizzazione delle regioni coinvolte nell'auto-associazione di questa proteina. Le canoniche tecniche biochimiche e spettroscopiche hanno inizialmente permesso di constatare che Gadd45 $\beta$  è presente in soluzione acquosa sotto forma di un omodimero e che, contrariamente all'omologa Gadd45 $\alpha$ , Gadd45 $\beta$  non ha una spiccata tendenza ad oligomerizzare. La realizzazione di saggi immunologici di tipo Elisa ha permesso di determinare una costante di autoassociazione nell'ordine di 100 nM e tale valore è risultato essere in accordo con la concentrazione della famiglia delle proteine Gadd stimata nei tessuti cellulari. La proteolisi enzimatica della proteina Gadd45 $\beta$  ha consentito di ottenere una miscela di frammenti peptidici successivamente purificati e caratterizzati per HPLC ed LC-MS/MS, ed impiegati come competitori in un saggio Elisa. Dal confronto dei risultati ottenuti con i dati di modeling riportati in letteratura è stato possibile identificare nelle eliche putative H1 e H5 le due regioni responsabili della autoassociazione di Gadd45 $\beta$ . Si e' visto come queste due eliche interagiscono in maniera non covalente ed antiparallela con le

corrispondenti regioni di un'altra unità monomerica determinando la formazione una compatta struttura dimerica in grado di interagire selettivamente con MKK7.

Ottenute e caratterizzate le due proteine ricombinanti, e dopo aver studiato il complesso che esse formano (MKK7- Gadd45 $\beta$  –Gadd45 $\beta$  –MKK7) è stato seguito un approccio combinatoriale allo scopo di individuare un antagonista specifico per tale interazione. In particolare la strategia adottata e' stata improntata sulla sintesi di collezioni peptidiche coordinata alla successiva deconvoluzione mediante saggi immunologici.

Le collezioni di tetrapeptidi sono state disegnate seguendo una struttura generale del tipo:

### **Fmoc-( $\beta$ Ala)<sub>2</sub>-Y1-X2-X3-X4-CONH<sub>2</sub>**

Il gruppo protettore aromatico Fmoc (9-fluorenil-metossi-carbonil) è stato inserito all' N-terminale in modo da facilitare l'utilizzo delle collezioni in saggi immunologici e per eventuali studi di fluorescenza; come spaziatore molecolare sono stati utilizzati due amminoacidi  $\beta$ -Alanina; i simboli **Y** e **X** rappresentano rispettivamente amminoacidi noti e miscele randomizzate. La sintesi dei peptidi lineari e' stata condotta in fase solida (SPPS) applicando la tecnica del premiscelamento ed inizialmente sono stati selezionati ed utilizzati solo 12 dei 20 amminoacidi naturali. La collezione era costituita da un numero teorico di 20736 differenti peptidi ( $12^4$ ) in 12 diverse frazioni, ognuna delle quali presentava un diverso amminoacido in posizione **Y**. La libreria è stata utilizzata in saggi ELISA di competizione utilizzando la proteina MKK7 immobilizzata sulla superficie delle piastre (42 nM) e Gadd45 $\beta$  biotinilata (21 nM) in soluzione.

La deconvoluzione delle collezioni peptidiche è stata condotta in maniera iterativa seguendo il seguente schema:

Fmoc-(βAla) <sub>2</sub> -Y <sub>1</sub> -X <sub>2</sub> -X <sub>3</sub> -X <sub>4</sub> -CONH <sub>2</sub>	20736 peptidi (12 <sup>4</sup> )
Fmoc-(βAla) <sub>2</sub> -5-X <sub>2</sub> -X <sub>3</sub> -X <sub>4</sub> -CONH <sub>2</sub>	1728 peptidi (12 <sup>3</sup> )
Fmoc-(βAla) <sub>2</sub> -5-12-X <sub>3</sub> -X <sub>4</sub> -CONH <sub>2</sub>	144 peptidi (12 <sup>2</sup> )
Fmoc-(βAla) <sub>2</sub> -5-12-11-X <sub>4</sub> -CONH <sub>2</sub>	12 peptidi (12 <sup>1</sup> )
Fmoc-(βAla) <sub>2</sub> -5-12-11-9-CONH <sub>2</sub>	1 peptide

Questo approccio combinatoriale ha permesso di identificare un'antagonista (**Lead 1**) che è risultato essere in grado di spiazzare l'interazione tra Gadd45β ed MKK7 a concentrazioni nano molarì (**IC<sub>50</sub> di circa 1 nM**).

Dopo aver selezionato il peptide *Lead 1*, la sequenza è stata successivamente ottimizzata realizzando una nuova collezione nella quale sono stati inseriti i residui amminoacidici esclusi precedentemente. Sono stati quindi disegnati e sintetizzati 24 diversi tetrapeptidi privi della porzione Fmoc-(βAla)<sub>2</sub>, in modo da incrementarne la solubilità. La deconvoluzione di questa collezione di seconda generazione ha permesso di identificare un nuovo antagonista dotato di IC<sub>50</sub> sub-nanomolare (**Lead 2**). I due peptidi selezionati presentano una serie di notevoli somiglianze sia strutturali che di natura chimico-fisica, entrambi conciliando un'elevata efficienza operativa ad una notevole solubilità in soluzione acquosa. Tali caratteristiche abbinate agli indiscutibili vantaggi della sintesi peptidica contribuiscono a promuovere questi tetrapeptidi come candidati ideali per future applicazioni terapeutiche.

L'integrazione della chimica combinatoriale con le basilari tecniche di ingegnerizzazione molecolare ha permesso di migliorare la stabilità nei mezzi biologici degli antagonisti selezionati. Infatti sintetizzando tali peptidi come retroinversi, sono stati resi immuni alla degradazione proteasica e quindi impiegabili in una serie di saggi cellulari essenziali per poter valutare un plausibile potenziale terapeutico dei *lead compounds 1 e 2*.

Sono stati allestiti una serie di saggi chinasi utilizzando estratti cellulari di 293T pre- trattati con TNFα o P/I in modo da avere MKK7 nella sua forma attiva fosforilata; JNK e Gadd45β sono stati prodotti da batteri in forma ricombinante come proteine di fusione della GST.

In accordo con i riferimenti bibliografici l'attività chinasi di MKK7 è stata controllata verificando la fosforilazione del substrato GST-JNK che risultava essere completamente inibita dalla presenza di GST-Gadd45β. Il ripristino

dell'attività fosforilativa di MKK7 è stato invece verificato utilizzando nei saggi chinasici *Lead compounds* 1 e 2 a concentrazioni nanomolari e sub-nanomolari.

I dati ottenuti non solo hanno confermato l'efficienza dei peptidi selezionati ma hanno anche evidenziato che gli antagonisti selezionati non determinano alcun effetto inibitorio sull'attività chinastica di MKK7.

Tale risultato è particolarmente incoraggiante se si considerano le numerose problematiche relative alla selezione di inibitori attivi nei cicli chinastici. In letteratura sono riportati numerosi studi incentrati sulla modulazione dell'attività chinastica ed il loro denominatore comune può essere sinteticamente riassunto nell'espressione provocatoria "**Specific inhibition for non-specific effect**".

Il paradosso dell'inibizione chinastica risulta essere strettamente correlato all'elevato grado di omologia di sequenza riscontrato nella struttura dei domini catalitici. Quindi le molecole che modulano l'attività chinastica interagendo a livello della tasca dell'ATP non hanno una particolare selettività e ciò determina un'aspecifica inattivazione costitutiva del kinoma. Di conseguenza l'impiego di antagonisti ATP – competitivi determina una serie di effetti collaterali difficilmente controllabili che possono compromettere la delicata rete fosforilativa che è alla base della trasduzione dei segnali cellulari (*cell- signalling*).

L'utilizzo di una strategia combinatoriale, integrata e validata da mirati saggi d'attività ha reso possibile l'identificazione due tetrapeptidi in grado di destabilizzare l'interazione tra Gadd45 $\beta$  ed MKK7 usati a concentrazioni nano e sub nanomolari. Gli antagonisti selezionati oltre a mostrare un'elevata efficienza presentano anche una serie di caratteristiche chimiche e stereochemiche comparabili a quelle di piccole molecole organiche e per questo risultano essere candidati ideali per l'ingegnerizzazione di una futura classe di agenti terapeutici per malattie croniche infiammatorie e proliferative come il cancro.

## A.2 Summary: Interactions between proteins and identification of high affinity antagonists

The relationship between the pathological processes of infection, inflammation and cancer is correlated to the role of the transcription factor NF- $\kappa$ B in cellular homeostasis. Therefore studying NF- $\kappa$ B target genes makes it possible to understand the molecular mechanisms of inflammation, of tumor growth and progression.

Gadd45 $\beta$  is one of the anti-apoptotic regulators controlled by NF- $\kappa$ B in response to pro-inflammatory stimuli and genotoxic stress exerting its functions by interacting with several partners such as MAP kinases and DNA clamp protein. The interaction between Gadd45 $\beta$  and MKK7 has been described as a molecular link between the NF- $\kappa$ B cytoprotective effects and the suppression of the signaling of JNK, one of the main MKK7 substrates that strongly promotes apoptosis. Understanding this complex network of interactions and finding effective antagonists is of preeminent importance for elucidating the balance between cell death and cell survival and to modulate cell homeostasis for therapeutic applications.

For this reason, this PhD project has been focused on the structural and functional characterization of the Gadd45 $\beta$ -MKK7 complex and on the identification of compounds able to disrupt this interaction. In fact, developing molecules able to block the pro-survival action of NF- $\kappa$ B without significantly compromising the innate activation of the immune system is an effective way to suppress the proliferative effects induced by Gadd45 $\beta$  expression.

Biochemical analyses confirmed that Gadd45 $\beta$  exists in solution prevalently as a non covalent dimer in a 1:1 stoichiometry. The self-association dissociation constant was estimated to be about 100 nM and by limited proteolysis we identified the regions of Gadd45 $\beta$  involved in the self-association as corresponding to the predicted helix 1 (H1) and helix 5 (H5) of the protein. The biochemical analysis of Gadd45 $\beta$ -MKK7 complex has been investigated and provided a new context for dissecting the structure-activity relationship of this interaction which exhibited a KD of about 13 nM.

To select antagonists of the Gadd45 $\beta$ -MKK7 interaction, a combinatorial chemistry approach has been followed. By this process, **Lead Compounds 1 and 2** have been selected from deconvolution of two generations of tetrapeptide libraries. These novel antagonists can disrupt very efficiently the interaction between Gadd45 $\beta$  and MKK7 at concentrations in the low nanomolar range. Further investigations by co-immunoprecipitation and kinase assays have confirmed that the measured antagonistic activity matches perfectly with the IC<sub>50</sub> values from ELISA data.

Additionally, the results suggest that the selected peptides disrupt the interaction between Gadd45 $\beta$  and MKK7 without directly interfering with the kinase activity. Indeed several kinase assays have confirmed that both Lead Compounds do not block JNK phosphorylation, therefore they do not enter the kinase ATP binding site. These results suggest that Lead Peptides 1 and 2 have the potential of becoming very useful new drug candidates, since the selective inhibition of NF- $\kappa$ B downstream targets, such as Gadd45 $\beta$ , could be a way to convert inflammation-driven tumor growth into inflammation-induced tumor suppression.

## **INTRODUCTION**

## 1.1 Drug discovery and protein-protein interactions

Drug discovery has become a whole interdisciplinary and independent field of research and is gaining an increasing attention from pharmaceutical industry and academic researchers (1).

This is a multi-step process that aims at finding new potential drugs or at improving the performances of those already on the market (2).

Another major task of drug discovery is also the delivery of drugs at the right time in a safe and reproducible manner to a specific target organ at the required level (3). Disciplines involved in this process include cell biology, bioinformatics, organic and protein chemistry, high-throughput automation and ultimately functional *in vivo* studies (3). Therefore discovering new drugs in most cases also leads to the elucidation of cellular mechanisms underlying a given disease phenotype (4). Understanding the molecular and cellular mechanisms regulating a given disease is a major issue for the identification of new drugs and the related clinical development and plays a key role for reducing the attrition rate and to speed up the process (5). An outstanding support to the process of drug discovery is come from the completion of the human genomic sequence and by the introduction of novel genomics and proteomics technologies. A further contribution has been provided by the development of new disciplines, like System Biology, that study the complex network of interactions established by a set of proteins and their association with pathologies, making predictions of new potential interactions and on alterations induced by the down- or up-regulation of a given target protein. New challenges are thereby now open and they concern the identification of new cellular targets specifically associated with diseases and the development of small molecules that can modulate protein-protein interactions instead of enzymatic functions (6;7;8).

The number of new Therapeutic Strategies based on inhibiting protein-protein interactions is steadily increasing and it is now estimated that 30-35% of the discovery programs deal with interactions between proteins (9). However the development of inhibitors of enzyme activity is still a valid approach for several viral diseases, for cancer and inflammation and, in this field, the selective inhibition of kinases is far the approach of widest interest. (10;11).

This trend is not surprising because protein kinases are the cornerstones of many cell signalling systems (12). In fact protein phosphorylation plays a key role in the regulation of a diverse range of cellular functions. Especially **Mitogen Activated Protein Kinases** (MAPKs) are involved in different aspects of immune response and various pathological conditions (13). This family of Ser/Thr protein kinases are activated by a wide spectrum of extracellular stimuli. Their activity is usually crucial in inflammation as well as in proliferative diseases such as cancer (14). MAPK pathways coordinate gene transcription activation, protein synthesis, and all cell cycle. They are components of signal transduction that feature a core triple phosphorylative cascade (15). Furthermore phylogenetic analyses confirm that the basic assembly of MAPK pathways in a three-component module is conserved from yeast to human (16). These transductional ways can be regulated by different sets of stimuli, including growth factors, inflammatory cytokines, chemical insults and radiant stresses (17). Duration and degree of kinase

activity are influenced by the delicate balance between activating signals and inactivating mechanism (18;19). Especially in mammals, the multiple MAPK pathways are often in conjunction with nuclear factors (NF) (20;21;22) which are regulative elements of gene transcription. This linker explains how the MAPK are pivotal to stress and inflammatory response (17;23;24).

In figure 2 are schematized the two major groups of MAPKs in mammalian cells:

- the extracellular signal regulated protein kinases (ERK) (25)
- the stress activated protein kinase (SAPk) family that includes SAPK-1/JNK and SAPK-2/P38 (26;27).

The relevance of kinase proteins in the modulation of immune response and human diseases suggests MAPK inhibitors to be used as anti-inflammatory and immunoregulatory molecules (18;26;28).

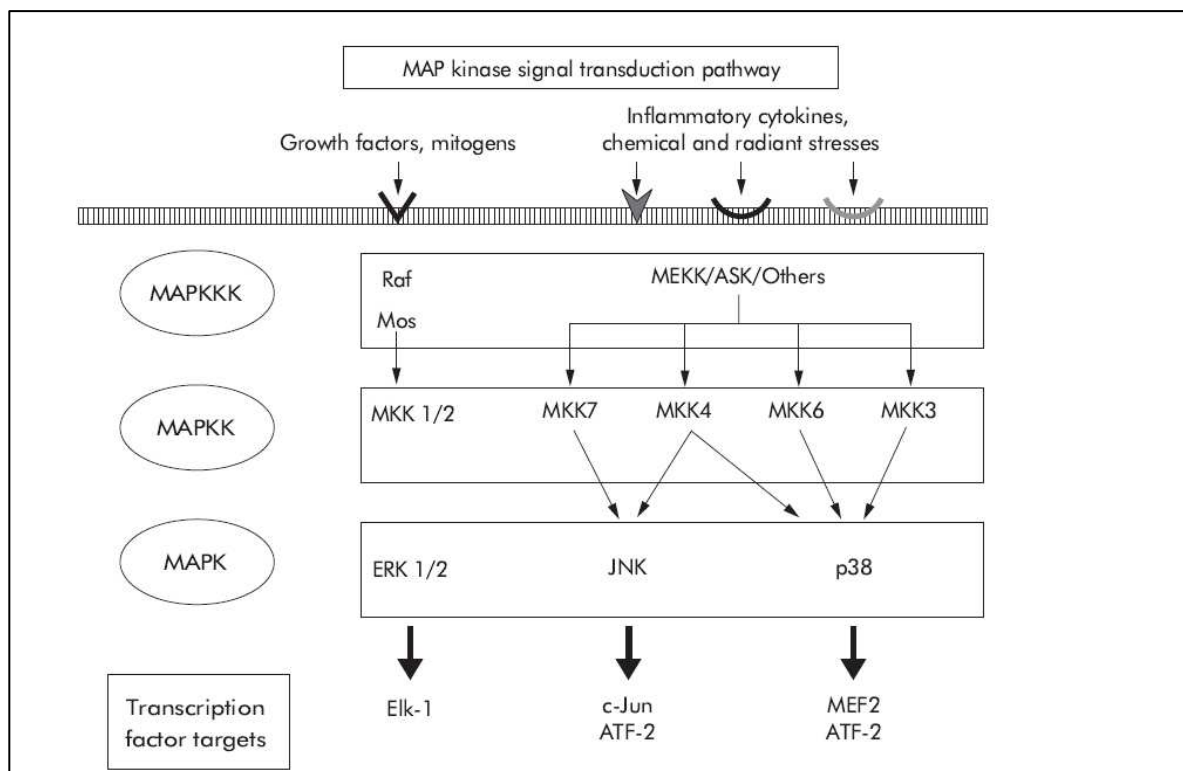


**Fig. 1: Organization of mammalian MAPK kinase.** The MAPK cascade consist of a series of three protein kinases: a MAPK and two upstream components, MAPK kinase (MAPKK) and MAPKK kinase (MAPKKKs). These last are often component of more than one signalling pathways as presented here. MAPKs can phosporylate transcriptional target directly or through downstream protein kinases.

## 1.2 Protein Kinases in Drug discovery and Development

The MAPKs have a “master-switch” function in balancing between cell proliferation and programmed cell death, controlling cellular architecture and polarity (13). These enzymes regulate multiple cellular processes that contribute to tumour development and progression, including cell growth, differentiation, migration, and apoptosis (29;30).

Extensive efforts have been made to develop kinase-specific inhibitors to treat diseases caused by the deregulation of signalling pathways (10;31), but this goal, because of the large structure similarity between all components of the family, especially at the level of the kinase domain, is a very challenging task (32). In addition, given the complexity of MAPK signal-transduction networks, the criteria that qualify a particular kinase as a putative drug-target are not straightforward (33;34).

Ten years ago only seven kinase inhibitors were under clinical evaluation, instead today they are more than 400 from early pre-clinical to marketed drugs in cancer treatment (35;36). Among the various approaches for the modulation of protein kinase activity, the inhibition by low-molecular-weight compounds appears to be the most interesting (29;37). Nevertheless, this kind of highly selective small-molecule inhibitors frequently presents problems of selectivity. In fact the vast majority of these compounds bind the hot spot of kinase domains: the ATP pocket (38). Considering that the catalytic kinase site is the most conserved in sequence and structure, the ATP competitive inhibitors show obviously a multi activity against human kinome (16). Significant is the case of SP 600125 selected as a direct JNK inhibitor. This anthrapyrazole was identified in a screening of chemical library (39) and it has been successively evaluated in animal models for arthritis rheumatoid showing anti-inflammatory effects (40). Subsequent assays against a broad range of kinases confirmed that SP 600125 inhibited 20 of the 30 kinases tested. As a consequence, the *in vivo* results previously obtained present an ambiguous interpretation (41). This example can explain why despite a significant quantity of disease-associated protein kinases, only a limited number of kinases have been successfully targeted.

The paradigm of inhibiting a specific kinase pathway can be extensively explored identifying new drug targets (42).

In fact the kinase inhibition or activation is often mediated by physical interaction with proteins up-regulated from transcriptional factors (12;43-46). Therefore these pivotal mediators could be more desirable targets for inflammatory and anti cancer therapy (47) and their characterization and validation as targets could open the way to new Therapeutic Strategies based on modulating interactions between proteins instead of blocking highly conserved enzymes.

### 1.3 Gadd45 Family: Key proteins of cell signalling

Gadd45 proteins have such highly regulative properties and it is widely accepted that they are implicated in cell signalling at several levels (47).

The gadd45 growth arrest and DNA damage-inducible family of genes, comprising gadd45a, gadd45b and gadd45g, encode for the corresponding Gadd45 $\alpha$ , Gadd45 $\beta$  and Gadd45 $\gamma$  acidic proteins of about 18 kDa. They are ubiquitously expressed and exert the primary function of growth arrest and apoptosis induction in response to several genotoxic stresses thus contributing to cellular homeostasis (44;47-51).

Numerous studies confirm the pivotal role of Gadd45 family in a variety of cell functions such as DNA replication and repair (52), cell cycle regulation (53) and, depending on cell type and cell metabolic state, also in cell survival (50). However, in literature there is no reported enzymatic activity for Gadd45 proteins. Then the members of Gadd45 family are significant examples of *key-proteins* exerting their biological functions by interaction with several protein partners. Indeed, highly specific interactions with PCNA (44;48;52;54;55) cdc2 (48) waf/p21 (44;48;56;57) cdk1/cyclinB1(44), MEKK4(58) and CRIF1(59) are involved in Gadd45 regulation of the cell cycle and the response to external cell stimuli.

### 1.4 Gadd45 $\beta$ in the cell system: functional - structural characterization

Gadd45 $\beta$  is one of the most important member of Gadd45 family (48) ; it has been described as an NF- $\kappa$ B –inducible gene and as a prominent mediator of NF- $\kappa$ B protective response to TNF- $\alpha$  and UV-induced apoptosis (43;15-60). However this aspect is still controversial and several reports indicate Gadd45 $\beta$  as an effective pro-apoptotic factor, too (47;51;52). The mechanisms by which Gadd45 $\beta$  can promote cell survival have been extensively investigated and it has been found that in MEFs and other cells, upon NF- $\kappa$ B induction, it provides selective JNK inactivation by inhibition of the upstream MKK7 kinase (19;43;61;50) (Fig 3). In hematopoietic cells, instead, it blocks JNK activation by binding to MKK4 (48;50), and in B cells it is a critical mediator of the pro-survival activity of CD40 elicited in response to Fas stimulation (63).

The primary sequences of Gadd45 proteins share an overall 70% homology (about 60% identity, See Fig. 2A e 2B ) and all contain six cysteines, five of which (from the 2nd to the 6th) are located in highly conserved positions.

Importantly, it has been reported that Gadd45 proteins are also able to homo- and hetero-dimerize or oligomerize (64).

```

GA45B_HUMAN      MTLEELVACDNA---AQKMQTVTAAVEELLVAAQRQDRLTVGVYESAKLM
GA45A_HUMAN      MTLEEFSAGEQK---TERMDKVGDALEEVLKALSQRTITTVGVYEAAKLL
GA45G_HUMAN      MTLEEVRGQDTVPESTARMQAGAKALHELLLSAQRQGCLTAGVYESAKVL
                  ***** . . : : : * : * : * * * * : * . ***** : * : :

GA45B_HUMAN      NVDPDSVVLCLLAIDEEEEEDDIALQIHFTLIQSFCCDNDINIVRVSGMQR
GA45A_HUMAN      NVDPDNVVLCLLAADEDDDRDVALQIHFTLIQAFCCENDINILRVSNPGR
GA45G_HUMAN      NVDPDNVTFCVLAAGEEDEGDIALQIHFTLIQAFCCENDIDIVRVGDVQR
                  ***** . * . : * : * * . * : : : * : ***** : * : * : * : * : * . . *

GA45B_HUMAN      LAQLLG-----EPAETQGTTEARDLHCLLVTNPHTDAWKSHGLVEVASYC
GA45A_HUMAN      LAELLLLETDAGPAASEGAEQPPDLHCVLVTNPHSSQWKDPALSQLICFC
GA45G_HUMAN      LAAIVG-----AGEEEAGAPGDLHCILISNPNEDAWKDPALEKLSLFC
                  ** : : : : . ***** : * : * : * . ** . * : : : *

GA45B_HUMAN      EESRGNNQWVPYISLQER
GA45A_HUMAN      RESRYMDQWVPVINLPER
GA45G_HUMAN      EESRSVNDWVPSITLPE-
                  . *** : : * * * * . * * *

```

**Fig.2A: Alignment of Gadd45 $\alpha$ ,  $\beta$  and  $\gamma$  sequences.** An identity of about 60% is observed. Most differences are present in the region corresponding to the second acidic loop, with a Gadd45g pentapeptide stretch remaining unpaired with the other two sequences. To correctly align the Gadd45 $\alpha$  variant, an 8-residue long stretch is required. Within the acidic loop (61), residues Asp67 of Gadd45 $\beta$  is mutated to Arg in the  $\alpha$  variant and to Gly in Gadd45g. Regions involved in self-association are underlined.

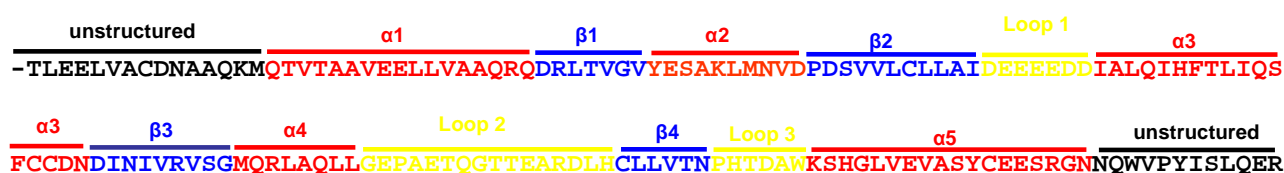


**Fig.2B: Representation of the protein secondary structure is schematized based on the model described in reference (61).**

## 1.5 Gadd45 $\beta$ and MKK7: a potential target for anti-cancer and anti – inflammatory therapies

The coordination between immune and inflammatory responses is correlated to the activation of the NF- $\kappa$ B/Rel transcription factors. As a consequence, they control cell survival (43). Activation of NF- $\kappa$ B antagonizes apoptosis or programmed cell death by numerous triggers, including the ligand engagement of death receptors, such as tumour-necrosis factor (TNF) receptor or TRAIL (20). The anti-apoptotic activity of NF- $\kappa$ B is also crucial to oncogenesis and to chemo- and radio-resistance in cancer (23). Cytoprotection by NF- $\kappa$ B involves the activation of pro-survival genes which down regulates the c-Jun amino terminal kinase (JNK) cascade (75) (Fig.3). It has widely been described how Gadd45 $\beta$  mediates the NF- $\kappa$ B suppression of JNK signalling by physically interacting with MKK7 (47).

Then Gadd45 $\beta$  – MKK7 interaction is a molecular crosslink between the anti-apoptotic activity of NF- $\kappa$ B and the suppression of the JNK cascade, thereby it acts as a key checkpoint to control cell fate downstream of TNF-Rs (19;61;47).

The structural basis of this interaction has been extensively described in literature (19;47;61;68). Gadd45 $\beta$  associates with MKK7 through an extensive network of interaction mediated by residues comprised within its putative  $\alpha$ 3, loop 1 and  $\alpha$ 4-loop 2 regions. The model proposed in the paper by Papa et al, explains the structural basis of Gadd45 $\beta$ -mediated inactivation of MMK7. The complex Gadd45 $\beta$ -MKK7 is stabilized by electrostatic interaction and H-bonds formed between charge/polar residues positioned at the interface between the two proteins and Gadd45 $\beta$  inactivates MKK7 by masking critical residues, such as the Lys149 required for ATP binding, causing conformational changes that impede the proper catalytic kinase function (Fig 4). This molecular scenario is further complicated by the presence of multiple equilibriums of self-association between Gadd45 $\beta$  and MKK7 monomers, as both reportedly have at least a dimeric structure. The occurrence of such homo-oligomeric forms could be a regulative element of the interaction between the two proteins and their effects need additional investigations.

The suppression of JNK signalling dependent on NF- $\kappa$ B activity is a constant in chronic inflammatory conditions such as rheumatoid arthritis and inflammatory bowel disease and several malignancies (65). Therefore the interaction between Gadd45 $\beta$  and MKK7 can be indicated as a potential therapeutic target and identifying compounds that disrupt this binding can represent a valid approach for the treatment of several diseases, such as cancer and inflammation. If provided with a sufficient selectivity, they can be potent therapeutic agents with a novel mechanism of action, whereby the effects of NF- $\kappa$ B activation are largely impaired without suppressing the physiological JNK signalling.

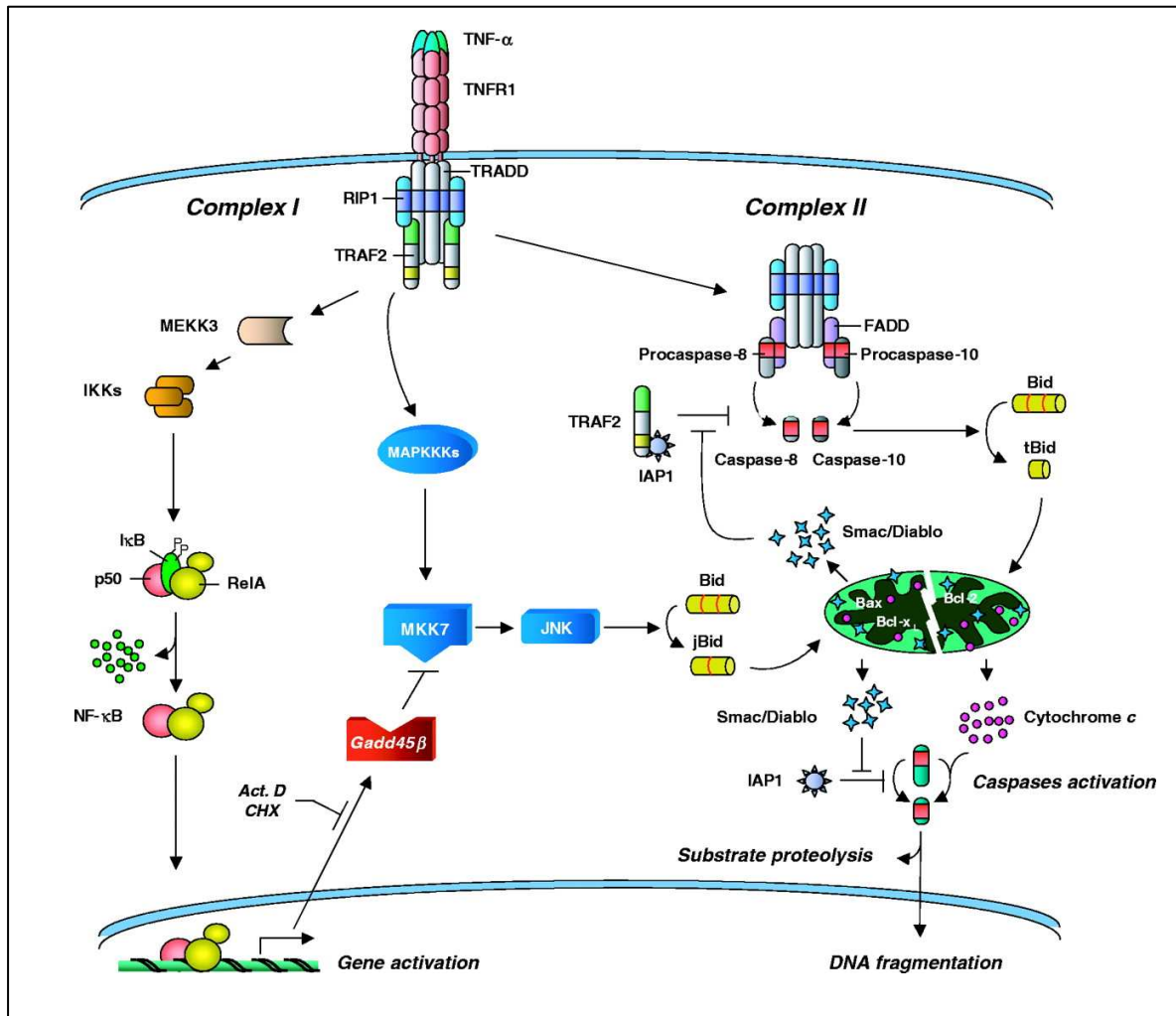


**Fig. 3: TNFR1-induced pathways modulating apoptosis.** Formation of complex I lead to NF- $\kappa$ B activation, Gadd45 $\beta$  induction, JNK inhibition and cell survival. Usually, ubiquitous NF- $\kappa$ B dimers are sequestered in the cytoplasm by inhibitory I $\kappa$ B proteins (I $\kappa$ B $\alpha$ , I $\kappa$ B $\beta$  and I $\kappa$ B $\epsilon$ ). Stimulation by TNF $\alpha$  induces a sequential phosphorylation and subsequently proteolysis of I $\kappa$ Bs, but after removal of the inhibitors, NF- $\kappa$ B dimers enter nuclei to induce expression of coordinated sets of target genes that regulate innate and adaptive immunity, inflammation, cell growth and cell survival. Gadd45 $\beta$  expression is up-regulated by TNF and mediated by NF- $\kappa$ B. Gadd45 $\beta$  strongly interacts with MKK7, an upstream JNK activator, inhibiting its kinase activity.

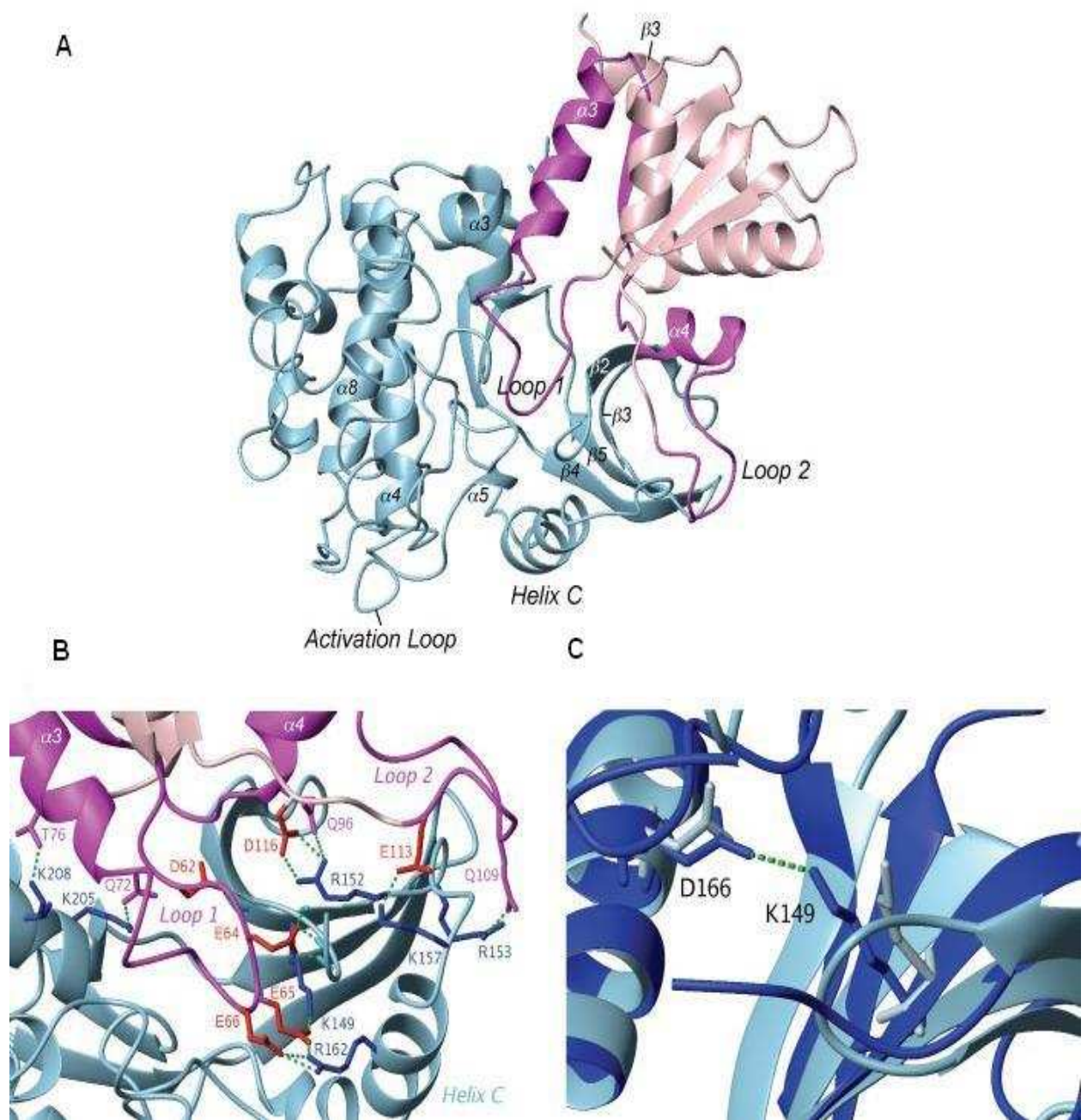


**Fig. 4:** Model of the Gadd45 $\beta$ -MKK7 complex represented in ribbon by MD simulation: MKK7 is in light blue and Gadd45 $\beta$  is in pink (A). Interface of interaction: basic residues of MKK7 are in blue instead the acidic residues of Gadd45 $\beta$  are in red; 60–114 region is reported in magenta and H-bonds are depicted as green dotted lines (B). Detail of H-bond (green) between Asp166 and Lys149 (C).

## 1.6 Bio-molecular Engineering and Combinatorial Design: two alternative approaches in drug discovery

The introduction of new pharmaceuticals is a lengthy and very expensive process (fig.5) that, starting from a given medical need, proceeds through the identification of validated targets, the selection of chemical leads and the identification of drug candidates that are subsequently developed in the preclinical (toxicology) and the clinical phases. The several phases of development (5). The original strategy, based on the random screening of proprietary compound collections and of plant extracts has been gradually superseded by the introduction of powerful design techniques (favoured by the advent of the structural biology) and of combinatorial chemistry and High Throughput technologies. The primary objective of the combinatorial chemistry is the generation of random or focused libraries composed of large numbers of molecules that are successively screened (66) to identify new leads. Random peptide libraries have been largely employed in the past decade for the rapid identification of new leads that have then converted into small molecules endowed with improved pharmacological and stability profiles. They offer the great advantage of being easily prepared and screened and, due to the very robust synthesis procedures, can be used in mixture-based formats (67). Active peptides can be isolated by these mixtures and identified following different deconvolution strategies (68). However, peptides generally do not fulfil the requirements of low conformational flexibility, stability and bioavailability needed for good drug candidates and peptide "leads" with high potency and selectivity are often made "druggable" by conversion to more stable structures with improved pharmacological profiles. This approach makes the screening of peptide libraries still a valuable tool for drug discovery (69), though it has been integrated with techniques of rational design, *in silico* screening and biomolecular engineering to facilitate the transition from peptides to useful drug candidates (6).

## 1.7 Therapeutic Peptides: interesting perspectives in Medicinal chemistry

The therapeutic application of peptides has often been hampered by their lack of *in vivo* stability and poor biodistribution and delivery properties. Due to protease degradation, the half-life of peptides is extremely short and they are typically cleared from bloodstream after few hours from administration. In addition they cannot cross cell membranes, therefore, even peptides with high potency *in vitro* do not show effects *in vivo* because their exposure to the target tissue is insufficient (70). Despite their poor bioavailability properties, the premise of transforming peptides into good therapeutics still holds. Indeed they offer several advantages over small molecules and proteins (71), especially to antagonize protein-protein interactions. For example, they have large recognition surfaces that can match better with the large interfaces underlining protein-protein contact regions; in addition their flexibility provides them with higher affinities and specificity for the targets. Peptides also have

low toxicity profiles and, differently from proteins, also exhibit higher stability at room temperature and higher tissue penetration (70). The therapeutic properties of bioactive peptides can be improved by several techniques that include the incorporation of D-amino acids (72) and cyclization (73), which can increase proteolytic stability and improve the conformational flexibility which are fundamental prerequisites for getting optimal lead compounds.

## 1.8 Aim of the project

The aim of this research project was twofold. In a first part of the work we wanted to study the oligomeric assembly of the proteins Gadd45 $\beta$  and MKK7 and their relevance in the mechanism of inactivation of the kinase by Gadd45 $\beta$ . Indeed, as both proteins are known to oligomerize or dimerize, this event could be a regulative mechanism of the interaction. This goal has been pursued by first studying the oligomerization status of the proteins and by next defining the regions of self-interaction on Gadd45 $\beta$ . Using a combination of biochemical and spectroscopical techniques, the secondary structure elements participating in self-association will be identified and correlated to the known structural elements mediating the interaction with MKK7. Identification of Gadd45 $\beta$  fragments involved in self-association will be performed using a method of protein digestion, peptide fractionation by HPLC and competitive ELISA assays.

In a second phase of the project, we will develop peptide antagonists of the interaction between Gadd45 $\beta$  and MKK7. This goal will be pursued by performing a screening of combinatorial peptide libraries made of synthetic tetrapeptides. The screening will be carried out utilizing an ELISA-like assay on a library built in a simplified format, whereby only 12 out of 20 natural aminoacids will be used. The advantage of using tetrapeptides relies on the easiness of preparation and the rapidity of screening. Furthermore, short peptides with only few residues have structural properties more similar to small molecules to which they can be easily converted. The synthesis of the library will be performed following the Mix-and-Split method that leads to combinatorial mixtures. The screening will be carried out by a competitive ELISA assay. The selected peptides will be next engineered to possibly improve the affinity and increase the peptide stability toward a set of proteases. Finally the peptides will be submitted to cell assays to assess the efficacy also in a more physiological environment and verify that the antagonists only block the interaction, without affecting the kinase activity.

# The Drug Design Process

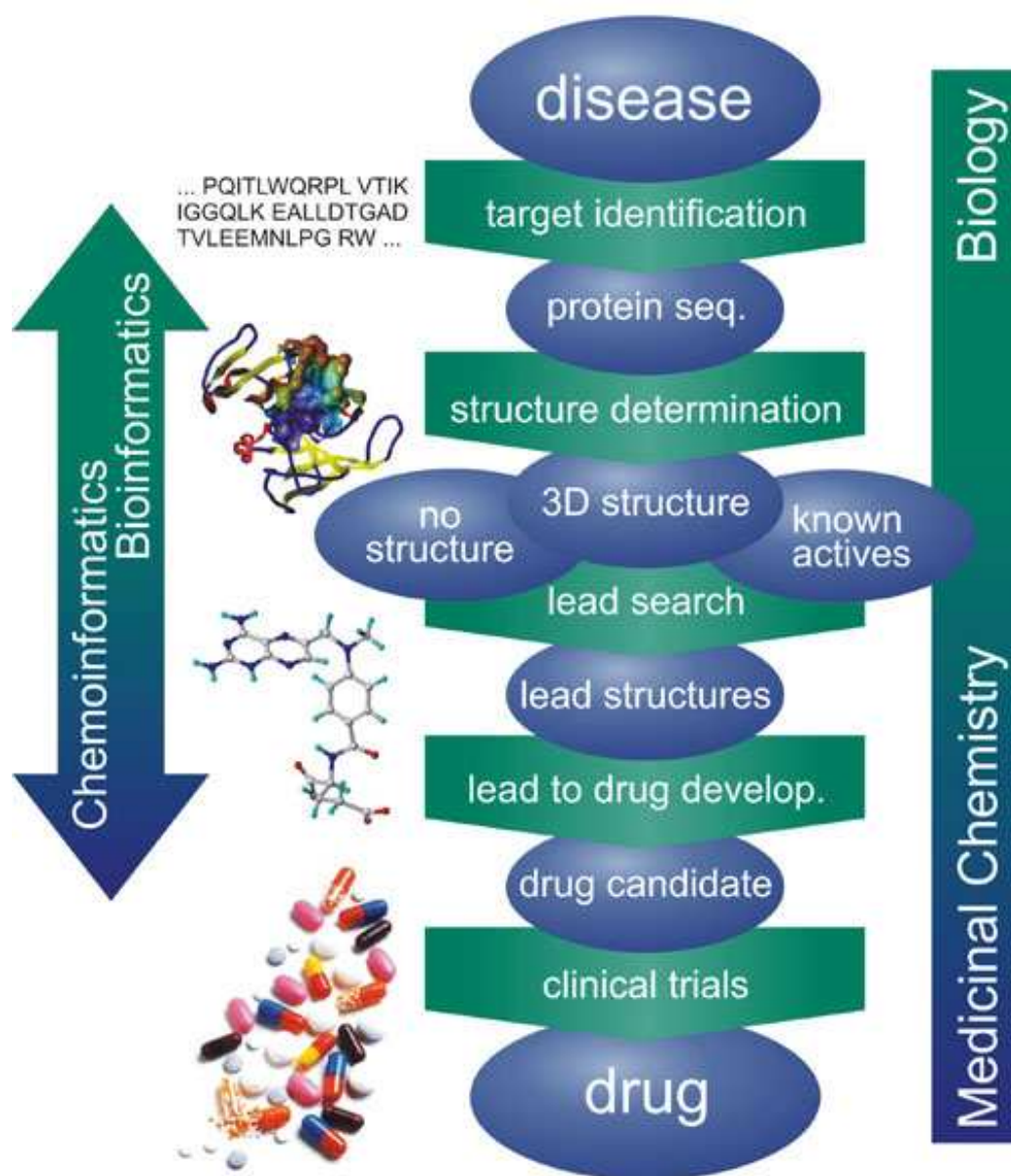


**Fig 5: The diagram illustrates the early phase of drug discovery in which the aim is to identify target and lead molecules.** Instead of isolated problems, drug discovery incorporates a whole series of challenges spanning from the biological problem of characterising a disease on a molecular level, to finally bringing a drug to the market. While Bioinformatics approaches deal mostly with the early stages of target selection and structure identification, Cheminformatics addresses the later stage problems like lead identification and lead optimization. *Source: Nat Rev Drug Discov. 2007 Nov;6(11):891-903.*

## **MATERIALS AND METHODS**

## 2.1 Cloning expression and purification of recombinant protein

### 2.1.1 Cloning

hGadd45b and hMKK7 were PCR amplified using the oligonucleotides reported in table 1, then double digested with proper restriction enzymes (see table 1). Digested fragments were extracted from 0.8% agarose gel using QIAquick Gel Extraction Kit and cloned into pGEX6P-1 vector, previously digested and dephosphorylated. Ligation products were electroporated into TOP10F' cells and recombinant colonies were isolated using QIAprep Spin Miniprep kit according to the manufacturer's instructions.

These clonings allowed the expression of the proteins of interest as GST-fusion products containing a highly specific cleavage site for PreScission Protease upstream the protein sequence.

**Table 1: Cloning conditions**

<b>Samples</b>	<b>Oligonucleotides</b>	<b>Enzyme restriction</b>
<b>GST hGadd45β</b>	3' CGC GCG <u>CCA TGG</u> GCA TGA CGC TGG AAG AGC TCG TGG 5'	NcoI
	5' CGC GCG <u>CTCGAG</u> TTA CTA GCG TTC CTG AAG AGA TGA TGG 3' * *	XhoI
<b>GST hMKK7</b>	3' CGC GCG <u>GGATCC</u> ATG GCG GCG TCC TCC CTG GAA CAG 5'	BAMHI
	3' CGC GCG <u>CTC GAG</u> TTA CTA CTT CTT CGC CAT GAC ATC CTT GAA CCA 5' * *	XhoI
Enzyme site = underlined * = stop codon		

## **2.1.2 Expression**

The expression of recombinant proteins: hGadd45 $\beta$ , hMKK7 and hJNK were induced by treatment for 16h of BL21(DE3)trxB bacterial strain with 0.1 mM isopropyl- $\beta$ -D-thiogalactopyranoside (IPTG) at 22 °C. In every case a 200 mL pellet was re-suspended in 20 mL of cold lysis buffer (see table 2) supplemented with protease inhibitor mixture (1 mM PMSF, 1.0  $\mu$ g/mL of aprotinin, 1.0  $\mu$ g/mL of leupeptin, 1.0  $\mu$ g/mL of pepstatin, and 1.0 mg/mL of lysozyme) and incubated at room temperature for 30 min. Cells were disrupted by sonication on ice with 10 s on/10 s off cycles for a total of 10 min on. After centrifugation at 15,000 rpm for 30 min at 4 °C, the supernatant was opportunely purified on an ÄKTA FPLC chromatography system using either HisTrap HP or GSTrapFF (GE Healthcare) columns. Column were washed with lysis buffer without Triton and inhibitors. The elution of the proteins was carried out using proper buffers (see table 2) and monitored by measuring absorbance at 280 nm. The resulting fractions were analyzed by 15% SDS-PAGE. The eluted fractions were dialyzed against opportune buffers as requested in the next analysis or purification steps.

To try to carry out accurate structural characterization of hGadd45 $\beta$  and hMKK7, aliquots of the fusion proteins were digested with PreScission protease (GE Healthcare) to remove the GST protein (see table 3).

After tag removal, proteins were submitted to other purification steps (MonoQ and gel-filtration, see table 2) in order to obtain highly purified material (95-98% pure).

**Table 2: Purification Buffers**

<b>Samples</b>	<b>Type of Purification</b>	<b>Loading Buffer</b>	<b>Elution Buffer</b>
<b>His6- hGadd45<math>\beta</math></b>	His trapHP	25 mM Tris, 500 mM NaCl, 10mM Imidazole, 1 mM DTT, 0.05% (v/v) Triton X-100, pH 7.5	Gradient of 10mM–500mM imidazole.
<b>GST hGadd45<math>\beta</math></b>	GSTrap FF	20 mM Tris-HCl [pH 7.0], 100 mM NaCl, 100 $\mu$ M PMSF, 1.0 mM EDTA	50mM Tris pH 8.0 10mM GSH
<b>GST hMKK7</b>	GSTrap FF	20 mM Tris-HCl [pH 7.0], 100 mM NaCl, 100 $\mu$ M PMSF, 1.0 mM EDTA	50mM Tris pH 8.0 10mM GSH
<b>GST hJNK</b>	GSTrap FF	PBS	50mM Tris pH 8.0 10mM GSH
<b>hGadd45<math>\beta</math></b>	MonoQ HR 5/5 column	20 mM Tris-HCl [pH 7.0], 100 mM NaCl, 100 $\mu$ M PMSF, 1.0 mM EDTA	Step gradient 20, 40, 60, 80, 100% of 20 mM Tris-HCl [pH 7.0], 500 mM NaCl, 100 $\mu$ M PMSF, 1.0 mM EDTA
<b>hGadd45<math>\beta</math> – hMkk7</b>	Superdex 75 10/30	20 mM Tris-HCl (pH 7.0) 150 mM NaCl , 1mM EDTA and with or without 1mM DTT	-

**Table 3: Digestion conditions**

<b>Samples</b>	<b>Cleavage Buffer</b>	<b>Units of PreScission Protease</b>	<b>Time</b>
<b>GST hGadd45<math>\beta</math></b>	50U	6°C for 4 hrs	50 mM Tris-HCl [pH 7.0], 100 mM NaCl, 1.0 mM EDTA 1mM DTT
<b>GST hMKK7</b>	160 U	4°C for 5 days	50 mM Tris-HCl [pH 7.0], 100 mM NaCl, 1.0 mM EDTA 1mM DTT

## 2.2 Peptides synthesis and purification

Peptides corresponding to different regions of Gadd45 $\beta$  and MKK7 (see table 4) were designed on the basis of a predicted model (61) and prepared by solid-phase synthesis as C-terminally amidated and N-terminally acetylated derivatives following standard Fmoc chemistry protocols. A Rink-amide MBHA resin (substitution 1.1 mmol/g) and amino acid derivatives with standard protections were used in all syntheses. Cleavage from the solid support, performed by treatment with a TFA/triisopropylsilane (TIS)/water (90:5:5, by vol.) mixture for 90 min at room temperature, afforded the crude peptides that were precipitated in cold ether, dissolved in a water/acetonitrile (1:1, v/v) mixture and lyophilised. Products were purified by RP-HPLC using a C18 Jupiter column (50 mm  $\times$  22 mm) applying a linear gradient acetonitrile 0.1% TFA between 5% and 70% over 30 minutes. Peptide purity and integrity were confirmed by LC-MS mass measurements using a Surveyor LC system coupled to an LCQ Deca XP mass spectrometer equipped with an OPTON ESI source. The peptide corresponding to fragment G132-N156 of MKK7 (61) and the shortest region of Gadd45 $\beta$  still able to bind and block MKK (47) were also prepared and purified. The highly acidic peptide Gadd45 $\beta$  (A60-D86) was purified by RP-HPLC using a C18 Jupiter column (50 mm  $\times$  22 mm) applying a linear gradient of acetonitrile from 5% to 70% over 30 minutes, using 10 mM phosphate buffer pH 7.0 as eluent A.

**Table 4: Synthetic peptides corresponding the different Gadd45b helices**

Synthetic Peptides	Sequence	Molecular Weight (Da)
eHelix 1 (A12-R32), eH1	Ac-AAQKMQTVTAAVEELLVAAQRQDR-NH <sub>2</sub>	2669.3 $\pm$ 0.2
eHelix 4 (R91-E104), eH4	Ac-RVSGMQRLAQLLGE-NH <sub>2</sub>	1343.6 $\pm$ 0.3
eHelix 5 (A129-N148), eH5	Ac-AWKSHGLVEVASYCEESRGN-NH <sub>2</sub>	2262.6 $\pm$ 0.3
hGadd45 $\beta$ (A60-D86)	Ac-AIDEEEEDDIALQIHFTLIQSFCDDN-NH <sub>2</sub>	3166.4 $\pm$ 0.5
hMKK7 (G132-N156)	Fmoc-( $\beta$ Ala) <sub>2</sub> GPVWKMRFRKTGHVIAVKQMRRSGN-NH <sub>2</sub>	3335.5 $\pm$ 0.4

## 2.3 Digestion with trypsin and peptide fractionation

An aliquot of Gadd45 $\beta$  (1.0 mg; 0.052  $\mu$ mol) was dissolved in 2.0 mL of 50 mM Tris, 20 mM CaCl<sub>2</sub>, pH 8.0. TPCK-treated trypsin (Sigma) was added at a final enzyme-substrate ratio of 1:100 and the reaction kept at 37 °C with gentle agitation for 16 h. A protein sample (0.4  $\mu$ g) was then analyzed by LC-MS/MS to assess protein digestion using a BioBasic 30 mm  $\times$  2 mm ID C18 column. The column was equilibrated at 200  $\mu$ L/min with 5% CH<sub>3</sub>CN, 0.05% trifluoroacetic acid (TFA), then a gradient of CH<sub>3</sub>CN from 5% to 55% over 65 min was applied and monitored by both photodiode array and MS. The MS analysis was conducted by alternatively recording full mass spectra and data-dependent mass analysis to obtain sequence information from peptide fragmentation. The remaining digested protein sample was finally injected on a 250 mm  $\times$  4.6 mm ID C18 column equilibrated at 1.5 mL/min flow-rate with 5% CH<sub>3</sub>CN, 0.1%TFA, applying a 5%–55% gradient of CH<sub>3</sub>CN over 65 min to elute the peptides; 13 fractions of 5 min each were collected from time zero to time 65 min, and were analyzed (4  $\mu$ L) by LC-MS/MS as reported. Lyophilised fractions were stored at –80 °C.

## 2.4 Spectroscopic characterization of hGadd45 $\beta$ and hMKK7

### 2.4.1 CD analysis of native proteins

CD spectra were recorded using a Jasco J-810 spectropolarimeter (JASCO Corp) equipped with a Peltier-type temperature control system. Spectra were recorded in the wavelength range between 195 and 250 nm, at a scanning speed of 20 nm/min, a band width of 2 nm, and a temperature of 20°C, under constant N<sub>2</sub> flow. The recorded spectra were then signal-averaged over at least three scans, and the baseline was corrected by subtracting the spectrum obtained with sample buffer. The value of molar ellipticity per mean residue  $[\theta]$ , expressed in deg $\times$ cm<sup>2</sup> $\times$ dmol<sup>-1</sup>, was finally calculated using the following equation:  $[\theta] = [\theta]_{\text{obs}} \text{mrw}/10.l.C$ , where  $[\theta]_{\text{obs}}$  is the ellipticity measured in millidegrees, mrw is the mean MW of the residues of the protein, C is the protein concentration in g/L, and l is the optical path length of the cell used, expressed in cm. The protein concentration to be used for acquisition of the CD spectra was optimized in preliminary acquisitions. hGadd45 $\beta$  and hMKK7 were analysed at a concentration of  $5.5 \times 10^{-5}$  M in water in order to minimize salt interference in the far UV region

### 2.4.2 Gadd45 $\beta$ Stability against Chemical Denaturants

CD spectra were recorded as previously described, native Gadd45 $\beta$  was diluted with water to obtain a final concentration of  $5.5 \times 10^{-5}$  M. A blank run was carried out before every experiment and subtracted from the protein CD spectra. Chemically induced denaturation was carried out on native Gadd45 $\beta$  performing 1 degree.(°C) increment every 2 min from 20 °C to 80 °C, monitoring the CD signal at 222 nm. The temperature was returned to 20 °C to investigate the refolding capacity of the thermally denatured protein. CD spectra were again collected after each 2 degrees (°C) change. To investigate the effects of concentration on protein oligomerization, serially diluted solutions at concentrations ranging from  $5.5 \times 10^{-5}$  M to  $5.5 \times 10^{-6}$  M were analyzed using cuvettes with increasing path-lengths in order to compensate the signal loss due to dilution. Chemical denaturation experiments were carried out evaluating the effect of urea and GdnHCl on Gadd45 $\beta$  denaturation as described (74). Briefly, pH-controlled solutions with different concentrations of urea and GdnHCl, with protein at a constant concentration of  $5.5 \times 10^{-5}$  M were prepared and incubated for 16 h at 20 °C. Chemically induced denaturation was monitored by recording the CD value at 222 nm for each sample. The reversibility of the denaturation was controlled after removal of denaturants from the unfolded protein sample by dialysis overnight. The capacity of the recovered protein to recognise MKK7 was also evaluated by direct ELISA binding. Corresponding blanks were always recorded and subtracted. CD spectra were registered at 25 °C. CD analysis was also done on the synthetic peptides used in the ELISA assays. The concentration of peptides was kept at  $1.0 \times 10^{-5}$  M and a 0.1 cm path-length quartz cuvette was used. Spectra were acquired in a 10 mM sodium

phosphate buffer at pH 7.0 and in the presence of increasing concentrations of TFE, up to 20% (v/v).

## **2.5 Characterization of Gadd45 $\beta$ structure by hydrodynamic methods and LC-MS.**

### **2.5.1 Native gels**

Laemmli discontinuous system without SDS was used for native gel separations. Mobilities of proteins were determined in 8, 10, 12, and 15% gels by loading 18  $\mu$ g of pure proteins from a 1.8 mg/mL solution (100  $\mu$ M). Relative electrophoretic mobilities were calculated relative to the mobility of bromphenol blue. Calibration curves were obtained and molecular masses calculated according to Sigma protocol (technical bulletin No. MKR-137).

### **2.5.2 Size exclusion chromatography**

Size exclusion chromatography was used as a final step in the purification of Gadd45 $\beta$  and to determine the oligomeric state of the protein. To this purpose 5.0  $\mu$ M solutions were subjected to gel-filtration chromatography on a Superdex 75 10/30 (Amersham Pharmacia Biotech) column equilibrated with the buffers shown in the table 2. For calibration, molecular mass markers for gel-filtration chromatography were run on the column under the same conditions in duplicate. Elution of dextran blue was used to determine the void volume of the column. Elution volumes and partition coefficients of the standards and samples were calculated according to Amersham Pharmacia Biotech protocol.

### **2.5.3 LC-MS**

To further characterize protein purity and MW, we performed LC-MS analyses using 5  $\mu$ l of a 0.1 mg/ml sample and a LCQ DCA XP Ion Trap mass spectrometer (ThermoElectron, Milan, Italy). This was equipped with an OPTON ESI source (operating at a needle voltage of 4.2 kV and a temperature of 320 $^{\circ}$ C) and a complete Surveyor HPLC system (including a MS pump, an autosampler and a photo diode array [PDA]). Analyses were performed using a 300  $\text{\AA}$  narrow bore 250x2 mm C4 Jupiter column (Phenomenex, Torrance, CA) and applying a gradient of solvent B (0.05% TFA in CH<sub>3</sub>CN) on solvent A (0.08% TFA in H<sub>2</sub>O) from 30% to 70%, over a period of 40 min. During this time, the sample tray was kept at either 4 or 20 $^{\circ}$ C, whereas the column was kept at 25 $^{\circ}$ C. Mass spectra were recorded continuously in the mass interval 400-2000 amu, in positive mode (LC-MS, condition 1). Multicharge spectra were then deconvoluted using the BioMass program implemented in the Bioworks 3.1 package provided by the

manufacturer. Mass calibration was performed automatically by means of selected multiple charged ions, in the presence of a calibrant (UltraMark; ThermoElectron, Milan). All masses were reported as average values.

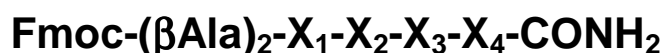
## 2.5.4 Protein alkylation assays

For an assessment of the presence of free cysteines, 50 µg of purified native Gadd45β (2 mg/ml) was denatured in 50 µl of a solution containing 250 mM Tris-HCl (pH 8.5), 1.0 mM EDTA, and 6 M guanidinium chloride for 30 min at 45°C, in the absence of any reducing agent. The protein was then subjected to alkylation by incubation of the sample mix to 0.12 M 4-vinyl-pyridine (4-VP) (Sigma-Aldrich) at 25°C for 60 min, after which time the reaction was terminated by quenching at 4°C with DTT. Finally, alkylation was assessed using LC-MS. For experiments of limited alkylation, preliminary assays were carried out using 6 µg of purified hGadd45β and 0.1 M 4-VP and performing incubations in 50 µl of 50 mM Tris.HCl, pH 7.5, at room temperature. Alkylation kinetics were monitored by LC-MS at 0, 10, 40, 70 and 90 min, using LC-MS, upon quenching the reactions by cooling at 4°C. Optimal conditions were identified (i.e. reaction time 10 min, room temperature), and free 4-VP was removed by filtration on Vivaspin concentrators with a 5-kDa cut-off at 4°C.

## 2.6 Combinatorial tetrapeptides library: synthesis and iterative deconvolution

The peptide library and single peptides were prepared using all commercially available L-α amino acids (listed in Table 5). All residues were 9-Fluorenylmethoxycarbonyl (Fmoc)-derivatized (>99%) and were utilized without any further purification. The library was chemically synthesized following the Fmoc methodology and sequence randomization was achieved by applying the Mix-and-Split method which therefore required an iterative selection and enhancement process to identify lead peptides. See also Fig. A and B for schematic examples of the Mix-and-Split process and of the iterative screening processes. The tetrapeptide library was generated using a simplified peptide library (67) where only 12 out 20 natural aminoacids were utilized in order to simplify the synthesis and screening process and, at the same time, to take into account the chemical complexity of the side chains functional groups and to eliminate several “quasi-duplicates”. Indeed, the synthesis of random combinatorial libraries of peptides generates large numbers of “quasi-duplicates” deriving from the strong similarity between several side chains. Using natural amino acids, in L- or D- configuration, sequences where Glu is replaced by Asp, Leu by Ile or Val, Gln by Asn and so on, can display very similar properties. Such residues, although being different in their propensity to adopt secondary structures, they can be considered almost equivalent in terms of intrinsic physical-chemical properties, as for example the capacity to establish external interactions or to fit in a given recognition site. Thereby, in preliminary screenings, a selection

of non-overlapping structures can be chosen, which are subsequently optimized introducing the excluded residues. The list of selected amino acids used for our study is reported in Table 5, along with a description of chemical and physical properties of the single residue. The first generation library was thus composed of 20736 peptides (all combinations of 12 amino acids at four positions:  $12^4=20736$ ). Twelve mixtures were generated such that the first position was individually defined with 12 amino acids and each mixture contained the 1728 different tetrapeptides beginning with the particular amino acid ( $Y_1XXX-NH_2$ , "Y" represents a single amino acid, while "X" represents all the 12 amino acids). The iterative process was carried out re-preparing the most active mixture identified. Each of the X positions from  $Y_1XXX-NH_2$ , were successively defined with each of the 12 amino acids (i.e.,  $Y_1XXX-NH_2 \rightarrow A_1Y_2XX-NH_2 \rightarrow A_1B_2Y_3X-NH_2 \rightarrow A_1B_2C_3Y_4-NH_2 \rightarrow A_1B_2C_3D_4-NH_2$ ; the letter A, B, C and D represent the identified position). The most active sequence(s) in this process was thus identified by the systematic reduction in the number of compounds in the most active mixture  $1728 \rightarrow 144 \rightarrow 12 \rightarrow 1$ . Three additional syntheses were required for each active mixture identified in the original library. The next step was to synthesize a library of II generation where the excluded aminoacids were introduced, thus arriving at the choice of a series of 24 single compounds. The particular library prepared and used in our study, had the following general formula:



The Fmoc group was introduced in order to have a large hydrophobic and fluorescent probe helpful in screening assays. The two  $\beta$  alanines were instead introduced as spacer between the library structure and the Fmoc group  $CONH_2$  represents an amide group at the C-terminus.

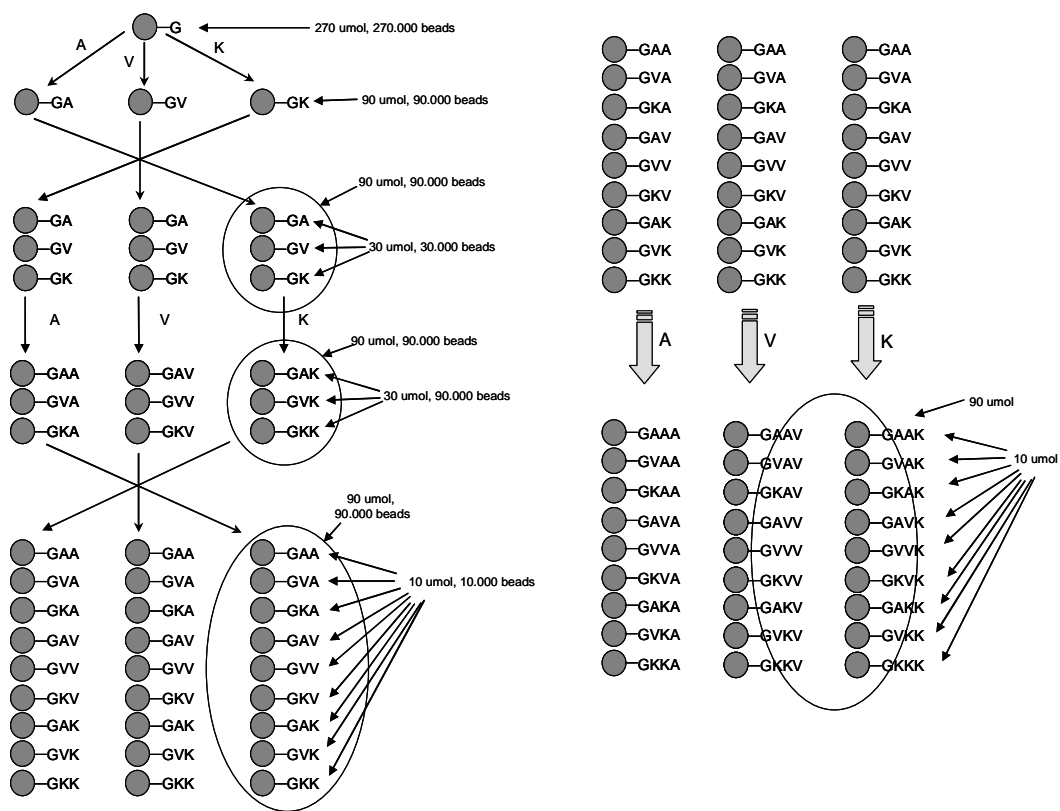


**Fig. A. Mix and Split method for the generation of combinatorial libraries of peptides.** The method is exemplified for the synthesis of tripeptide libraries with 3 different amino acids using a resin batch of 270000 resin beads. By this method, repetitive cycles of resin mixing and re-pooling are performed until the requested length and complexity are reached. The resin beads are distributed in 3 equal aliquots of 90.000 beads, then single residues are coupled (Ala, Val, Lys). After the washing and deprotection steps, the three aliquots are pooled and carefully mixed. By repeating this procedure for N times, a complexity of  $3^N$  is achieved. In this example, after three randomization rounds, three peptide pools, each with 9 different sequences, are generated. In an ideal synthesis, each sequence is present on 10.000 beads, thus accounts for 10 μmoles of the starting 270 μmoles.

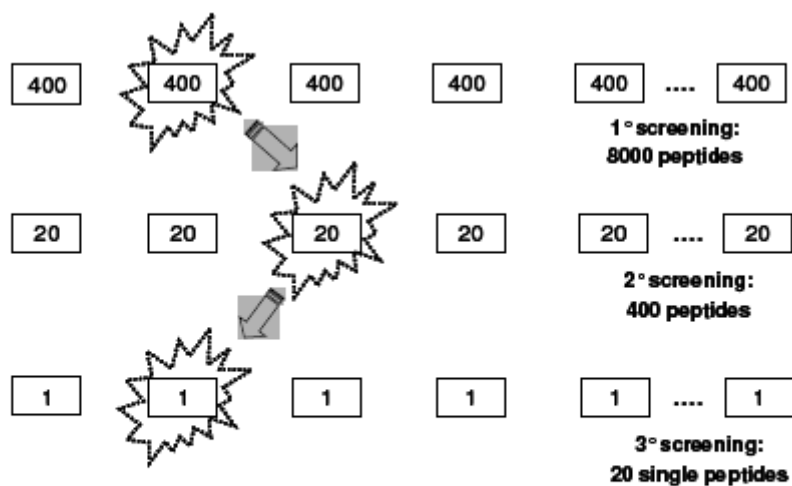
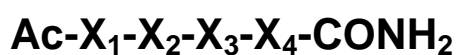


**Fig. B. Schematic representation of the deconvolution of peptide libraries by an iterative screening approach..** The screening of a tripeptide library with 20 different building blocks is exemplified. In the first screening round 8000 compounds arranged in 20 pools of 400 peptides each is submitted to a screening assay, whereby a single 400-components pool is selected. In the second screening round, the selected 400 peptides present in the selected pool, are re-synthesized in a format where 20 sub-pools of 20 molecules each are arranged. A 20-components sub-pool is selected using the same assay, then the 20 isolated compounds are singularly prepared and tested, arriving to the identification of the most active component.

**Table 5: Properties of “Amino acidic Building blocks” used in the library design**

<b>Selected Amino Acid</b>	<b>1-Letter</b>	<b>Side chain</b>	<b>Side chain properties</b>		
<b>Glutamine</b>	Q	-CH <sub>2</sub> CH <sub>2</sub> CONH <sub>2</sub>	polar	neutral	Amide
<b>Serine</b>	S	-CH <sub>2</sub> OH	polar	neutral	Hydrophobic
<b>Arginine</b>	R	-(CH <sub>2</sub> ) <sub>3</sub> NHC(NH)NH <sub>2</sub>	polar	Basic (strongly)	
<b>Alanine</b>	A	-CH <sub>3</sub>	Non polar	neutral	Hydrophobic
<b>Tyrosine</b>	Y	-CH <sub>2</sub> -C <sub>6</sub> H <sub>4</sub> OH	polar	neutral	Aromatic
<b>Proline</b>	P	-CH <sub>2</sub> CH <sub>2</sub> CH <sub>2</sub>	Non polar	neutral	Hydrophobic
<b>Methionine</b>	M	-CH <sub>2</sub> CH <sub>2</sub> SCH <sub>3</sub>	Non polar	neutral	Hydrophobic
<b>Cysteine</b>	C	-CH <sub>2</sub> SH	Non polar	neutral	
<b>Phenylalanine</b>	F	-CH <sub>2</sub> C <sub>6</sub> H <sub>5</sub>	Non polar	neutral	Aromatic
<b>Leucine</b>	L	-CH <sub>2</sub> CH(CH <sub>3</sub> ) <sub>2</sub>	Non polar	Neutral	Aliphatic
<b>Histidine</b>	H	-CH <sub>2</sub> -C <sub>3</sub> H <sub>3</sub> N <sub>2</sub>	polar	Basic (weakly)	Aromatic
<b>Aspartic acid</b>	D	-CH <sub>2</sub> COOH	polar	acidic	

The Fmoc group and the spacer were subsequently removed and replaced by an acetyl group; therefore all active peptides had a general formula as follows:



## **2.7 Binding and competitive Enzyme-Linked Immunosorbent Assay (ELISA)**

### **2.7.1 Biotinylation of Gadd45 $\beta$**

Fractions of Gadd45 $\beta$  (1 mg/ml) were biotinylated using an EZ Link NHS-LC-biotin kit (Pierce), according to the manufacturer's instructions, but with slight modifications. One volume of 2 mg/mL NHS-LC-biotin was added to 20 volumes of protein and incubated on ice for 1 h; the reaction was then stopped by addition of one volume of 50 mM glycine. Biotinylated samples were dialyzed against buffer A (25 mM Tris, 150 mM NaCl 1 mM EDTA, 1 mM DTT, pH 7.5) to remove excess glycine and free biotin, and stored at  $-80\text{ }^{\circ}\text{C}$ . The incorporation of one biotin moieties per molecule of protein was recorded by LC-MS analysis.

### **2.7.2 Gadd45 $\beta$ -MKK7 association and competition ELISA assays**

Association between Gadd45 $\beta$  and MKK7 was investigated by ELISA assays by coating the GST-fused full length kinase for 16 h at  $4\text{ }^{\circ}\text{C}$ , at a concentration of 42 nM in buffer A (25mM Tris pH 7.5, 150mM NaCl, 1mM DTT and 1mM EDTA) into a 96-well microtiter plate (Coating). Some wells were filled with buffer alone and were used as blanks. After incubation for 16 h at  $4\text{ }^{\circ}\text{C}$ , the solutions were removed and the wells filled with 350  $\mu\text{L}$  of a 1% (w/v) solution of NFDM (Non Fat Dry Milk) in PBS (Blocking). The plate was incubated for 1 h at  $37\text{ }^{\circ}\text{C}$  in the dark. After washing with buffer T-PBS (PBS with 0.004% (v/v) Tween), the wells were filled with 100  $\mu\text{L}$  of biotinylated Gadd45 $\beta$  at concentrations ranging between 8.4 nM to 168 nM (Binding). Each data point was performed in triplicate. Following incubation for 1 h in the dark at  $37\text{ }^{\circ}\text{C}$  the solutions were removed and the wells again washed with T-PBS. Then 100  $\mu\text{L}$  of 1:1000 horseradish peroxidase-conjugated streptavidin dissolved in buffer was added to each well and the plate incubated for 1 h at  $37\text{ }^{\circ}\text{C}$  in the dark (Binding Signal amplification). After removal of the enzyme solution and washing, 100  $\mu\text{L}$  of the chromogenic substrate o-phenyldiamine (0.4 mg/mL in 50 mM sodium phosphate-citrate buffer, containing 0.4 mg/mL of urea in hydrogen peroxide) was added and the colour was allowed to develop in the dark for 5 min. The reaction was stopped by adding 50  $\mu\text{L}$  of 2.5M  $\text{H}_2\text{SO}_4$  (Detection). The absorbance at 490 nm was measured in all wells and the values were averaged after subtracting the corresponding blanks. Bound protein was then detected as described above. KD values were estimated as the concentration of protein able to give half of the saturation signal. Binding competition assays were performed by coating GST-MKK7 at 42 nM as described, a concentration of biotinylated Gadd45 $\beta$  of 21 nM (pre-saturation conditions 1:0.5 mol/mol ratio) and using 12 pools of peptides as competitors at a 2:1 competitor/soluble protein ratio (total concentration of competitors 42 nM assuming an average molecular weight of 1000 Da for each peptide). Competition results are reported as  $(B/B_0)\times 100$ , where B means the average

OD from the triplicate data point for a given analyte and  $B_0$  is the average OD determined without competitors (Analysis). Data were all fitted using the GraphPad Software, GraphPad, San Diego, California, USA.

### ***2.7.2 Dose dependent competition assay***

Dose-dependent competition assays were carried out to monitor the efficiency of antagonist selected from combinatorial libraries. For this purpose, 100  $\mu\text{L}$  of 42 nM GST-fused full-length kinase in buffer A was coated on multi-well plates overnight at 4  $^{\circ}\text{C}$ . After blocking with NFDM for 1 h and washing with TPBS, increasing concentrations (from 0.168 nM to 0.105  $\mu\text{M}$ ) of lead compound 1 and 2 and one negative control were pre-incubated with 21nM biotinylated Gadd45 $\beta$  for 30 min before addition to each well. The subsequent steps of the ELISA assays were carried out as described before.

### ***2.7.3 Gadd45 $\beta$ self-association and competition ELISA assays***

An ELISA-like assay was used to monitor Gadd45 $\beta$  dimerization. For this purpose, Gadd45 $\beta$  at concentration of 0.52  $\mu\text{M}$  in buffer A was dispensed into a 96-well microtiter plate. The steps of coating, washing, blocking, signal amplification and detection were performed as previously described. Instead the step of binding was carried out filling the wells with 100  $\mu\text{L}$  of biotinylated Gadd45 $\beta$  at concentrations ranging between 16  $\mu\text{M}$  and 2.1  $\mu\text{M}$ .

A binding curve was obtained and the concentration of biotinylated Gadd45 $\beta$  resulting in a 50% of maximum binding was taken as an estimate of the dissociation constant of self-association.

For the competition experiments, 100  $\mu\text{L}$  aliquots of 0.52  $\mu\text{M}$  His6-Gadd45 $\beta$  were coated on the wells of a microtiter plate and 0.26  $\mu\text{M}$  biotinylated His6-Gadd45 $\beta$  (molar ratio 1:0.5) was used throughout (presaturation condition). Peptides (0.52  $\mu\text{M}$ ) from trypsin digestion or the synthetic peptides corresponding to the protein helices, were used as competitors at a molar ratio of 1:1 to coated unbiotinylated protein. Competitors were pre-incubated with 0.26  $\mu\text{M}$  biotinylated Gadd45 $\beta$  for 30 min at 4  $^{\circ}\text{C}$  before addition to each well. Peptides derived from the trypsin digestion were used at a nominal concentration of 0.52  $\mu\text{M}$ , calculated assuming a 100% trypsin cleavage and a 100% recovery from the HPLC fractionation. GST-MKK7, Gadd45 $\beta$  eH1, eH4, and eH5, and the synthetic peptides MKK7(G132-N156) and Gadd45 $\beta$ (A60-D86), were always used at a concentration of 0.52  $\mu\text{M}$ . ELISA assays were carried out at least in duplicate. Competition results are reported as  $(B/B_0) \times 100$ , where B is the average absorbance from the triplicate data points for a given analyte and  $B_0$  is the average absorbance determined without competitor.

## 2.8 Tissue culture and transfection assays

Human epithelial cells (HEK293) were cultured using Dulbecco's modified Eagle's medium (DMEM) supplemented with 10% fetal calf serum, 100 units/ml penicillin, 100 mg/ml streptomycin, and 1% glutamine. HEK293 cells ( $2.2 \times 10^6$ ) were seeded in 10 cm dishes the day before the transfection in DMEM. They were transfected with 1  $\mu$ g of pEGFP and 25  $\mu$ g of pcDNAFlagMKK7 or 25  $\mu$ g of pcDNAHAGadd45 $\beta$ , using  $\text{Ca}_3(\text{PO}_4)_2$  precipitation technique. Forty-eight hours after the initiation of transfection, the efficiency was determined using a FACScalibur (Becton Dickinson) instrument, with the help of the Cellquest software to detect the variation of GFP fluorescence intensity between untransfected and transfected cells. Subsequent data analyses were obtained using the Flow Jo program.

The co-transfection of two proteins was carried out as previously described, using ever 1  $\mu$ g of pEGFP to monitor the efficiency of transfection and different DNA ratio pcDNAFlagMKK7:pcDNAHAGadd45 $\beta$ .

## 2.9 Cell lysis and western blot analysis

The transfected cells were washed once with PBS, lysed for 30 min at 4°C in buffer B (20 mM HEPES, 350 mM NaCl 20% glycerol 1 mM  $\text{MgCl}_2$ , 0.2 mM EGTA, 1 mM DTT, 1 mM  $\text{Na}_3\text{VO}_4$  and 50 mM NaF), supplemented with 1 mM phenylmethylsulfonylfluoride, 10  $\mu$ M of chymostatin, 2  $\mu$ g/ml of aprotinin, and 2  $\mu$ g/ml of leupeptin with occasional gentle shaking. The lysed cells were collected and centrifuged at 20000xg for 20 min, and cleared lysates were used for further analysis. The protein concentration in the supernatants was determined by the Bradford method. Lysates were fractionated by 15% SDS-PAGE gels under reducing conditions and then electrotransferred to nitrocellulose. The nitrocellulose filters were blocked for 1h at room temperature and then incubated with opportune primary antibody for 90 min. After three washes with TBS/0.1% Tween 20, the blots were incubated for 1h with proper horseradish peroxidase-conjugated (HRP) secondary antibody, washed extensively and developed by enhanced chemiluminescence (ECL, Amersham, Arlington Heights, IL), according to the manufacturer's instructions.

**Table 6: Antibody**

<b>Detected samples</b>	<b>Primary Antibody</b>	<b>Secondary Antibody</b>
<b>Gadd45<math>\beta</math></b>	$\alpha$ Gadd45 $\beta$ 1: 100	$\alpha$ Mouse 1: 2000
<b>Mkk7</b>	MEK-7 (T-19) 1: 2000	$\alpha$ goat 1:2000
<b>HAGadd45<math>\beta</math>/HA MKK7</b>	HA-probe (Y-11) 1: 200	$\alpha$ Rabbit 1:1500
<b>Flag Gadd45<math>\beta</math>/Flag MKK7</b>	$\alpha$ Flag 1: 2000	$\alpha$ Mouse 1:5000
<b>Phospho-SAPK/JNK</b>	$\alpha$ Phospho-SAPK/JNK (Thr183/Tyr185) 1: 200	$\alpha$ Rabbit 1:1500

## **2.10 Activation of MKK7 immunoprecipitation and kinase assays**

Transient transfections of pcDNAFlagMKK7 were performed with the  $\text{Ca}_3(\text{PO}_4)_2$  precipitation technique. After 36h, the cells were serum-starved overnight and treated with TNF $\alpha$  (2000 u/mL) and Pma/ionomycin (100 ng/ml – 1 $\mu$ M), respectively, for 10 min and 30 min at 37 $^\circ$ C. Cell extracts were prepared as previously described. In pull-down experiments, 50  $\mu$ g of Flag-MKK7 cell lysate was incubated with 20  $\mu$ l of anti-FLAG<sup>®</sup> M2 Affinity Gel (SIGMA), for 1h at 4 $^\circ$ C with rotation. The immunoprecipitates were washed three times with lysis buffer without inhibitors and subjected to SDS-PAGE. After immunoprecipitation, the beads were washed 3 times in lysis buffer, and twice in Kinase Buffer (10 mM HEPES, 5 mM MgCl<sub>2</sub>, 1 mM MnCl<sub>2</sub>, 12.5 mM  $\beta$ -glycerophosphate, 2 mM DTT, 4 mM NaF and 0.1 mM Na<sub>3</sub>VO<sub>4</sub>). The MAPK activity was measured at 30 $^\circ$ C for 20 min in 20  $\mu$ l of kinase buffer containing 2  $\mu$ M of recombinant GST-JNK and 0.2 mM ATP or 5  $\mu$ Ci of [ $\gamma$ -<sup>32</sup>P]ATP). The reactions were terminated by addition of Laemmli sample buffer. Proteins were resolved by 10% SDS-PAGE and identified by Western Blotting or autoradiography. The incorporation of [<sup>32</sup>P] phosphate into the GST fusion protein was quantitated by Phosphor Imager analysis.

## **2.11 Binding and Competition Assay by combined Immunoprecipitation, Kinase Assay and Western Blotting**

To monitor MKK7 inactivation by Gadd45 $\beta$  and the ability of peptides antagonists to revert this effect by disrupting the Gadd45 $\beta$ -MKK7 interaction, cell lysate immunoprecipitated Flag-MKK7 (50  $\mu$ g, obtained as previously described, was pre-incubated for 10 min in absence and in presence of synthetic peptides (at different concentration from 1 nM to 1  $\mu$ M). The mixtures were next incubated with 5  $\mu$ M GST-Gadd45 $\beta$  and 2  $\mu$ M GST-JNK (purified from bacterial lysates) and the incorporation of [ $^{32}$ P] phosphate groups into GST-JNK was monitored Phosphor Imager analysis.

## **RESULTS AND DISCUSSION**

### 3.1. Gadd45 $\beta$ cloning, expression and purification

The recombinant construct pGEX6P-GADD45 $\beta$  allowed the expression of the protein as a GST-fusion product containing a highly specific cleavage site for PreScission Protease upstream of the Gadd45 $\beta$  protein. The applied overexpression system was quite efficient, producing more than 6 mg of highly purified protein from 1 L of induced culture under optimized conditions, as described in materials and methods. The isolated protein was 98% pure after a purification step on anionic exchange column and was characterized by SDS-PAGE and LC-MS to assess purity and MW. The MW was in very good agreement with that calculated  $18096.6 \pm 1.0/18096$  (inclusive of the GPLGS linker left from proteolytic cleavage). The investigation of Gadd45 $\beta$  cysteines redox state was carried out through extensively alkylation of cysteine thiols with 4-VP and subsequent analysis by LC-MS to determine the exact MW. The Gadd45 $\beta$  mass spectrum after 4-VP alkylation shows that the protein undergoes an increase of molecular weight of 630 Da, corresponding to the incorporation of six 4VP-moieties, confirming the absence of any disulfide bridge between the six cysteines. SDS analyses of Gadd45 $\beta$  purified fractions and LC-MS characterization before and after alkylation are shown in the following panel A.

Human Gadd45 $\beta$  was expressed also as a recombinant protein with an N-terminal His6 tag using the vector pET28aGADD45 $\beta$ .

The expression conditions were optimized obtaining more than 7 mg of pure protein from 1 L of bacterial culture. The protein after two purification steps by affinity and anionic change chromatography was about 95% pure. Furthermore, this protein was efficiently derivatized with biotin as described in the Methods section. Protein derivatization was assessed by mass spectrometry showing that about 90% of the protein harboured one biotin molecule, while the remaining appeared underivatized. The experimental MW of 19196.5 amu as determined by LC-MS was consistent with that expected on the basis of the sequence and one biotin molecule (19196.52 amu). His6-Gadd45 $\beta$  was used in ELISA assays to identify regions involved in auto-association. SDS-PAGE analysis of the recombinant protein and the successive LC-MS characterization are reported in the panel B.

## Panel A: Expression and LC/MS characterization of hGadd45 $\beta$

Gadd45 $\beta$  was cloned in the pGex6P-1 expression vector allowing the expression of the protein as GST-fusion product containing a highly specific cleavage site for PreScission Protease upstream of Gadd protein. The purification was achieved on a Glutathione Sepharose 4B and on-column cleavage was carried out at 6 °C for 4h (Fig. 1A). The final purification step was realized on an anionic exchange column (Fig. 2A). In order to investigate the presence of reduced cysteines, was carried out an extensive alkylation of the protein which was subsequently analyzed by LC-MS (Fig 3A and 4A).

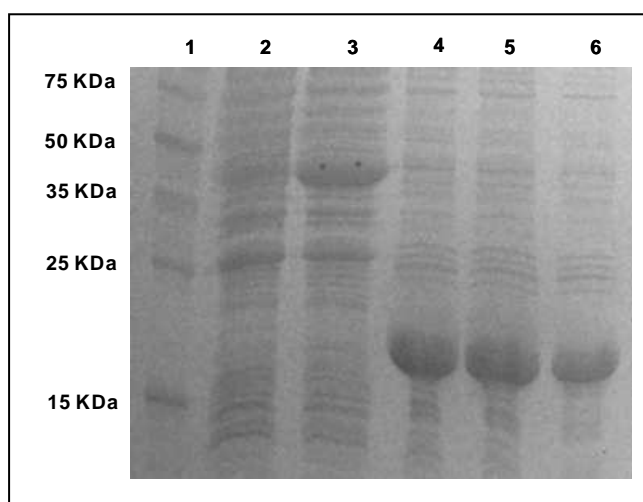


**Fig. 1A:** 15% SDS-PAGE analysis of the recombinant protein; Lane 1: Perfect Protein Marker, 15-150 kDa; Lane 2: clarified bacterial lysate of BL21(DE3)TrxB transfected with pGEX6P-1/GADD45 $\beta$  vector; Lane 3: flow through; Lane 4-5-6: eluates containing the cleaved protein.

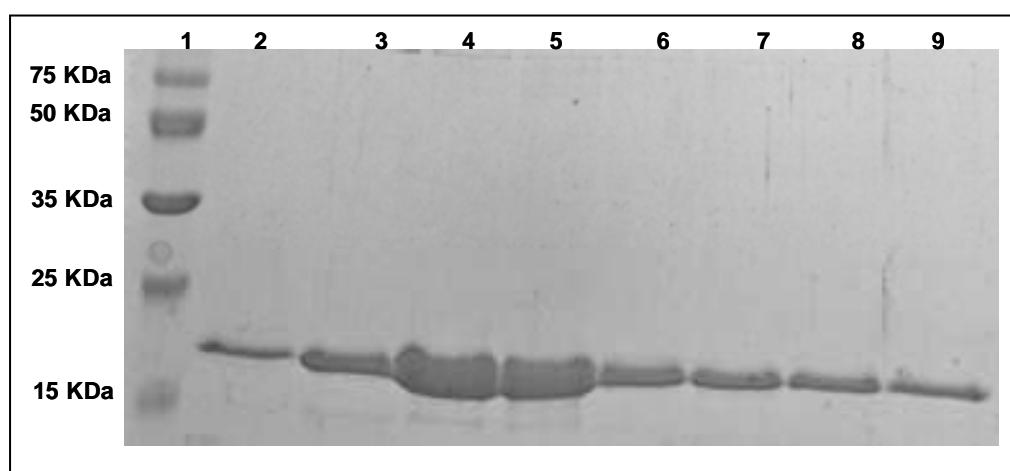


**Fig. 2A:** 15% SDS-PAGE of purified fractions; Lane 1: Perfect Protein Marker, 15-150 kDa; Lane 2: pool of fractions purified from Glutathione Sepharose matrix; Lane 3: flow through; Lane 4-9: eluates at 340 mM NaCl containing Gadd45 $\beta$  with a purity of 98%.

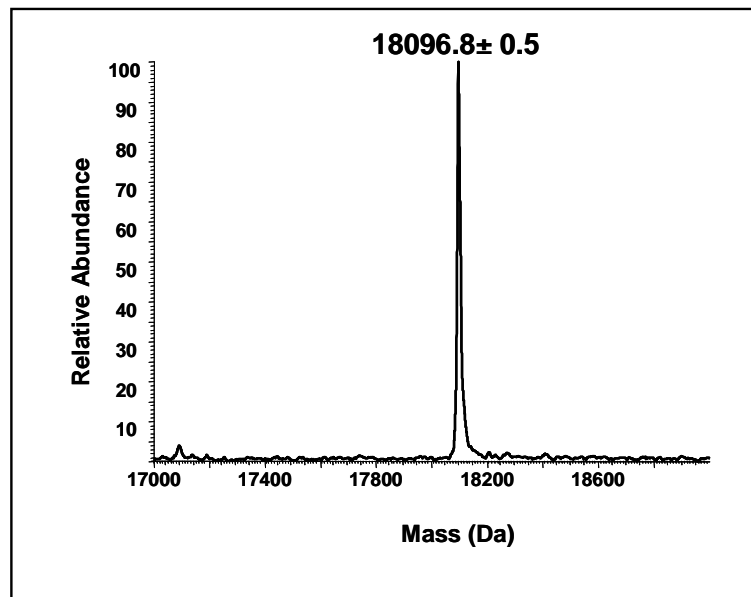


**Fig. 3A:** Deconvoluted mass spectrum of underivatized Gadd45 $\beta$  showing a molecular weight of  $18096.6 \pm 0.5$  Da, in very good agreement with the theoretical value of 18098.3 Da, assuming that all cysteines were in the reduced state.

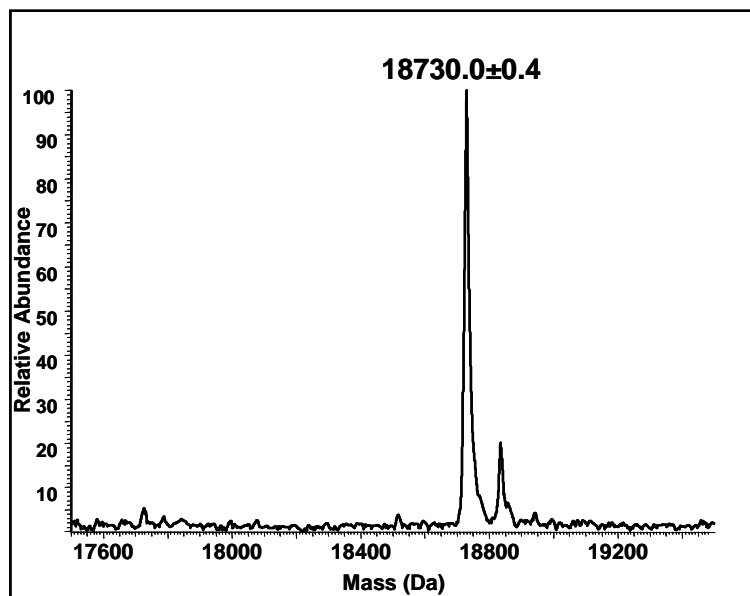


**Fig. 4A:** Deconvoluted mass spectrum of Gadd45 $\beta$  after 4-VP alkylation. The spectrum shows that the protein undergoes an increase of molecular weight of 630 Da, corresponding to the incorporation of six 4VP-moieties, confirming the reduced state of all the six cysteines.

## PANEL B: Expression and derivatization of His6Gadd45 $\beta$

Human Gadd45 $\beta$  was expressed as a recombinant protein with an N-terminal His6 using the vector pET28GADD45 $\beta$ . Purification was achieved on His Trap Hp, 1mL prepacked with precharged Ni-Sepharose. The bound protein was eluted using an imidazole gradient from 10 to 500 mM (Fig. 1B). The protein was efficiently derivatized with biotin (Fig. 2B) and used in Elisa assays

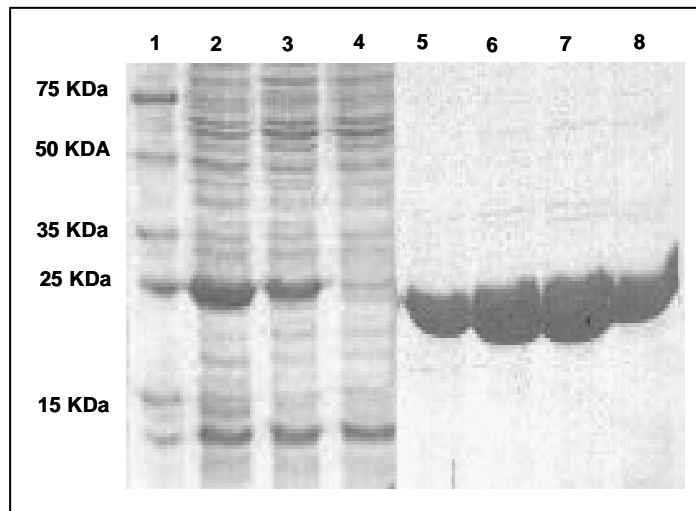


**Fig. 1B:** 15% SDS-PAGE analysis of the recombinant protein; Lane 1: Perfect Protein Marker, 15-150 kDa; Lane 2: total bacterial lysate of BL21(DE3) transfected with pET28-GADD45 $\beta$  vector; Lane 3: clarified bacterial lysate of BL21(DE3) transfected with pET28-GADD45 $\beta$  vector; Lane 4: flow through; Lane 5-8: Eluates containing the purified protein.

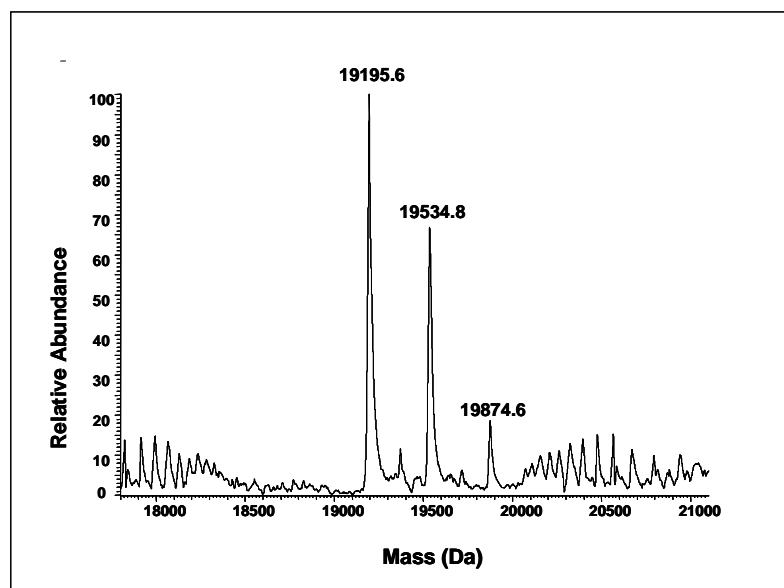


**Fig. 2B:** Assessment by mass spectrometry of Gadd45 $\beta$  derivatized with biotin. About 90% of the protein harboured one biotin molecule, while the remaining appeared underivatized.

### **3.2. MKK7 cloning, expression and purification**

MKK7 was produced in bacteria as a soluble GST-MKK7 fusion product. About 7 mg/L of the fusion protein were obtained in typical fermentations. The protein was initially purified by standard GSTrap and the GST was removed by on-column PreScission protease cleavage. The material recovered was further purified by gel filtration chromatography, obtaining a product more than 95% pure. MKK7 characterization by SDS-PAGE, circular dichroism and exclusion chromatography are reported in panel C. The folding of MKK7 was assessed by CD analysis observing, as expected on the basis of its high similarity with other kinases a spectrum with a mixed  $\alpha$ - $\beta$  content. Gel filtration analysis confirmed the oligomeric state of the protein. Indeed, MKK7 eluted on the gel filtration column as a dimer (apparent MW of about 90 kDa), in agreement with previous reports on other similar kinases (75) Importantly, also the fusion protein GST-MKK7, used in several assays in this study, eluted from the gel filtration column as a dimer.

## Panel C : Expression and characterization of hMKK7

Human MKK7 kinase was expressed as a recombinant protein with an N-terminal GST using the vector pGex6p1-MKK7 (Fig 1C). The fusion protein has been removed by PreScission protease cleavage (Fig 2C). The preliminary structural characterization showed that the recombinant human MKK7 is properly folded exhibiting a prevailing alpha-helical conformation (Fig. 3C). The protein appears to be dimeric upon gel filtration analysis (Fig. 4C).

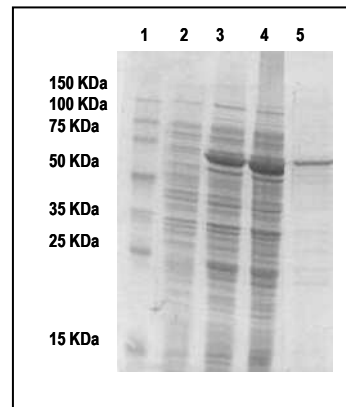


**Fig. 1C:** 12% SDS-PAGE analysis of purified GST-MKK7. Lane 1: protein marker 15-150KDa; Lane 2: pGex6P1-MKK7 transformed into BL21 (DE3) trxB but not induced; Lane 3: total bacterial lysate after induction; Lane 4: clarified bacterial lysate; Lane 5: eluate containing the protein GST-MKK7.

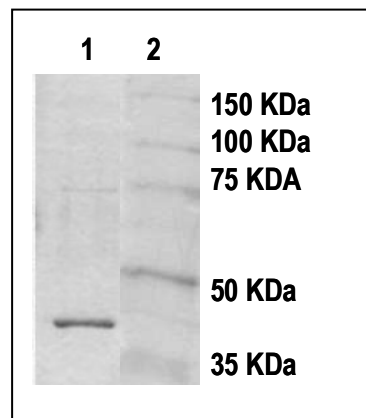


**Fig. 2C:** 12% SDS-PAGE analysis of purified cleaved MKK7. Lane 1: fraction containing the cleaved protein; Lane 2: protein marker 15-150KDa.

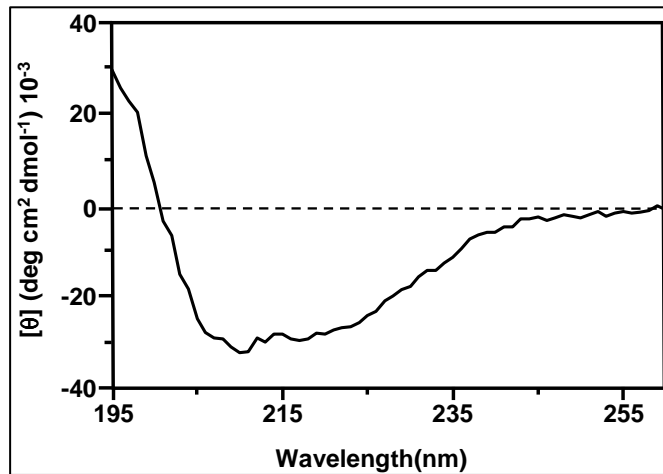


**Fig. 3C:** CD spectrum in the near UV of MKK7 showing that the protein adopts a prevailing alpha helical conformation, as expected on the basis of a very high sequence conservation with other kinases whose structures have been solved.

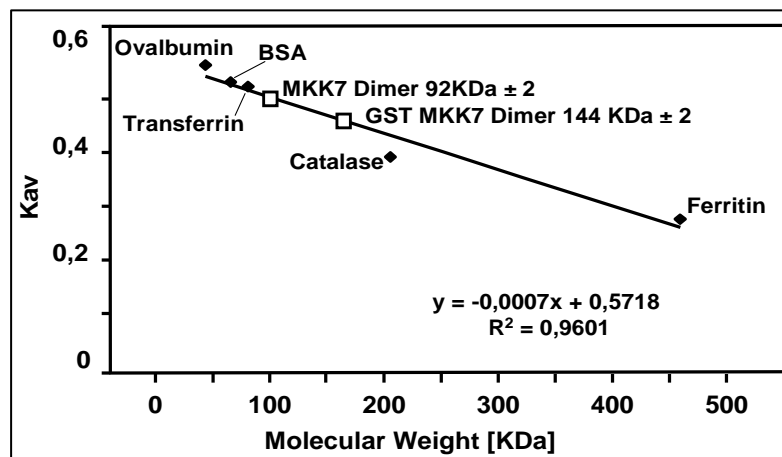


**Fig. 4C:** Calibration curve used to determine the apparent MW of recombinant MKK7 protein by gel filtration analysis. Ovalbumin, 44 kDa; BSA, 66 kDa; Transferrin, 81 kDa; Catalase, 206 kDa; Ferritin, 460 kDa. The protein appears to be dimeric. All determinations were carried out under the same conditions and repeated at least twice.

### **3.3 Investigation of Gadd45 $\beta$ oligomerization by size exclusion chromatography analysis**

Since previous studies reported on the capacity of Gadd45 proteins to oligomerize (64), this issue was investigated by carrying out a gel filtration analysis in the presence and/or absence of DTT and by native electrophoresis experiments. Gel filtration analysis of protein aliquots at the concentration of 5.0  $\mu$ M, showed that, in absence of DTT, two peaks were eluted at column volumes corresponding to a dimeric and tetrameric protein, that is 36 kDa and 72 kDa, respectively (panel D, Fig. 1D and 3D). Conversely, under reducing conditions, the tetramer peak disappeared (Fig. 2D), indicating that it was held together by disulfide bridges, whereas the dimer was associated through strong non-covalent interactions. The presence of protein dimer or oligomer was also investigated by native gels, observing in this case the dimer and the monomer (Fig. 4D). According to these data, Gadd45 $\beta$  seemingly exists in solution prevalently as a dimeric protein, in partial equilibrium – under certain conditions (the non-denaturing gel) – with the monomer. Indeed, no higher order oligomers have been detected by either techniques.

## Panel D: The assessment of Gadd45 $\beta$ oligomeric state by hydrodynamic methods

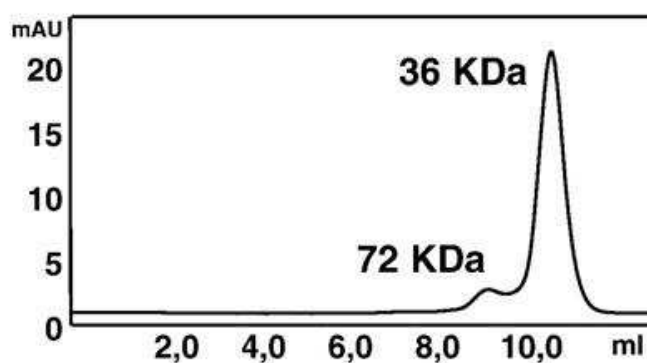


**Fig. 1D:** Gel filtration analysis on a Superdex 75 10/30 of Gadd45 $\beta$  protein under non reducing conditions. Two peaks at elution volumes compatible with dimeric and tetrameric forms are detected.

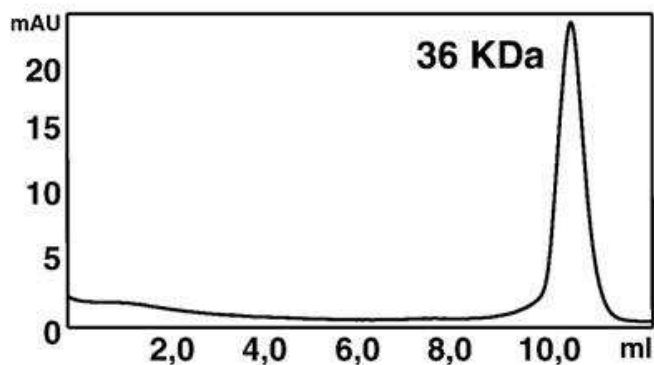


**Fig. 2D:** Analysis by size exclusion chromatography carried out after addition of 1 mM DTT in the running buffer. The peak at lower elution volumes disappeared, suggesting that it is due to covalent disulfide bridges.

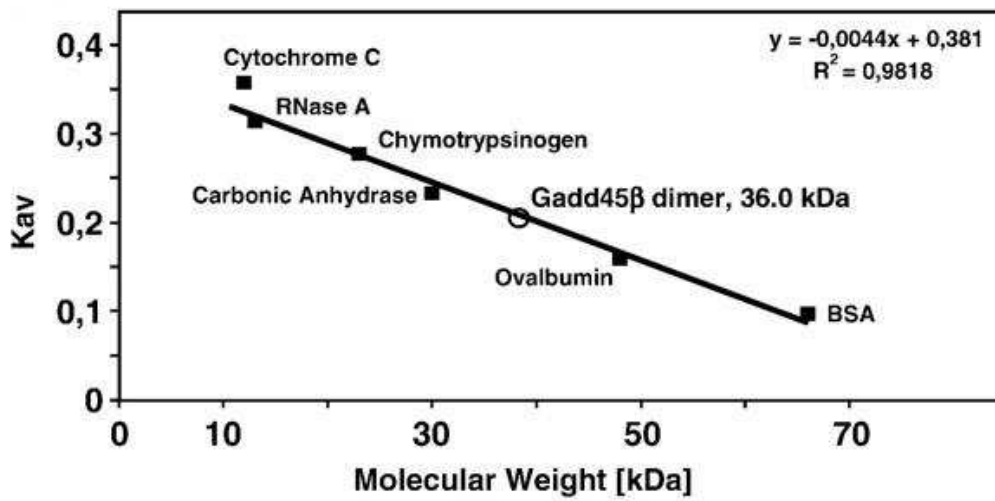


**Fig. 3D:** Calibration graph of partition coefficient ( $K_{av}$ ) versus molecular mass of several protein standards: Cytochrome C, 12.4 kDa; RNase A, 14.7 kDa; Chymotrypsinogen, 25.0 kDa; Carbonic anhydrase, 29.0 kDa; Ovalbumin, 44.0 kDa; BSA, 66.0 kDa. All determinations have been performed at least twice.

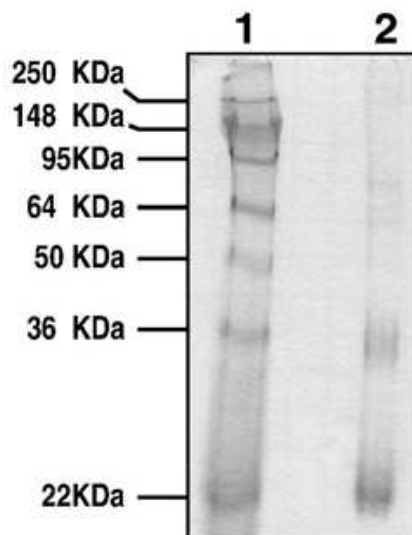


**Fig. 4D:** Non-denaturing polyacrylamide gel analysis of Gadd45β. Lane 1: Sea Blue marker (250-22 KDa); Lane 2: Gadd45β at a concentration of 1.8 mg/mL (100 μM).

### 3.4 Spectroscopic characterization of Gadd45 $\beta$

The far-UV CD spectrum of Gadd45 $\beta$  ( $11 \times 10^{-6}$  M) in aqueous solution showed two negative bands at 209 and 222 nm and a positive band at 195 nm indicative of a high content of  $\alpha$ -helical conformations (See panel E, Fig. 1), as previously reported (61). Importantly, also the His6-Gadd45 $\beta$ , utilized in different assays exhibited a very similar CD spectrum (not shown). The occurrence of oligomers was also investigated by this technique by comparative analysis of protein solutions at different concentrations. No differences were detectable between CD curves recorded on protein solutions at concentrations ranging between  $5.5 \times 10^{-5}$  M and  $5.5 \times 10^{-6}$  M (data not shown) suggesting that dilution, at least in the range of the explored concentrations, did not affect the protein global folding nor the quaternary structure. Therefore, no indications could be obtained on the actual monomer-dimer status of the protein by this experiment. A CD analysis of the dependence on denaturant concentration was also performed to further assess the protein structure stability or the capacity to eventually dissociate into monomers. Chemical denaturation data (Fig. 2E and 3E) showed that Gadd45 $\beta$  unfolds cooperatively at about 2.0 M GdnHCl and 3.0 M urea. This may indicate that electrostatic interactions, which are more efficiently weakened by GdnHCl than by urea (74), play an important role in stabilization of Gadd45 $\beta$ .

Upon denaturant removal, the protein secondary structure was recovered (Fig. 1E), suggesting that denaturation, as well as the eventual dimer dissociation (assuming it occurs at high denaturant concentration), is a reversible event. Also thermal denaturation experiments were carried out to confirm these observations; a single transition was observed at about 46.5  $^{\circ}$ C, but, most importantly, after slow cooling back to 20  $^{\circ}$ C, the protein could not recover the original structure because of disulfide cross-linking. The melting temperature is quite low in comparison to those of other globular proteins indicating that Gadd45 $\beta$  is not a thermodynamically stable protein, according to the predicted structure that exhibits large and flexible loops (67)

## Panel E: Circular dichroism characterization of the recombinant Gadd45 $\beta$

CD spectra of the recombinant protein before and after denaturation with guanidinium and urea are reported in Fig. 1E. The protein appeared to properly refold after the chemical treatment. Spectra at 7.5 M urea and guanidinium (dotted lines) are also reported. The curves of chemical denaturation are representative of at least two independent experiments. CD curves were obtained by averaging at least three consecutive acquisitions. In Fig. 2E the chemical denaturation by GdnHCl is reported. The protein unfolds in a cooperative way at guanidinium concentrations higher than about 2.5 M (See also Fig. 1E). In Fig 3E the chemical denaturation by urea is also reported. In this case the protein unfolds cooperatively at concentrations higher than about 4.0 M.

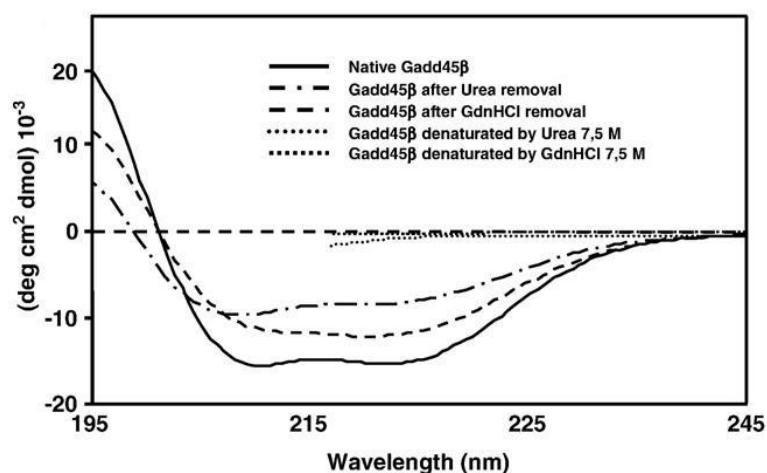


Fig. 1E

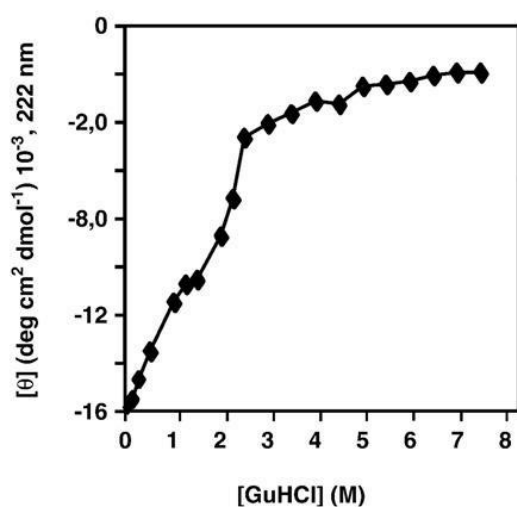


Fig. 2E

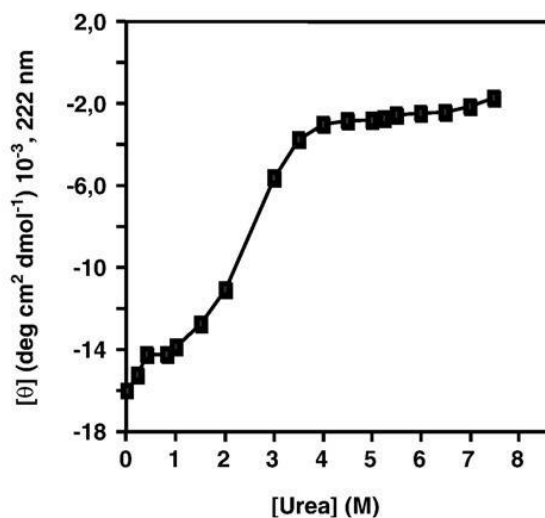


Fig. 3E

## **3.5 Identification of regions of Gadd45 $\beta$ involved in auto-association**

### ***3.5.1 The rationale of the strategy***

Identifying interaction sites between proteins requires powerful techniques and methodologies such X-Ray diffraction and high field NMR, for which large amounts of highly pure proteins are needed. Secondary structure motifs and small protein domains can be used as models isolated from the protein context and investigated by several techniques to gain structural insights on the protein global structure and to modulate interactions with external partners. While awful progresses have been made in this field by using *de novo* designed synthetic peptides, the idea of using protein fragments obtained by chemical or enzymatic methods have been only rarely pursued. Chemical methods, though equally selective in cleaving proteins on selected residues, are always carried out under harsh conditions that invariably lead to protein unfolding. On the other hand, enzymatic proteolysis of folded proteins under mild conditions, acting preferentially on exposed and less structured sites, can help to isolate shorter polypeptides with partially preserved secondary and tertiary structures. These structurally selected protein blocks could work as “reminders” of the original structure and, as such, can be usefully utilized as probes for structural studies and as tools for the identification of protein-protein interaction contacts. We have optimized this process and developed a novel method to rapidly and cheaply obtain useful insights on protein-protein interaction sites that can be successively utilized to support or refine available structural data by classical techniques. The methods is based on the use of ELISA assays, whereby protein binding is firstly optimized in order to determine affinity constants and the pre-saturation concentrations needed to carry out binding competition assays. Proteins are subsequently degraded by trypsin, and the resulting peptide fragments are utilized as competitors to select those able to disrupt the binding. Following this approach regions of Gadd45 $\beta$  implicated in self-association were identified and characterized.

### 3.5.2 Characterization of regions of Gadd45 $\beta$ involved in auto-association

Firstly an ELISA assay to monitor Gadd45 $\beta$  self-association was carried out by coating the His6-protein on the surface of microtiter wells. Protein association was followed by adding increasing amounts of biotinylated His6-Gadd45 $\beta$  and detecting the bound protein by using HRP-STRV. As shown in Panel F (Fig. 1F), the protein efficiently associated in a dose-dependent way, reaching signal saturation at a nearly 1:1 (mol/mol) ratio, as expected by a dimeric complex. The concentration of His6-Gadd45 $\beta$  resulting in a 50% of maximum binding was around 100 nM and it was taken as an estimation of the dissociation constant of self-association.

Subsequently, an extensive digestion of a protein aliquot was carried out with trypsin which resulted in complete digestion and formation of fragments of suitable length to ensure a complete coverage of the protein primary structure (See panel F; Table 1). Upon RP-HPLC fractionation (13 fractions), Gadd45 $\beta$  peptides, identified by MW and MS/MS sequencing, were essentially distributed along 7 main fractions, since fractions 1-5 contained no material and fraction 11 contained only very small amounts (less than 4%) of fragment L46-R91. All identified trypsin fragments are reported in Table 1 along with a correspondence with the predicted Gadd45 $\beta$  secondary structure (67). Fractions 6, 7, 8, 9, 10, 12 and 13 contained relevant amounts of the protein fragments. Notably, fraction 6 only contained the C-terminal G147-R160 peptide (unstructured); fraction 7 contained, in a 1:1 ratio, fragments L36-K45 (Part of  $\beta$ 1 and part of  $\alpha$ 2) and L98-R115 (Part of  $\alpha$ 4; most of loop 2); fraction 8 contained (in a 85:15 ratio), a major fraction of fragments S132-R146 (87%, the central region of  $\alpha$ 5, hereafter H5 short) and the peptide D116-K131 ( $\beta$ 4); fraction 9 contained, in a 75:25 ratio, the N-terminal polyhistidine tag and a minor fraction of the peptide S132-R146 ( $\alpha$ 5); fraction 10 contained only the fragment M16-R32 (92%, the remaining being distributed along the contiguous fractions), corresponding to most of helix 1; fraction 12 and 13 contained the fragment L46-R91, corresponding to part of  $\alpha$ 2,  $\beta$ 2, loop1,  $\alpha$ 3, and part of  $\beta$ 3. Finally, to identify the Gadd45 $\beta$  regions involved in protein dimerization, binding competition assays were carried out using peptide fragments. The assays were performed using an invariable 1:0.5 (mol/mol) ratio of coated/soluble His6-Gadd45 $\beta$  and a 2:1 (mol/mol) ratio of peptide competitor/soluble protein. The results are summarized in the panel F, Fig. 1F where a plot of representative data is reported. Gadd45 $\beta$  trypsin fractions from 1 to 5 and fraction 11 were not utilized. Fractions 6, 7, 12 and 13 which contained consistent amounts of protein fragments (see Table 1), but they were essentially ineffective. In contrast, fractions 8 to 10 interfered with the association. In particular, fraction 8 exhibited a nearly 30% binding reduction, fraction 10, which virtually contained only fragment M16-R32 (see Table 1) corresponding to most residues of helix 1, decreased protein association to about 50%, whereas fraction 9, containing most residues of the tag and a minor part of fragment S132-R146, disrupted Gadd45 $\beta$  self-association by 25%. Interestingly, the synthetic peptides Gadd45 $\beta$  (A60-D86) and MKK7 (G132-N156), identified as forming the binding interface between Gadd45 $\beta$  and MKK7 (47;67) appeared totally ineffective in this assay. To further refine

the ELISA data, those fragments unable to disrupt Gadd45 $\beta$ -Gadd45 $\beta$  interaction were not considered; furthermore, on examination of the predicted Gadd45 $\beta$  3D model (panel F, Fig. 3F), it was decided to not further investigate the fragment D116-K131, present in fraction 8 at 15%, since it corresponds to the fourth  $\beta$ -strand which should be buried within the protein core and therefore virtually inaccessible to external interactions (panel F, Fig. 3F). The regions M16-R32 and S132-R146 corresponding to the regions within the putative H1 and H5, respectively have been successively investigate. Examining the protein model, (panel F, Fig. 3F) the peptides were opportunely designed by adding N- and C-terminal amino acids in order to complete the helices, hence the corresponding synthetic peptides, A12-R35 (hereafter extended Helix 1, eH1) and A129-N148 (hereafter extended Helix 5, eH5) were prepared by chemical synthesis and purified to homogeneity by RP-HPLC. The peptide R91-E104, corresponding to the extended predicted eH4, was also similarly prepared and utilized as a negative control. These peptides were then tested in the Gadd45 $\beta$ -Gadd45 $\beta$  competition assay, using the same protein-protein and protein-competitors ratios as described previously. As shown in the same panel F, Fig. 2F, eH1 and eH5 blocked the Gadd45 $\beta$  self association by 82% and 78%, respectively, supporting the hypothesis that these regions are strongly involved in the interaction. On the contrary, peptide R91-E104 (eH4), lying in the model in the close proximity of H1, as well as peptides Gadd45 $\beta$ (A60-D86) and MKK7(G132-N156) and the full length kinase did not interfere with the protein homodimerization. A dose-dependent competition assay carried out with eH1, eH5, the short H5, eH4 and full length MKK7, further confirmed the properties of H1 and H5 and the inefficacy of H4 to abrogate dimerization (Panel F, Fig. 4F). As expected, the full length kinase (fused to GST) was unable to block the Gadd45 $\beta$  self-association even at higher concentrations. Remarkably, the IC<sub>50</sub> for these competitors were 100 nM for H1, 180 nM for the extended Helix 5 and only 600 nM for the short H5, indicating that the full H5 was more than 3 times efficient in disrupting the protein self-association. These results might account for the relatively weak inhibition exhibited by fractions 8 (30%) and 9 (25%) which only contained the shorter variant of the H5. The combination of the method of limited enzymatic proteolysis and LC-MS characterization permitted to identify the regions of Gadd45 $\beta$  involved in the self association corresponding to the predicted H1 and H5 of protein. The results have been validated by model building which shows how the dimerization region can form a four-helix bundle (see Fig.5F). The contiguous disposition of H1 and H5 in one monomer creates a large hydrophilic surface interacting in an anti-parallel fashion with the corresponding helix of the other monomer. In particular the residues Gln13 Thr14 and Glu21 on H1 and Glu140, Tyr137, Glu133 and His 129 on H5 are involved in a network of intra-molecular polar interaction which stabilizes the structure of the complex. The 3D model still supports the view that Gadd45 $\beta$  is unable to form higher order complexes. In fact the absence of an alternative and independent site involved in the auto association does not permit an oligomerization. The predicted helix H4, being parallel to H1, virtually extends the interaction surface towards the protein Loop 2 but does not contribute to protein self-association. On the contrary it is reportedly involved in the binding with MKK7 (47;61).

## Panel F: Detection of Gadd45 $\beta$ regions implicated in self-association

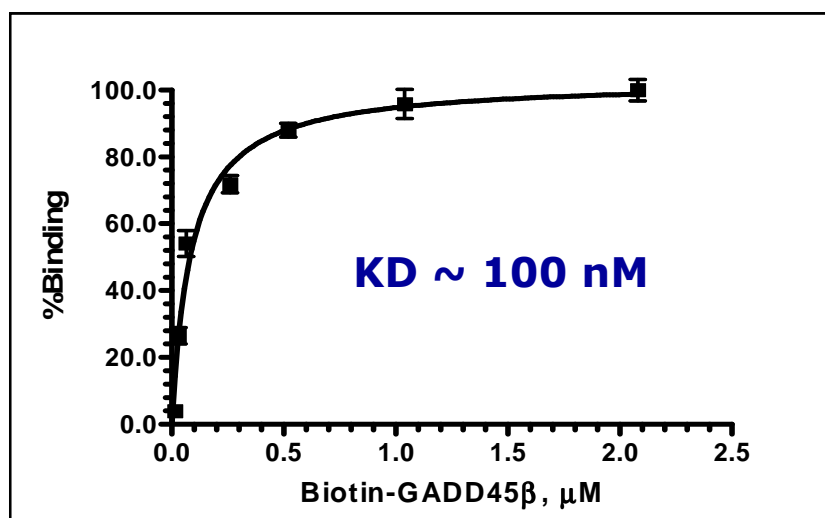


**Fig. 1F:** Dose-dependent binding of biotinylated Gadd45 $\beta$  to the plate-adsorbed protein: Gadd45 $\beta$  self associates with an estimated  $K_D$  of about 100 nM, assumed as the concentration of Gadd45 $\beta$  resulting in 50% maximum binding. Notably, the signal reaches saturation at a 1:1 protein ratio, suggesting the formation of dimers only.

Fraction	Gadd45 $\beta$ tryptic peptides	Relative distribution of fragments within fractions (%)	Relative composition of the fraction (%)	Predicted secondary structure*
6	G147-R160	98	100	Unstructured
7	L36-K45 L98-R115	98 99	50 50	Part of $\beta$ 1, part of $\alpha$ 2 Part of $\alpha$ 4; most of loop 2
8	S132-R146 D116-K131	87 99	85 15	$\alpha$ 5 $\beta$ 4
9	-13-15 S132-R146	100 5	75 25	Tag $\alpha$ 5
10	M16-R32	92	95	$\alpha$ 1
12	L46-R91	10	100	Part $\alpha$ 2, $\beta$ 2, loop1, $\alpha$ 3, part $\beta$ 3
13	L46-R91	87	100	Part $\alpha$ 2, $\beta$ 2, loop1, $\alpha$ 3, part $\beta$ 3

**Table 1:** Tryptic Gadd45 $\beta$  peptidic fragments have been identified by LC-MS/MS analysis. Fragments less than 5% were not considered. Relative distributions of fragments in column 3 were calculated by comparing area integration of extracted ion peaks from a given fragment taken from the different fractions. The relative composition within each fraction was derived by comparing area integrations of extracted ion peaks of all the fraction components. \*As reported in reference 1.

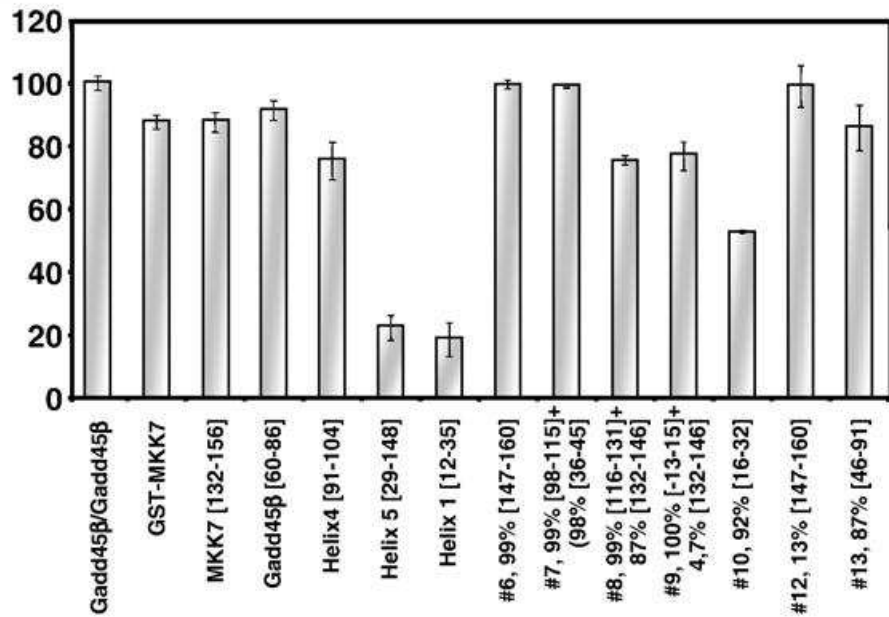


**Fig. 2F:** Competition assay of the Gadd45 $\beta$  self-association by the trypsin-generated protein fragments and by synthetic peptides designed to reproduce helices as predicted in the protein model (67).

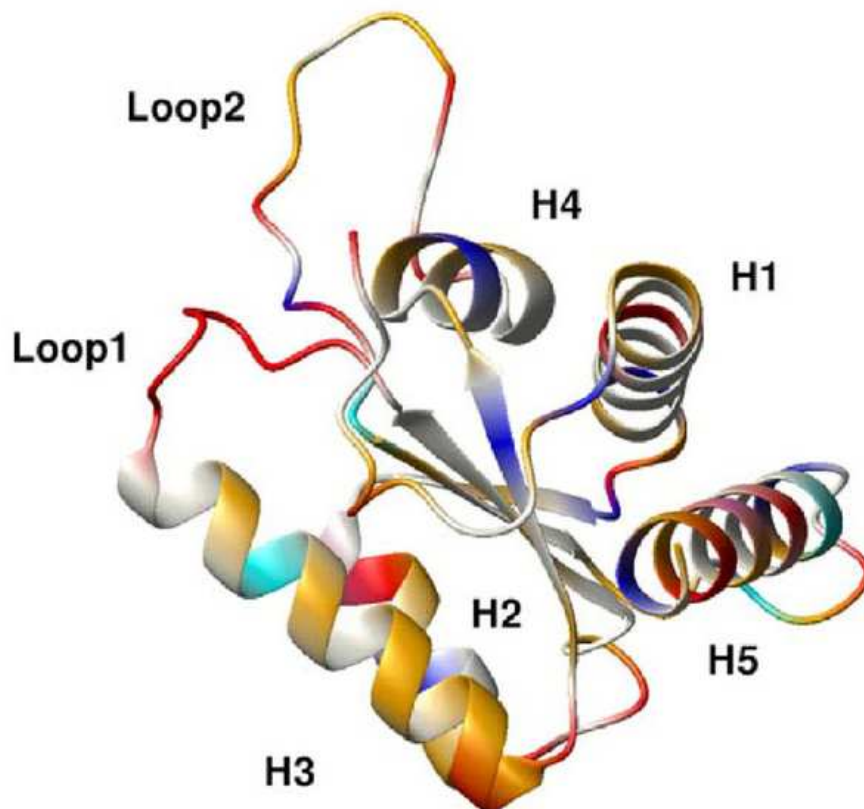


**Fig. 3F:** A ribbon representation of Gadd45 $\beta$  three-dimensional model, coloured by residue type according to the following scheme: hydrophobic residues, white; polar residues, yellow; acidic residues, red; basic residues, blue; histidine residues, cyan; tyrosine residues, in pink (67).

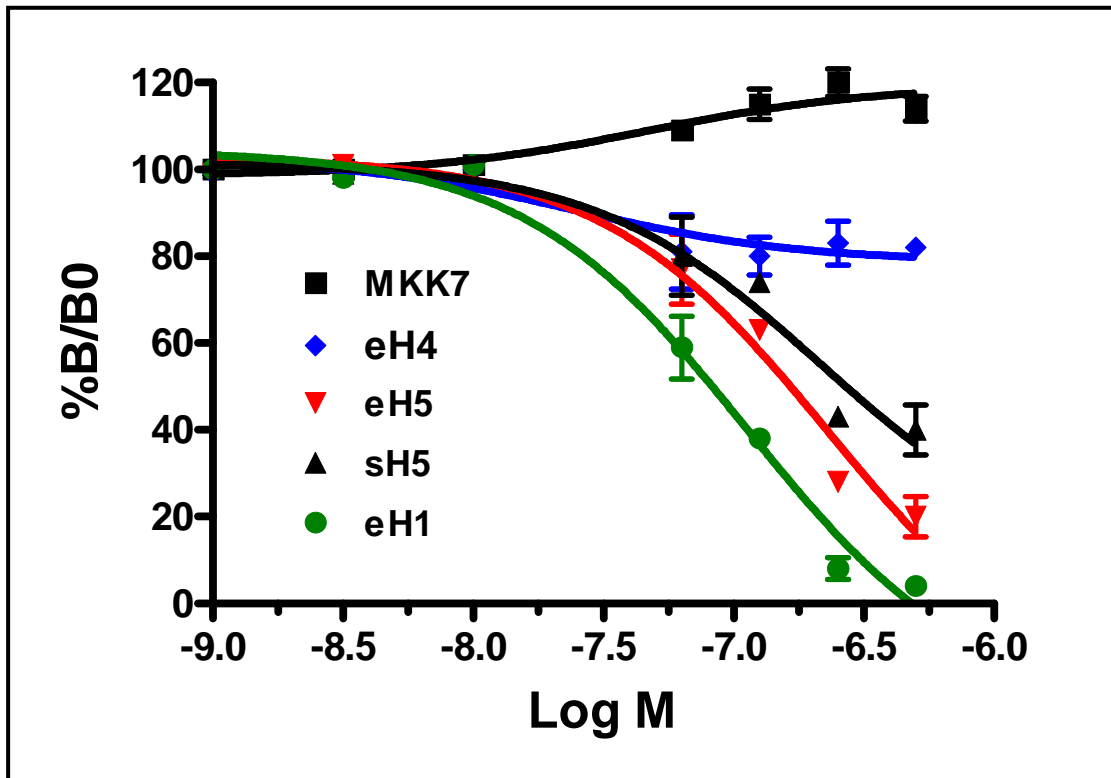


**Fig. 4F:** Dose-dependent inhibition of Gadd45 $\beta$  self-association by GST-MKK7 full length, eHelix 4 (residues 91-104), eHelix 5 (residues 129-148), eHelix 1 (residues 12-35) and the Helix 5 short (residues 132-146). While the kinase and the eHelix 4 are not able to block the Gadd45 $\beta$  self-association, peptides corresponding to eHelix 1 and eHelix 5, potentially reduce the association. The Helix 5 short, derived by trypsin cleavage, is less effective than the entire eHelix 5. Data are representative of at least 3 independent experiments.

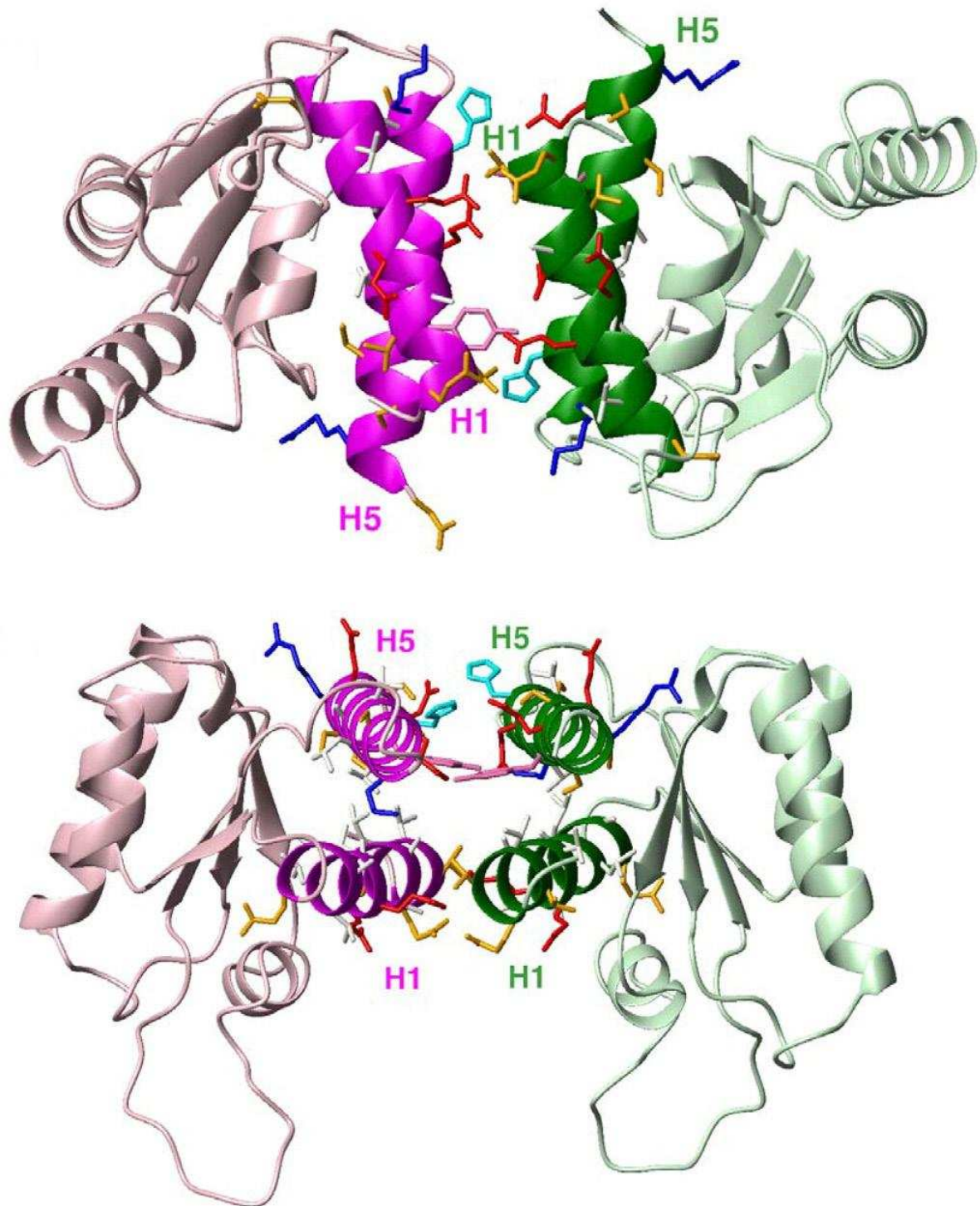


**Fig. 5F:** Two orthogonal views of Gadd45 $\beta$  homo-dimer three-dimensional model in ribbon representation, rotated around the horizontal axis of the figure. One monomer is colored in pink, the other in pale green. Helices H1 and H5 of each monomer are colored in magenta and dark green, respectively. Residues lying on these helices are shown in stick representation and colored according to the following scheme: hydrophobic residues in white, acidic residues in red, basic residues in blue, histidine in cyan and tyrosine in magenta.

### **3.5.4 Gadd45 $\beta$ eHelices characterization by CD**

The synthetic peptides reproducing eH1, eH5, the short H5 and the eH4 were analyzed by CD. The analyses were carried out in both phosphate buffer and in the presence of 20% TFE to measure the relative propensity of peptides to adopt  $\alpha$ -helical conformations. As reported in the Panel G, whereas eHelices 1, 4 and 5 adopted a partially folded structure in buffer and readily folded into  $\alpha$ -helices upon TFE addition, the short H5 remained in the unfolded state even after addition of the structuring solvent, suggesting an intrinsic incapacity to form organized structures. Thus, increasing the length at the N- and C-termini of the putative H5 provided a 5-fold increase in potency that can be partially ascribed to the lack of any structure of this peptide.

## Panel G: Spectroscopic characterization of Gadd45 $\beta$ helices

CD spectra of synthetic peptides eHelix 1, eHelix 4, eHelix 5, Helix 5 short in neutral buffers and in the presence of 20% TFE are reported in Fig. 1G, 2G, 3G and 4G, respectively. As shown, the complete predicted helices have a good propensity to adopt an  $\alpha$ -helical conformation, whereas the short Helix 5 persists in a random conformation even after addition of the structuring agent. This different property is likely contributing to the reduced peptide capacity to disrupt the MKK7-Gadd45 $\beta$  interaction. CD curves have been obtained by averaging at least three consecutive acquisitions.

Fig. 1G

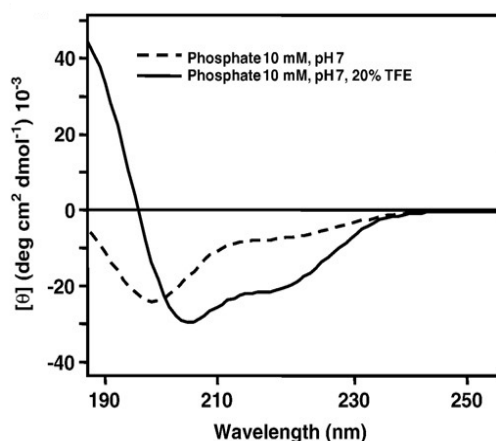


Fig. 2G

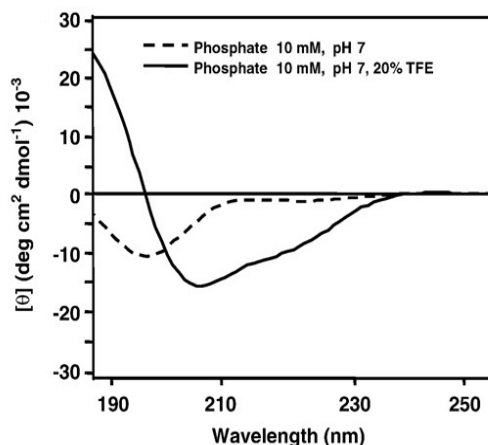


Fig. 3G

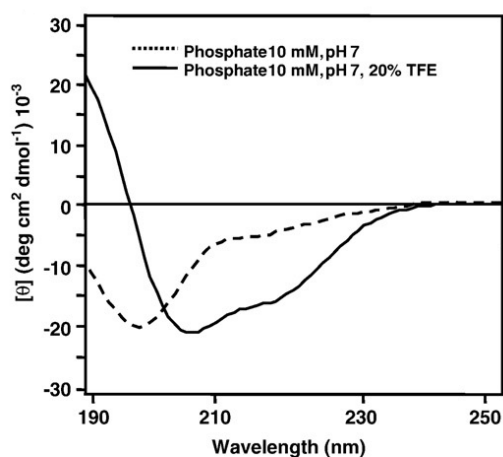
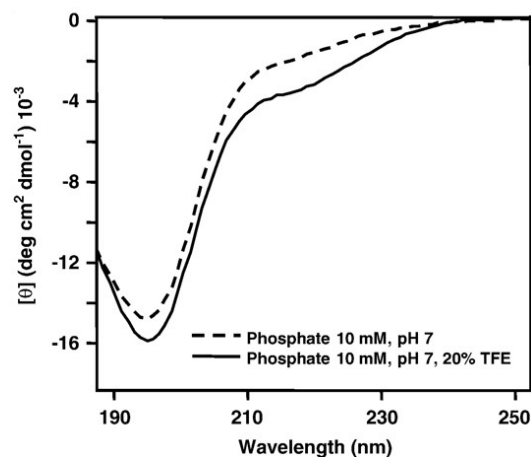


Fig. 4G



### **3.5.5 Gadd45 $\beta$ forms a homodimeric complex that binds tightly to MKK7**

To extend the knowledge of the interaction between the two monomers, an assay to monitor the binding between MKK7 and Gadd45 $\beta$  was carried out. Indeed this interaction has been thoroughly investigated in previous works by pull-down assays utilizing several point-mutated variants of both proteins (67). As shown in t Panel H (Fig. 1H), the association between the two purified proteins was very strong: a rough estimation of the KD, deduced by the Gadd45 $\beta$  concentration at half of the saturation signal, was about 13 nM. Noticeably, signal saturation was reached at an approximate 1:1 molar ratio, suggesting that one MKK7 molecule should be sufficient to bind to one molecule of Gadd45 $\beta$ . The competition experiment carried out using 42 nM MKK7, 21 nM Gadd45 $\beta$  and a twofold excess of competitors over the soluble protein, is reported in Fig. 2H. As shown, peptides corresponding to the putative extended Helices 1, 4 and 5, MKK7 (G132-N156) and Gadd45 $\beta$  (A60-D86) were utilized. Consistent with the notion that MKK7 proximity do not interfere with the Gadd45 $\beta$  dimerization, eH1 and eH5 do not affect the binding, whereas peptides Gadd45 $\beta$  (A60-D86) and MKK7 (G132-N156), believed to form part of the interface between the two proteins, completely abolish the interaction. The peptide R91-E104 corresponding to the putative eH4 and containing two key residues (M95/Q96) involved in kinase recognition (67), also proved ineffective to antagonize the Gadd45 $\beta$ -kinase binding, at the used concentration. Instead, soluble GST-MKK7, as expected, totally abolished the binding. Thus, these results corroborate the view that the Gadd45 $\beta$ -MKK7 interaction is essentially mediated by residues comprised within loop 1 and H3 (region A60-D86) (67), while other regions, such as H4, only partially contribute or may have only a structural role.

## Panel H: Gadd45b dimerization does not affect MKK7 binding and inhibition

Gadd45 $\beta$  and MKK7 strongly interact (Fig. 1F) and their association is not influenced by Helix 1 or Helix 5. Instead Gadd45 $\beta$  [A60-D86] and MKK7 [G132-N156], completely abolish the interaction. These data suggest that Gadd45 $\beta$  self association surface is distinct from that contacting the kinase MKK7 (Fig. 2F).

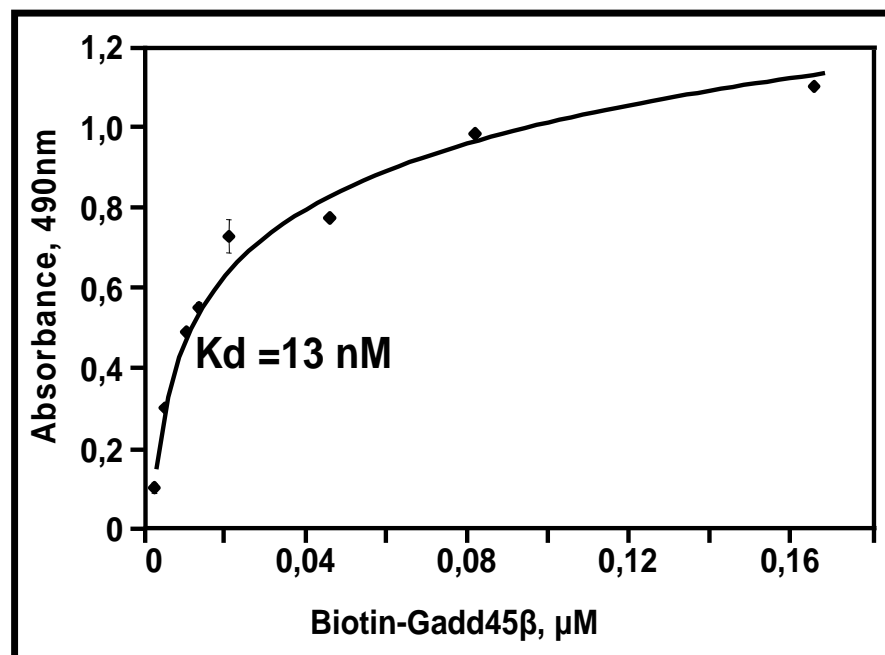


**Fig. 1H:** Binding curve of the association between GST-MKK7 and Gadd45 $\beta$ . The estimated KD is 13 nM.

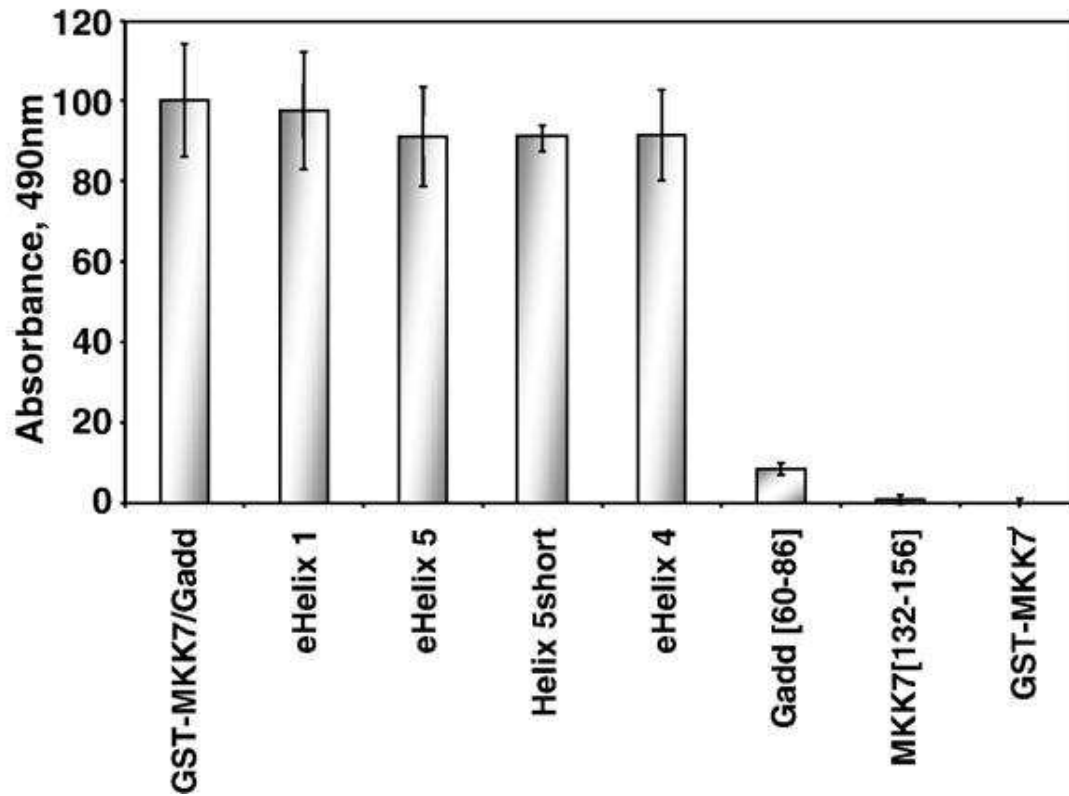


**Fig. 2H:** Binding competition of the MKK7- Gadd45 $\beta$  association by Gadd45 $\beta$  and MKK peptides. eHelix 1, eHelix 5, Helix 5 short and eHelix 4 cannot disrupt the binding, whereas Gadd45 $\beta$  [A60-D86] and MKK7 [G132-N156], corresponding to the interface between the two proteins, completely abolish the interaction. Also the GST-fused full length kinase abolishes the interaction as expected. Data are representative of at least 3 independent experiments.

## **3.6 Biomolecular engineering by combinatorial chemistry and high-throughput screening**

### ***3.6.1 Design of the combinatorial tetrapeptide library***

Designing and engineering small peptides that have specific structures or functions in biological pathways is a very challenging task. Indeed peptides have intrinsic flexible features and, despite the richness of side chain groups, they present an overall large structural similarity at the level of the backbone. Furthermore, as for the GADD45 $\beta$ -MKK7 complex only a theoretical model is available (61), we pursued an approach of screening random combinatorial libraries to select effective inhibitors of the interaction between the two proteins. Combinatorial libraries have gained widespread acceptance for the rapid preparation of enormous numbers of structurally related chemical compounds that are subsequently submitted to a screening assay to select active ingredients. In our case, a random tetrapeptides library in a simplified format (67) was designed and prepared to screen for effective peptide antagonists. To this purpose, a universal library was conceived with a minimum number of “non redundant” different amino acids (12 rather than 20) for the assembly of linear tetrapeptides. A tetrapeptide structure was chosen for it since it can mimic small molecules and can easily be re-converted in peptidomimetic compounds. Additionally they contain a limited number of rotatable bonds which restrains the amount conformational flexibility. The choice of the different amino acids was dictated by diversity in lipophilicity, MW, charge and polarity (See the Table 5 in Methods). Diverse monomers were chosen also to elude ambiguous sequencing by MS analysis. For example only Q and S were selected between the polar neutral amino acids, excluding their homologues N and T.

### **3.6.2 First generation simplified peptide libraries**

Peptide mixtures were obtained with a yield of about 70% (calculated on the basis of the final weight of crude products as compared to a theoretical MW obtained by averaging the molecular weight of residues). Peptide pools were characterized by LC-MS analyses, matching the experimental MW distribution with that expected by an equimolar mixture of the single peptides present in that mixture. Selected peptide mixtures were also characterized by pool aminoacid analysis, confirming the expected distribution of aminoacids (not shown). The success in preparing the peptide mixtures, was confirmed by the parallel synthesis of some test compounds having the same general structure and using the same synthetic procedures. Libraries were dissolved at a nominal concentration of 1 mM in pure DMSO (assuming an average MW of about 800 Da of all peptides) and dissolved in buffers in order to reach the concentrations required for screening.

In the first screening assay, carried out by incubating the soluble biotin-GADD45 $\beta$  with the different 12 sub-libraries (concentration 42 nM of total peptide concentration; the average concentration of the single peptides was about 24 pM), we observed that only the pool number 5 decreased the capacity of GADD45 $\beta$ -MKK7 binding by more than 98% (panel I, Fig 1). Therefore the sub-library Fmoc- $\beta$ Ala<sub>2</sub>-5-Y<sub>2</sub>-X<sub>3</sub>-X<sub>4</sub> was synthesized as a set of 12 new-sublibraries, each containing 144 different peptides. Also these libraries were characterized by LC-MS comparing the expected and the experimental MW distribution. Screening this second set of sub-libraries (concentration 42 nM of total peptide concentration; the average concentration of the single peptides was about 292 pM), we identified the pool 12 (panel I, Fig 2I) as the best competitor of the GADD45 $\beta$ -MKK7 binding, providing a 95% signal reduction at the indicated concentration. On the basis of these data, the sub-library Fmoc- $\beta$ Ala<sub>2</sub>-5-12-Y<sub>3</sub>-X<sub>4</sub> was re-prepared as a set of 12 sub-libraries each containing 12 different peptides. These peptide pools were easily characterized by LC-MS confirming the presence of all the expected molecules within the mixtures. By testing these sub-libraries (concentration 42 nM of total peptide concentration; the average concentration of the single peptides was about 3.5 nM), we observed that pools 3 and 12 resulted positive, showing almost complete blocking of the interaction (panel I, Fig 3I). Eventually, after further dose-dependent assays, sub-library 11 was chosen as the best working in that position. Finally, in the last screening cycle, 12 separated peptides with sequence Fmoc- $\beta$ Ala<sub>2</sub>-5-12-11-Y<sub>4</sub> were synthesized and screened. In this assay the single, purified peptides (fully characterized by LC-MS in terms of identity and purity), were all tested at a concentration of 42 nM; only the peptide Fmoc- $\beta$ Ala<sub>2</sub>-5-12-11-9, named lead peptide 1, turned out to be able to block the interaction (panel I, Fig 4I) and was selected as the best molecule to be further studied and developed.

## Panel I : Deconvolution of Combinatorial library

The library deconvolution has been realized by Elisa competition assays. Competition results are reported as  $(B/B_0) \times 100$ , where B is the average absorbance from the triplicate data points for a given analyte and  $B_0$  is the average absorbance determined without competitor

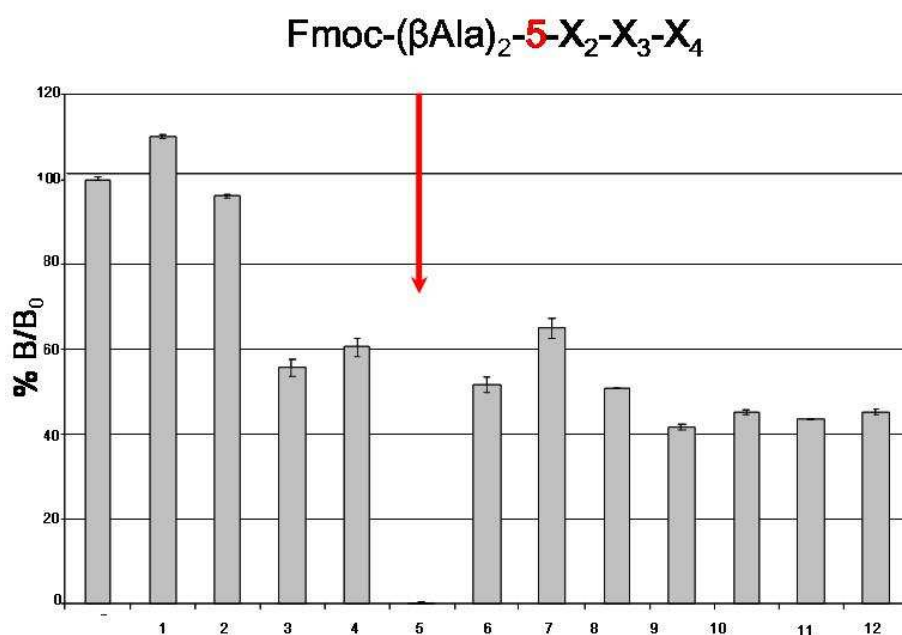


**Fig. 11 :** Screening of the library containing a theoretical total number of  $12^4 = 20736$  different peptides, arranged in 12 different sub-pools. The sub-library 5 decreases the capacity of GADD45 $\beta$ -MKK7 binding with efficiency more than 98%. Therefore it was selected for re-synthesis.

Fmoc-( $\beta$ Ala)<sub>2</sub>-5-12-X<sub>3</sub>-X<sub>4</sub>

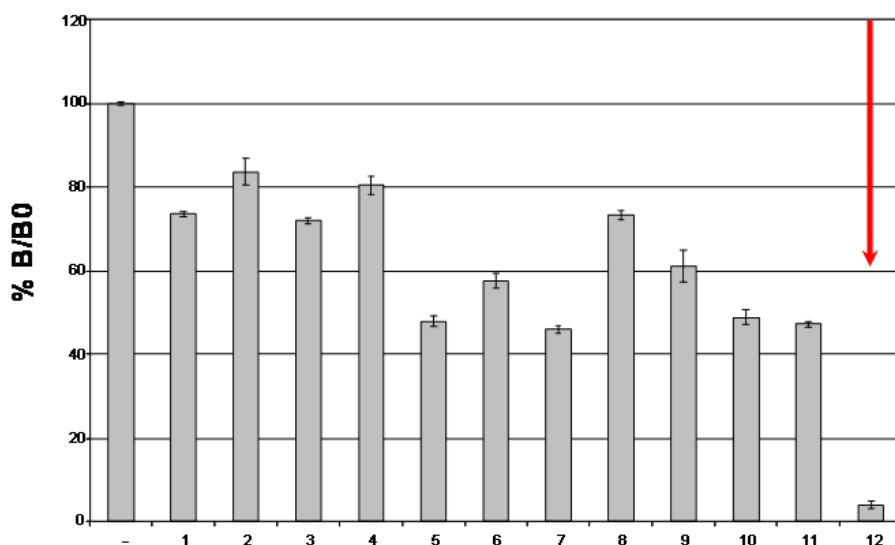


**Fig. 2I:** Deconvolution of the sub-libraries Fmoc-( $\beta$ Ala)<sub>2</sub>-5-Y2-X3-X4-NH2. A theoretical total number of 1728 different peptides were arranged in 12 different pools. Only the sub pool 12 was chosen for re-synthesis.

Fmoc-( $\beta$ Ala)<sub>2</sub>-5-12-11-X<sub>4</sub>

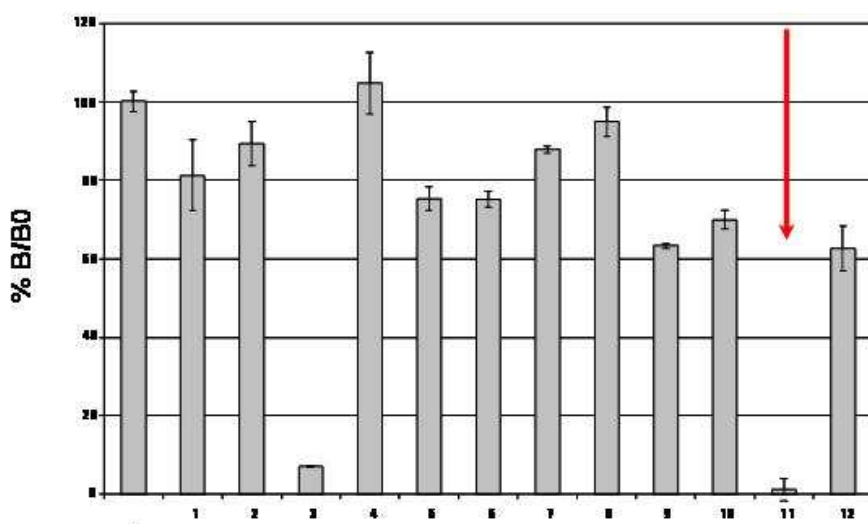


**Fig. 3I:** Screening of the library Fmoc-( $\beta$ Ala)<sub>2</sub>-5-12-Y3-X4-NH2. A theoretical total number of 144 different peptides were arranged in 12 different pools. Only the sub pool 11 was chosen for re-synthesis.

### Fmoc-( $\beta$ Ala)<sub>2</sub>-5-12-11-9

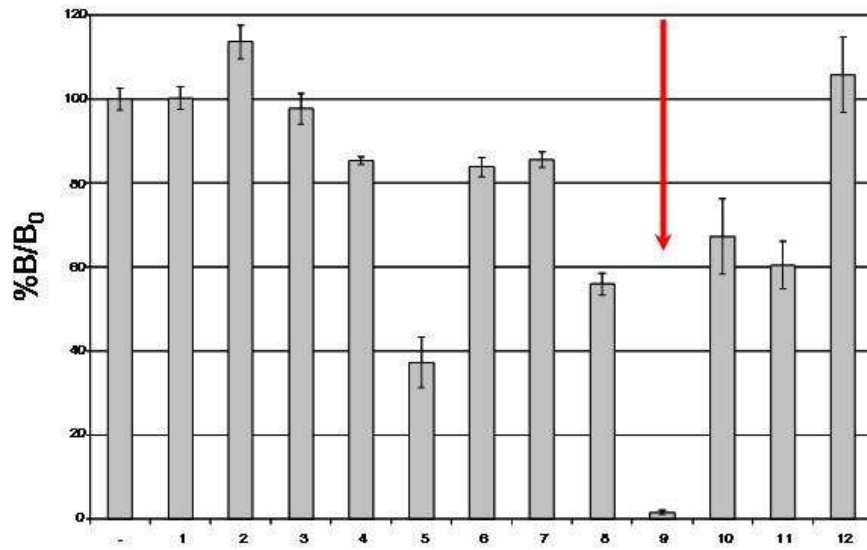


**Fig. 4I:** Last step of iterative deconvolution. This fourth library was constituted by single peptides. Fmoc-( $\beta$ Ala)<sub>2</sub>-5-12-11-9-NH<sub>2</sub>, named Lead Peptide 1, was selected as the best library component of the interaction between GADD45 $\beta$  and MKK7. Its efficiency has been estimated to be more than 98% at a concentration of 42nM.

### 3.6.3A new focused library of tetrapeptides

To take into account for the peptide sequences not generated within the simplified library, a set of new peptides was designed and prepared by chemical synthesis. This new set of compounds was designed on the basis of the sequence of the Lead Peptide 1. Also this part of the work is not disclosed for the patent filing purposes. However, to better understand the re-design process after the screening of a simplified peptide library, an example is given in Scheme 1.

The new series of compounds was named “II generation library”. As exemplified in the Scheme, each amino acid constituting the lead peptide sequence was replaced with the homologue amino acids, previously excluded from the first combinatorial library synthesis. Considering all possible amino acidic combinations, the lead peptide 1 and 24 new different peptides were synthesized and characterized by LC-MS analysis. In this new focused library, the hydrophobic tag and the molecular spacer were omitted to improve their solubility in solution.

From the screening of this library, where peptides were tested at a single 42 nM concentration, only peptides 8 and 24 disrupted the Gadd45 $\beta$ -MKK7 interaction with an efficiency similar to that of the Lead Peptide 1, (panel Y, Fig. 1Y). The remaining 22 peptides did not exhibit any antagonistic effect. Considering the strong sequence conservation between the Lead Peptide 1 and the other peptides, these results suggested a potent selectivity of the selected compounds. On the basis of its higher solubility, Peptide 8 was chosen as the best compound and was named Lead Peptide 2. To further validate this result, dose-dependent assays with Lead Peptides 1 and 2 and with a control peptide were carried out. The data are shown in Fig. 2Y. Again, these structures are not shown for the purpose of patent filing.

The sequence of the Lead Peptide 1 and the Lead Peptide 2 are not disclosed in this work, as a patent covering the potential applications of these molecules is being filed, therefore any dissemination or presentation of data would be considered as “prior art” and would annul the main requirement of originality.

#### Asp-Gln-His-Leu

Asp → Asp, Glu	2x
Gln → Gln, Asn	2x
Arg → Arg, Lys	2x
Leu → Leu, Val, Ile	3 =
	<hr/>
	24

**Scheme 1: Redesigning active sequences after the screening of simplified peptide libraries.** To complete the screening, taking into accounts the excluded residues, new sequences are re-designed by inserting homologous amino acids. In this scheme the redesign of sequences derived by a putative positive peptide has the sequence Asp-Gln-His-Leu. As shown, only 24 new peptides need to be prepared.

## Panel Y: Screening the II generation focused library

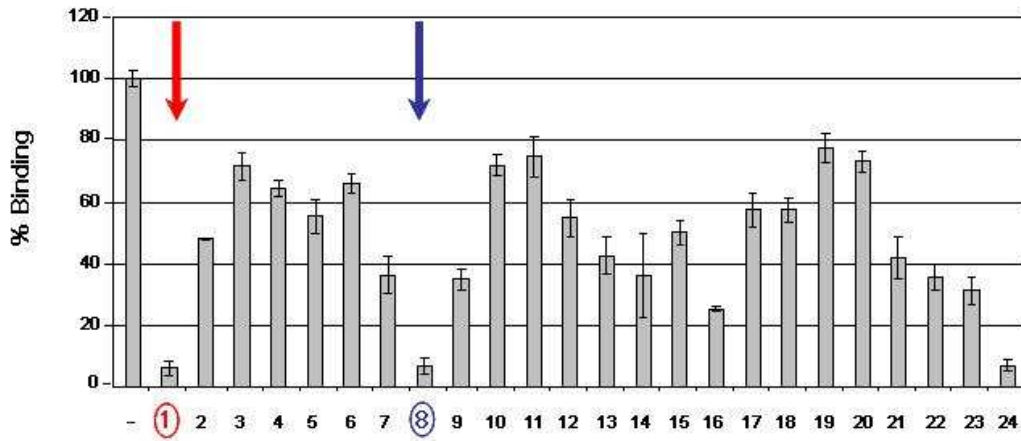


**Fig. 1 Y:** Selection of Lead Peptide 2 from the library of second generation.

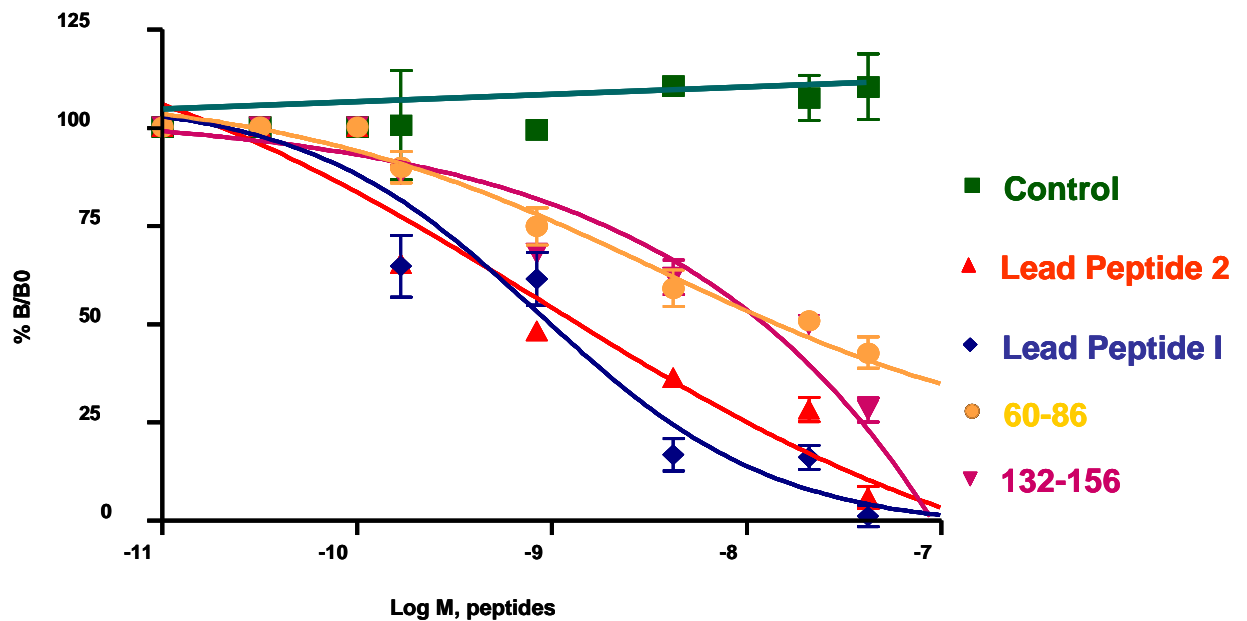


**Fig. 2 Y:** The concentration-dependent activity of Lead Peptides 1 and 2 has been compared to known antagonists by ELISA assay. The  $IC_{50}$  values extrapolated by non-linear fitting were: Lead Peptide 1: 1.3 nM; Lead Peptide 2: 0.18 nM.

### **3.6.4 Validation of the combinatorial approach**

In literature are described only two antagonists of the Gadd45 $\beta$ -MKK7 interaction (47) that are Gadd45 $\beta$  A60-D86 and MKK7 G132-N156. These two peptides were capable of disrupting the MKK7-Gadd45 $\beta$  binding because they mime the interface of protein-protein interaction.

Our hypothesis is that tetrapeptide antagonists can be more efficient than long peptides, because they can have chemical and stoichiometric characteristics comparable to those of small molecules.

For this reason, the peptides mentioned above and the two Lead Compounds 1 and 2, were tested in a dose-dependent Elisa competition. In this assay, every antagonist has shown a concentration-dependent activity (Panel Y Fig. 2Y). According to our hypothesis tetrapeptides functioned better than the antagonist described in literature. In fact the Lead Peptide 1 and 2 exhibited an EC<sub>50</sub> values of about 1.3nM and 0.18 nM respectively, while Gadd45 $\beta$  A60-D86 and MKK7 G132-N156 showed an EC<sub>50</sub> values of about 21nM.

These results suggest the high activity of two Lead Compounds identified and confirm the technical efficiency of the combinatorial strategy.

### **3.6.5 Lead peptides engineering**

The short half-life of peptides has been one of the major issues of peptide therapeutic. Peptides are typically cleared in the cell medium within minutes to hours after their administration. Therefore, to realize further characterization with some cell-based assays, the two Lead Peptides and one opportune negative control have been synthesized incorporating D-amino acids and tested again in Elisa assays. Their activity did not change. In this mode their stability has been substantially increased.

### 3.7 From combinatorial chemistry to validated hit: defining the mechanism of inhibition

In addition to screening strategies based on synthetic tetrapeptide libraries, it became necessary to validate the results obtained using alternative assessments. The selected lead compounds were further characterized with different cell-based assay in order to confirm their antagonist activities.

For this reason HA-Gadd45 $\beta$  was transiently co-expressed in HEK293T cells together with Flag-MKK7. Thus the intracellular localization of these proteins was assessed by immune-staining and further western blot, using properly antibodies (Fig. 1K). The interaction between Gadd45 $\beta$  and MKK7 was detected readily by immunoprecipitation of Flag-MKK7 and monitoring HA-Gadd45 $\beta$  co-precipitation.

To support the idea that the selected antagonists are able to disrupt Gadd45 $\beta$ -MKK7 interaction, co-immunoprecipitation assays were carried out with and without peptidic inhibitors. As expected, incubating the immunocomplex with 1 and 5 nM of Lead Compounds 1 and 2, the HA-Gadd45 $\beta$  co-immunoprecipitation decreased. Data shown in Fig. 2 K confirm the result previously observed throughout the deconvolution of combinatorial libraries. Indeed the Lead Peptides 1 and 2 exhibit a substantial activity at nanomolar concentration.

#### 3.7.1 Investigation of inhibition mechanism

To investigate whether the Lead Peptides 1 and 2 were MKK7 inhibitors several kinase assays were performed. This way was addressed by using HEK293 cells transiently transfected with Flag-tagged MKK7. The kinase activation was realized by stimulation either with TNF $\alpha$  or with P/I. The kinase assays confirmed that MKK7 was efficiently activated (Fig. 1L). In order to understand the level at which Gadd45 $\beta$  inhibits the JNK phosphorylation, another Kinase assay was carried out using the recombinant GST-Gadd45 $\beta$  as MKK7 competitor (Fig. 2L). After setting the best conditions of Gadd45 $\beta$  inhibitory activity at 5  $\mu$ M, Lead Peptides 1 and 2 and the opportune negative controls were finally tested.

Consistently with preliminary results, only the Lead Peptides 1 and 2 were able to prevent the MKK7-Gadd45 $\beta$  interaction. The results shown in Panel L suggest that they are active respectively in the range of concentration 1-5 nM and 0,5-1 nM (Fig. 3L). *In vitro* kinase assays established that their antagonist activity matched perfectly with the IC<sub>50</sub> value detected by Elisa fitting (see Panel Y, Fig. 2Y).

Additionally, the results previously described also suggested that the selected peptides disrupt the interaction between Gadd45 $\beta$  and MKK7 without interfering with the kinase activity directly. In order to investigate this particular issue, kinase assays were performed using only the peptides without the recombinant GST-Gadd45 $\beta$  protein.

The results revealed that both lead compounds do not block JNK phosphorylation acting as inhibitors ATP-no competitive (Panel 4K). Data obtained from *in vitro* studies on these inhibitors should generate interesting insight into the argument previously discussed. Actually, the vast majority of

kinase inhibitors work overlapping the ATP binding pocket. This competitive behavior often determine undesirable effects cross-reacting against other kinases.

*“Specific inhibition by a non specific effect”* is a provocative expression but could be applied to inhibitory effect of MAPK inhibitors.

As mentioned above in the introduction section, the signaling module composed by MAPK is an integrated system that means interaction between the different pathways.

Instead the lead compounds 1 and 2 have an activity non-ATP competitive. Therefore they have the potential of taking a leading role in development of new drug candidates having powerful Biotechnological applications.

**Panel K: Validation of results obtained by combinatorial approach with cell based assays**

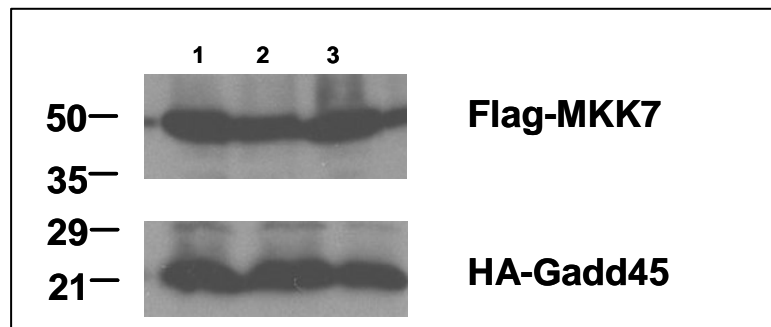


**Fig. 1K: Gadd45 $\beta$  physically interacts with MKK7.**

Western Blot showing the co-expression of HA-Gadd45 $\beta$  and Flag-MKK7 in 293 cells. Anti-Flag immunoprecipitates of lysates from 293 cells previously transfected with pcDNAFlag-MKK7 and pcDNAHA-Gadd45 $\beta$  using different ratios: 1:1 (line 1); 1:2 (line 2) and 1:5 (line 3).

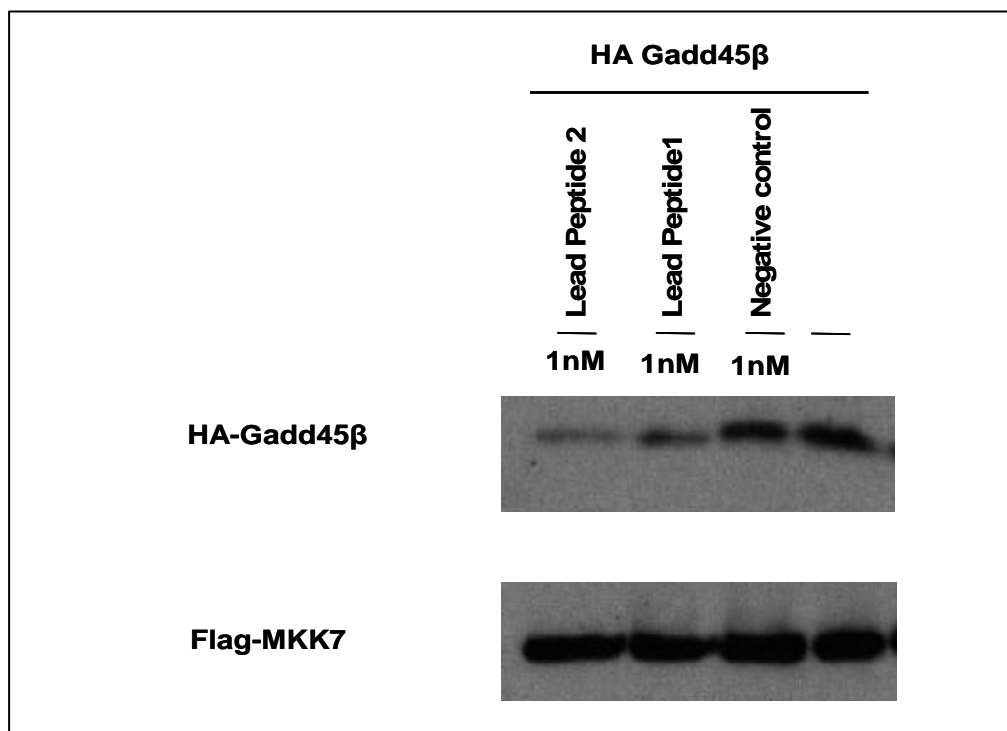


**Fig. 2K:** Immunoprecipitation followed by western blot, showing physical association between endogenous Gadd45 $\beta$  and MKK7 and the destruction of immunocomplex by Lead Peptides 1 and 2.

**Panel L: Lead compounds 1 and 2 disrupt Gadd-MKK7 interaction without blocking JNK phosphorylation**

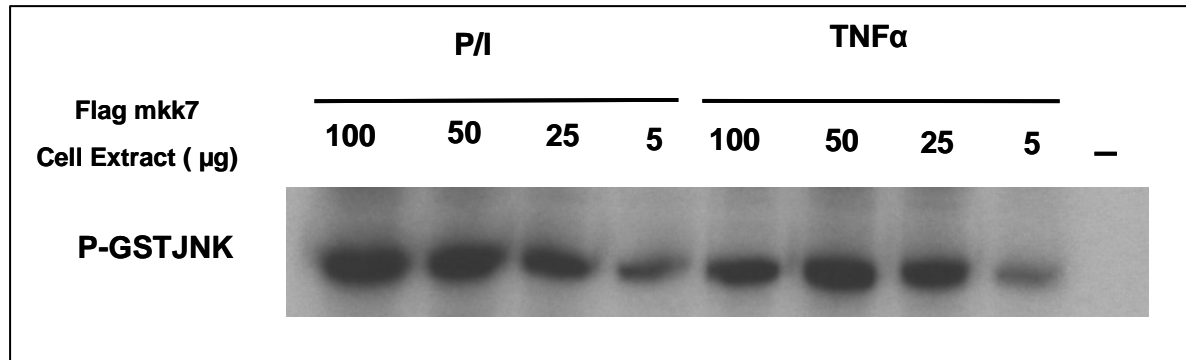


**Fig . 1L:** MKK7 activation with P/I and TNF $\alpha$  was monitored by combined immunoprecipitation (Resin anti Flag) and Kinase assay

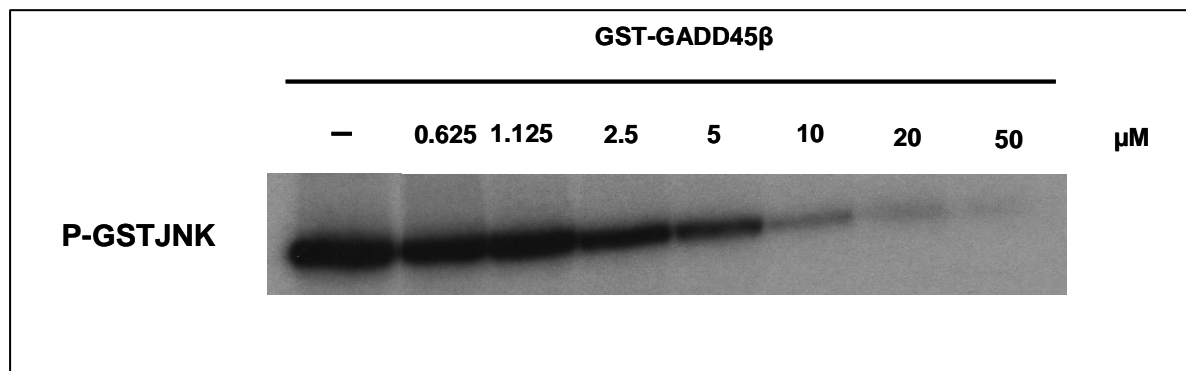


**Fig. 2L:** Kinase assays showing a specific inhibition of active Mkk7 by purified GST-Gadd45 $\beta$  in vitro. Flag-tagged kinase were immunoprecipitates from 293 cells treated with P/I (30 min) and pre-incubated with the indicated concentrations of Gadd45 $\beta$ .

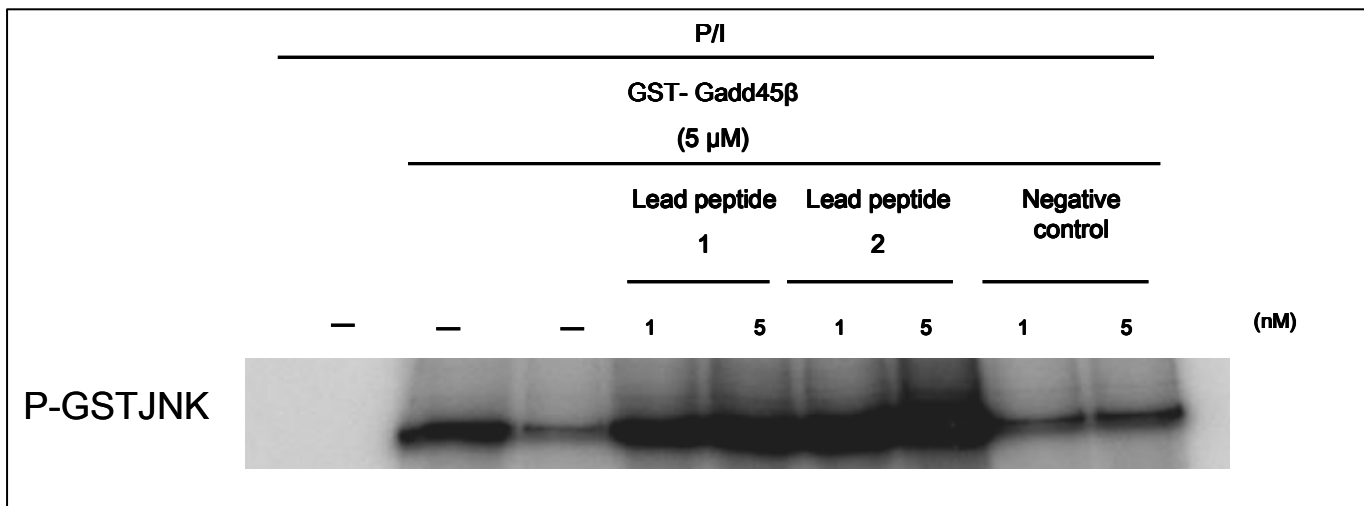


**Fig. 3L:** The ability of lead compounds 1 and 2 to disrupt the interaction between Gadd45 $\beta$  and Mkk7 has been confirmed by kinase assays.

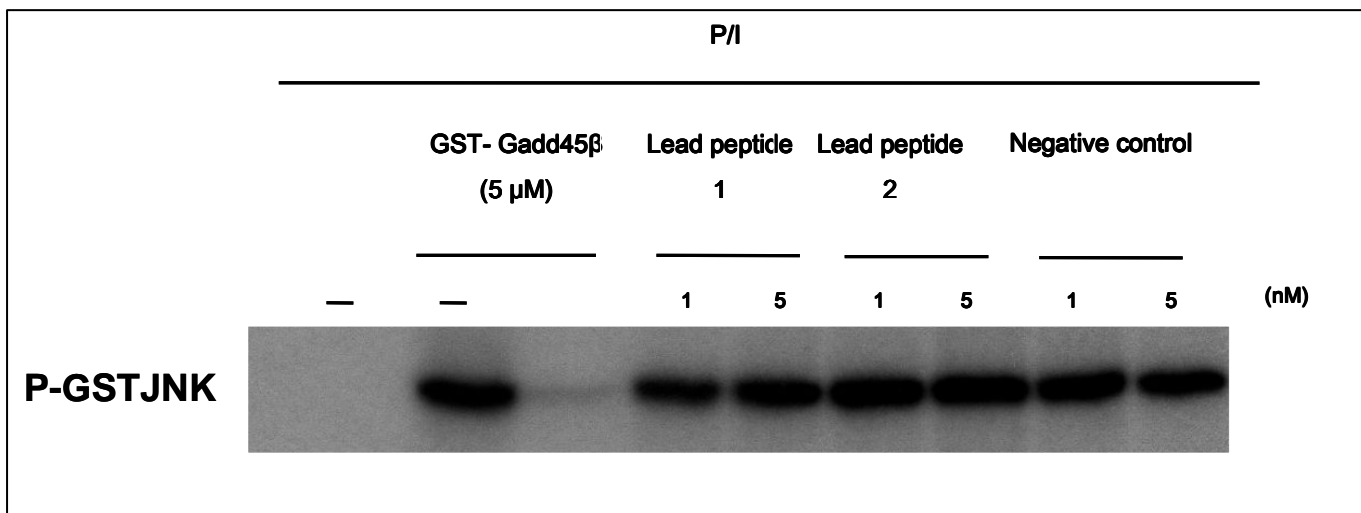


**Fig. 4L:** Kinase assays confirming that lead peptides 1 and 2 are non – ATP competitive inhibitors.

## **CONCLUSIONS AND PERSPECTIVES**

## **Antagonists of Gadd45 $\beta$ – Mkk7: from combinatorial approach to new therapeutic components**

The relationship between the pathological processes of infection, inflammation and cancer is correlated to the role of the transcription factor NF- $\kappa$ B in cellular homeostasis (24)

Therefore studying NF- $\kappa$ B target genes makes it is possible to understand the molecular mechanisms of inflammation, of tumor growth and progression.

Gadd45 $\beta$  is one of the anti-apoptotic regulators controlled by NF- $\kappa$ B in response to pro-inflammatory stimuli and genotoxic stress (43).

Gadd45 $\beta$  exerts its functions by interacting with several partners such as MAP kinases (43;47;50) and DNA clamp protein (52;76) .

In particular the physical interaction between Gadd45 $\beta$  and MKK7 has been widely described as a molecular link between the NF- $\kappa$ B cytoprotective effects and the suppression of the signaling of JNK, one of the main MKK7 substrates that strongly promotes apoptosis.

In addition it has been reported that both Gadd45 $\beta$  and MKK7 are able to dimerize or to oligomerize. Therefore their mutual interaction and the interaction with other partners can be regulated by this event. Understanding this complex network of interactions and finding effective antagonists is therefore of preeminent importance for elucidating in details the fine balance between cell death and cell survival and to modulate cell homeostasis for therapeutic applications.

Accordingly, this project has been focused on the structural and functional characterization of the Gadd45 $\beta$ -MKK7 complex and on the identification of compounds able to disrupt this interaction. In fact, developing molecules able to block the pro-survival action of NF- $\kappa$ B without significantly compromising the innate activation of the immune system is an effective way to suppress the proliferative effects induced by Gadd45 $\beta$  expression.

The first part of this study was dedicated to a complete investigation of the Gadd45 $\beta$  homodimerization by spectroscopic and biochemical techniques. Since Gadd45 proteins have no enzymatic activity, the self association could be a regulative mechanism under both physiological and pathological conditions.

Analyses by Size Exclusion Chromatography, circular dichroism and native gels unequivocally confirmed that Gadd45 $\beta$  exists in solution prevalently as a non covalent dimer. In agreement with previous findings, ELISA-like assays showed a 1:1 stoichiometry for the Gadd45 $\beta$  self-binding, while in contrast to previous data on Gadd45 $\alpha$ , Gadd45 $\beta$  is seemingly able to only form dimers.

Importantly, the self-association dissociation constant was estimated to be about 100 nM, a value which is similar to the cellular concentration estimated for proteins of this family (64;77). This high similarity suggests that equilibrium between monomers and dimers can occur in the cytoplasm, where up- and down-regulation of the protein could be a way to finely modulate self-association as well as other external interactions.

Applying a method of limited proteolysis of the protein, separation of the resulting fragments and binding competition assays, we have identified the

regions of Gadd45 $\beta$  involved in the self-association as corresponding to the predicted helix 1 (H1) and helix 5 (H5) of the protein (61).

With the help of a homology model of the Gadd45 $\beta$  dimer, we have hypothesized that the dimerization region can form a four-helix bundle, where the contiguous disposition of H1 and H5 in one monomer creates a large hydrophilic surface interacting in an anti-parallel fashion with the corresponding helix of the other monomer.

In particular residues Gln13, Thr14 and Glu21 on H1 and Glu140, Tyr137, Glu133 and His129 on H5 are involved in a network of intra-molecular polar interaction which stabilizes the structure of the complex.

The formation of a compact dimer is supported by studies of chemical denaturation with both GndHCl and urea, where it is seen that the protein, in the presence of up to 1M denaturants persists in the dimeric form, whereas it unfolds after reaching higher concentrations (74).

It has been recently reported the crystal structure of Gabb45 $\gamma$ , which reveals a fold comprising an  $\alpha\beta\alpha$  sandwich with a central five stranded mixed  $\beta$ -sheet with  $\alpha$ -helices packed on either side, similarly to the predicted Gadd45 $\beta$  model. By inspection of the crystal packing, Gabb45 $\gamma$  is a dimer, where the interface is formed by a four-helix bundle with predominant hydrophobic interactions. Residues Ile76-Leu80 of helix  $\alpha$ 3 and residues Tyr44-Lys48 of helix  $\alpha$ 2 contribute the vast majority of the interactions. It is worth to be noticed that the dimerization interface is formed by residues that are highly conserved among isoforms (78). The different dimerization surface between the Gadd protein family points out how even if some roles are common among the three isoforms, others are isoform- and cell-type-specific. In this regard, it is interesting to note that the Thr79 in Gadd 45 $\beta$  is implicated in its interactions with MKK7.

The predicted helix H4, being parallel to H1, virtually extends the interaction surface towards the protein Loop 2, but does not contribute to protein self-association. On the contrary it is reportedly involved in the binding with MKK7 (61).

In agreement with previous reports (61), and in contrast with others (50;79), Gadd45 $\beta$  and MKK7 strongly interact in vitro, exhibiting a KD of about 13 nM. This value is about 8-fold lower than that estimated for Gadd45 $\beta$  self-association, thus suggesting that the two proteins are also able to interact in the presence of monomeric Gadd45 $\beta$ . Consistently, the two proteins still strongly interact in the presence of both eH1 and eH5 that efficiently abrogate the Gadd45 $\beta$  dimerization.

By characterizing the recombinant MKK7, we found that, in agreement with other reports (76;80), also the folded kinase is dimeric suggesting that the interaction between Gadd45 $\beta$  and MKK7 takes place in the context of a large complex comprising at least two Gadd45 $\beta$  and two kinase units (MKK7/Gadd45 $\beta$ :Gadd45 $\beta$ /MKK7).

Integrating these findings with the literature data, Gadd45 $\beta$  appears to have a modular structure despite its small size.

In fact while the N- and C-termini are involved in self association, the central region, residues A60-A114 and the large acidic patches, is committed to kinase binding and regulation and to the interaction with core histones (region 72-124) (81).

The same sub-domains, however, have concomitantly a role in the recognition of other partners such as PCNA (56), which binds the terminal region 27-50 and 127-150 of Gadd45 $\alpha$ , and nucleophosmin (81), which interacts with the region 61-100, thereby regulating nuclear entry. Therefore, while dissociation of Gadd45 proteins would be required for interaction with PCNA, a key player of the DNA repair mechanism primarily regulated by Gadd45 proteins, it seems dispensable for binding to kinases, core histones and nucleophosmin.

The biochemical analysis of Gadd45 $\beta$ -MKK7 complex provided a new context for dissecting the structure-activity relationship of this interaction.

Given the crucial effect of Gadd45 $\beta$ -MKK7 interaction in NF- $\kappa$ B-mediated JNK activity suppression, the selection of antagonists becomes an attractive target for cancer prevention and therapy.

In the literature only two antagonist of the Gadd45 $\beta$ -MKK7 complex have been described: the peptides Gadd45 $\beta$  A60-D86 and MKK7 G132-N156 (47). These peptides are capable of disrupting the Gadd45 $\beta$ -MKK7 binding because they mimic the interface of protein-protein interaction.

To select antagonists of the Gadd45 $\beta$ -MKK7 interaction, a combinatorial chemistry approach has been followed. Synthesis and screening of random peptide libraries have been chosen to permit the rapid selection and optimization of leads to produce drug candidates.

By this process, **Lead Compounds 1 and 2** have been selected from deconvoluting of two generations of tetrapeptide libraries. These novel antagonists can disrupt very efficiently the interaction between Gadd45 $\beta$  and MKK7 at concentrations in the low nanomolar range. The high potency of these compounds is more evident when compared with their IC<sub>50</sub> values of about 0.8 nM with the value of about 21 nM calculated for Gadd45 $\beta$  A60-D86 and MKK7 G132-N156. Importantly, the final Lead Compounds selected have both a molecular weight below 500 Da and a potent inhibiting activity.

Further investigations by co-immunoprecipitation and kinase assays have confirmed that the measured antagonistic activity matches perfectly with the IC<sub>50</sub> values from ELISA data.

Additionally, the results suggest that the selected peptides disrupt the interaction between Gadd45 $\beta$  and MKK7 without directly interfering with the kinase activity. Indeed several kinase assays have confirmed that both Lead Compounds do not block JNK phosphorylation, therefore they do not enter the kinase ATP binding site.

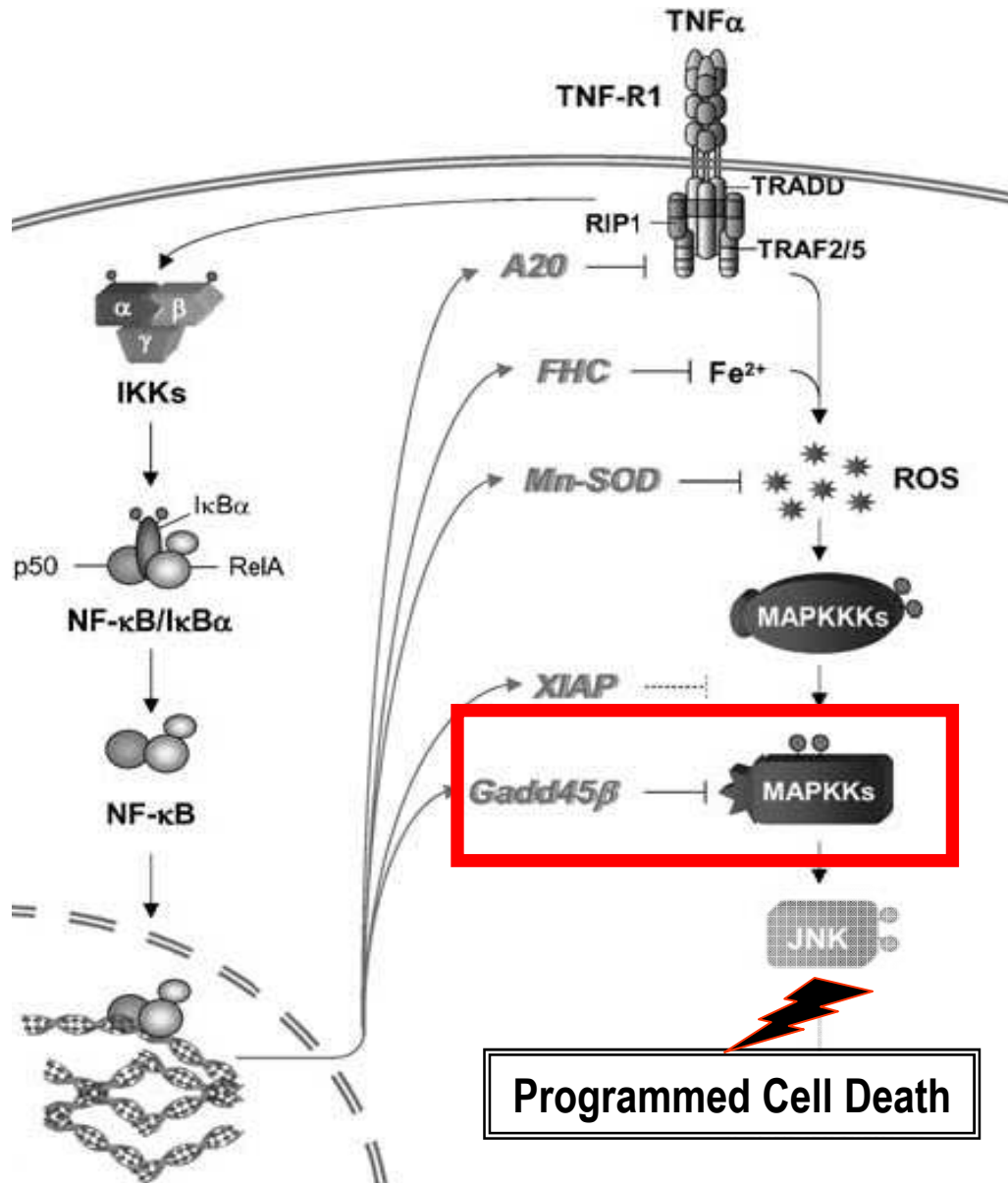
Considering the paradoxical contest of kinase inhibitors, these *in vitro* studies can open interesting prospective.

Actually, the vast majority of highly selective small compounds modulate the kinase activity overlapping the ATP binding pocket.

This kind of inhibitors, because of the high homology in sequence and structure of catalytic kinase sites (41), usually show undesirable effects by cross-reacting against several other kinases (11;38;82).

Consequently, non ATP-competitive small compounds, such as Lead Peptides 1 and 2, have the potential of becoming very useful new drug candidates, since the selective inhibition of NF- $\kappa$ B downstream targets, such as Gadd45 $\beta$ , could be a way to convert inflammation-driven tumor growth into inflammation-induced tumor suppression.

Future studies are required to translate these basic findings into deeper practice developing novel compounds. Indeed the potential of peptides as drug candidates is limited by their poor pharmacokinetic properties and by their difficulties to cross cell membranes. Several experiments will be carried out to establish the key pharmacokinetic characteristics of **Lead compounds 1 and 2** and to establish the effects of these antagonists on other NF- $\kappa$ B regulated pathways



**Gadd45 $\beta$ -Mkk7: critical molecular linker between NFKB citoprotective effect and JNK cascade suppression.**

Given the importance of this pathway both in inflammation-inducing oncogenesis and cancer chemoresistance, to develop antagonists targeting Gadd45 $\beta$  Mkk7 interaction should provide a new prospective for alternative cancer treatments.

## **REFERENCES**

1. Malik, N. N. (2008) *Drug Discov. Today*
2. Deb Carstoiu, B. D. o. S. M. R. a. A. V. D. B. H. P. A. D. G. B. M. D. o. A. B. L. W. E. M. Ph. D. W. E. (2008) *The Guide to Biotechnology* is compiled by the Biotechnology Industry Organization (BIO)
3. Waller, C. L., Shah, A., and Nolte, M. (2007) *Drug Discov. Today* **12**, 634-639.
4. Terstappen, G. C., Schlupen, C., Raggiaschi, R., and Gaviraghi, G. (2007) *Nat. Rev. Drug Discov.* **6**, 891-903
5. Searls, D. B. (2005) *Nat. Rev. Drug Discov.* **4**, 45-58
6. Guido, R. V., Oliva, G., and Andricopulo, A. D. (2008) *Curr. Med. Chem.* **15**, 37-46
7. Fry, D. C. and Vassilev, L. T. (2005) *J. Mol. Med.* **83**, 955-963
8. Fletcher, S. and Hamilton, A. D. (2006) *J. R. Soc. Interface* **3**, 215-233
9. Laudet, B., Prudent, R., Filhol, O., and Cochet, C. (2007) *Med. Sci. (Paris)* **23**, 273-278
10. Boldt, S. and Kolch, W. (2004) *Curr. Pharm. Des* **10**, 1885-1905
11. Bishop, A. C. (2004) *Chem. Biol.* **11**, 587-589
12. Aggarwal, B. B., Sethi, G., Baladandayuthapani, V., Krishnan, S., and Shishodia, S. (2007) *J. Cell Biochem.* **102**, 580-592
13. Boutros, T., Chevet, E., and Metrakos, P. (2008) *Pharmacol. Rev.* **60**, 261-310
14. Mitra, A. P. and Cote, R. J. (2008) *Annu. Rev. Pathol.*
15. Chang, L. and Karin, M. (2001) *Nature* **410**, 37-40
16. Vieth, M., Higgs, R. E., Robertson, D. H., Shapiro, M., Gragg, E. A., and Hemmerle, H. (2004) *Biochim. Biophys. Acta* **1697**, 243-257
17. Lawrence, M. C., Jivan, A., Shao, C., Duan, L., Goad, D., Zaganjor, E., Osborne, J., McGlynn, K., Stippec, S., Earnest, S., Chen, W., and Cobb, M. H. (2008) *Cell Res.* **18**, 436-442
18. Karin, M. (2004) *Ann. Rheum. Dis.* **63 Suppl 2**, ii62-ii64
19. Papa, S., Zazzeroni, F., Pham, C. G., Bubici, C., and Franzoso, G. (2004) *J. Cell Sci.* **117**, 5197-5208
20. Naugler, W. E. and Karin, M. (2008) *Curr. Opin. Genet. Dev.* **18**, 19-26

21. Halsey, T. A., Yang, L., Walker, J. R., Hogenesch, J. B., and Thomas, R. S. (2007) *Genome Biol.* **8**, R104
22. Roberts, P. J. and Der, C. J. (2007) *Oncogene* **26**, 3291-3310
23. Karin, M. (2006) *Mol. Carcinog.* **45**, 355-361
24. Karin, M. (2008) *Cell Res.* **18**, 334-342
25. Yang, R., Piperdi, S., and Gorlick, R. (2008) *Clin. Cancer Res.* **14**, 6396-6404
26. Kennedy, N. J. and Davis, R. J. (2003) *Cell Cycle* **2**, 199-201
27. Khatlani, T. S., Wislez, M., Sun, M., Srinivas, H., Iwanaga, K., Ma, L., Hanna, A. E., Liu, D., Girard, L., Kim, Y. H., Pollack, J. R., Minna, J. D., Wistuba, I. I., and Kurie, J. M. (2007) *Oncogene* **26**, 2658-2666
28. Hommes, D. W., Peppelenbosch, M. P., and van Deventer, S. J. (2003) *Gut* **52**, 144-151
29. Craig, E. A., Stevens, M. V., Vaillancourt, R. R., and Camenisch, T. D. (2008) *Dev. Dyn*
30. Thaimattam, R., Banerjee, R., Miglani, R., and Iqbal, J. (2007) *Curr. Pharm. Des* **13**, 2751-2765
31. Baselga, J. (2006) *Science* **312**, 1175-1178
32. Karaman, M. W., Herrgard, S., Treiber, D. K., Gallant, P., Atteridge, C. E., Campbell, B. T., Chan, K. W., Ciceri, P., Davis, M. I., Edeen, P. T., Faraoni, R., Floyd, M., Hunt, J. P., Lockhart, D. J., Milanov, Z. V., Morrison, M. J., Pallares, G., Patel, H. K., Pritchard, S., Wodicka, L. M., and Zarrinkar, P. P. (2008) *Nat. Biotechnol.* **26**, 127-132
33. Peters, E. C. and Gray, N. S. (2007) *ACS Chem. Biol.* **2**, 661-664
34. Traxler, P. (2003) *Expert. Opin. Ther. Targets.* **7**, 215-234
35. bioseeker, <http://www.bioseeker.com/component/page> (2008) kinase inhibitors.
36. Weinmann, H. and Metternich, R. (2005) *Chembiochem.* **6**, 455-459
37. Fabian, M. A., Biggs, W. H., III, Treiber, D. K., Atteridge, C. E., Azimioara, M. D., Benedetti, M. G., Carter, T. A., Ciceri, P., Edeen, P. T., Floyd, M., Ford, J. M., Galvin, M., Gerlach, J. L., Grotzfeld, R. M., Herrgard, S., Insko, D. E., Insko, M. A., Lai, A. G., Lelias, J. M., Mehta, S. A., Milanov, Z. V., Velasco, A. M., Wodicka, L. M., Patel, H. K., Zarrinkar, P. P., and Lockhart, D. J. (2005) *Nat. Biotechnol.* **23**, 329-336

38. Battistutta, R., Mazzorana, M., Cendron, L., Bortolato, A., Sarno, S., Kazimierczuk, Z., Zanotti, G., Moro, S., and Pinna, L. A. (2007) *Chembiochem.* **8**, 1804-1809
39. Bennett, B. L., Sasaki, D. T., Murray, B. W., O'Leary, E. C., Sakata, S. T., Xu, W., Leisten, J. C., Motiwala, A., Pierce, S., Satoh, Y., Bhagwat, S. S., Manning, A. M., and Anderson, D. W. (2001) *Proc. Natl. Acad. Sci. U. S. A* **98**, 13681-13686
40. Han, Z., Boyle, D. L., Chang, L., Bennett, B., Karin, M., Yang, L., Manning, A. M., and Firestein, G. S. (2001) *J. Clin. Invest* **108**, 73-81
41. Bain, J., Plater, L., Elliott, M., Shpiro, N., Hastie, C. J., McLauchlan, H., Klevernic, I., Arthur, J. S., Alessi, D. R., and Cohen, P. (2007) *Biochem. J.* **408**, 297-315
42. Jin, S., Antinore, M. J., Lung, F. D., Dong, X., Zhao, H., Fan, F., Colchagie, A. B., Blanck, P., Roller, P. P., Fornace, A. J., Jr., and Zhan, Q. (2000) *J. Biol. Chem.* **275**, 16602-16608
43. De, S. E., Zazzeroni, F., Papa, S., Nguyen, D. U., Jin, R., Jones, J., Cong, R., and Franzoso, G. (2001) *Nature* **414**, 308-313
44. Vairapandi, M., Balliet, A. G., Hoffman, B., and Liebermann, D. A. (2002) *J. Cell Physiol* **192**, 327-338
45. Wang, Q., Tang, X. N., and Yenari, M. A. (2007) *J. Neuroimmunol.* **184**, 53-68
46. Engelmann, A., Speidel, D., Bornkamm, G. W., Deppert, W., and Stocking, C. (2008) *Oncogene* **27**, 1429-1438
47. Papa, S., Zazzeroni, F., Bubici, C., Jayawardena, S., Alvarez, K., Matsuda, S., Nguyen, D. U., Pham, C. G., Nelsbach, A. H., Melis, T., De, S. E., Tang, W. J., D'Adamio, L., and Franzoso, G. (2004) *Nat. Cell Biol.* **6**, 146-153
48. Abdollahi, A., Lord, K. A., Hoffman-Liebermann, B., and Liebermann, D. A. (1991) *Cell Growth Differ.* **2**, 401-407
49. Amanullah, A., Azam, N., Balliet, A., Hollander, C., Hoffman, B., Fornace, A., and Liebermann, D. (2003) *Nature* **424**, 741
50. Gupta, M., Gupta, S. K., Hoffman, B., and Liebermann, D. A. (2006) *J. Biol. Chem.* **281**, 17552-17558
51. Takekawa, M. and Saito, H. (1998) *Cell* **95**, 521-530
52. Smith, M. L., Chen, I. T., Zhan, Q., Bae, I., Chen, C. Y., Gilmer, T. M., Kastan, M. B., O'Connor, P. M., and Fornace, A. J., Jr. (1994) *Science* **266**, 1376-1380

53. Wang, X. W., Zhan, Q., Coursen, J. D., Khan, M. A., Kontny, H. U., Yu, L., Hollander, M. C., O'Connor, P. M., Fornace, A. J., Jr., and Harris, C. C. (1999) *Proc. Natl. Acad. Sci. U. S. A* **96**, 3706-3711
54. Azam, N., Vairapandi, M., Zhang, W., Hoffman, B., and Liebermann, D. A. (2001) *J. Biol. Chem.* **276**, 2766-2774
55. Hall, P. A., Kearsley, J. M., Coates, P. J., Norman, D. G., Warbrick, E., and Cox, L. S. (1995) *Oncogene* **10**, 2427-2433
56. Vairapandi, M., Liebermann, D. A., Hoffman, B., and Duker, N. J. (2000) *J. Cell Biochem.* **79**, 249-260
57. Vairapandi, M., Balliet, A. G., Fornace, A. J., Jr., Hoffman, B., and Liebermann, D. A. (1996) *Oncogene* **12**, 2579-2594
58. Chi, H., Lu, B., Takekawa, M., Davis, R. J., and Flavell, R. A. (2004) *EMBO J.* **23**, 1576-1586
59. Chung, H. K., Yi, Y. W., Jung, N. C., Kim, D., Suh, J. M., Kim, H., Park, K. C., Song, J. H., Kim, D. W., Hwang, E. S., Yoon, S. H., Bae, Y. S., Kim, J. M., Bae, I., and Shong, M. (2003) *J. Biol. Chem.* **278**, 28079-28088
60. Yang, J., Zhu, H., Murphy, T. L., Ouyang, W., and Murphy, K. M. (2001) *Nat. Immunol.* **2**, 157-164
61. Papa, S., Monti, S. M., Vitale, R. M., Bubici, C., Jayawardena, S., Alvarez, K., De, S. E., Dathan, N., Pedone, C., Ruvo, M., and Franzoso, G. (2007) *J. Biol. Chem.* **282**, 19029-19041
62. Papa, S., Zazzeroni, F., Fu, Y. X., Bubici, C., Alvarez, K., Dean, K., Christiansen, P. A., Anders, R. A., and Franzoso, G. (2008) *J. Clin. Invest* **118**, 1911-1923
63. Ali, H. I., Ashida, N., and Nagamatsu, T. (2008) *Bioorg. Med. Chem.* **16**, 922-940
64. Kovalsky, O., Lung, F. D., Roller, P. P., and Fornace, A. J., Jr. (2001) *J. Biol. Chem.* **276**, 39330-39339
65. Orłowski, R. Z. and Baldwin, A. S., Jr. (2002) *Trends Mol. Med.* **8**, 385-389
66. Nefzi, A., Ostresh, J. M., Yu, Y., and Houghten, R. A. (2004) *J. Org. Chem.* **69**, 3603-3609
67. Marasco, D., Perretta, G., Sabatella, M., and Ruvo, M. (2008) *Curr. Protein Pept. Sci.* **9**, 447-467
68. Nordling, E. and Homan, E. (2004) *J. Chem. Inf. Comput. Sci.* **44**, 2207-2215
69. Sato, A. K., Viswanathan, M., Kent, R. B., and Wood, C. R. (2006) *Curr. Opin. Biotechnol.* **17**, 638-642

70. Werle, M. and Bernkop-Schnurch, A. (2006) *Amino. Acids* **30**, 351-36
71. Pini, A., Falciani, C., and Bracci, L. (2008) *Curr. Protein Pept. Sci.* **9**, 468-477
72. Jain, R. and Chawrai, S. (2005) *Mini. Rev. Med. Chem.* **5**, 469-477
73. Landon, L. A., Zou, J., and Deutscher, S. L. (2004) *Curr. Drug Discov. Technol.* **1**, 113-132
74. Granata, V., Graziano, G., Ruggiero, A., Raimo, G., Masullo, M., Arcari, P., Vitagliano, L., and Zagari, A. (2006) *Biochemistry* **45**, 719-726
75. Cobb, M. H. and Goldsmith, E. J. (2000) *Trends Biochem. Sci.* **25**, 7-9
76. Zhan, Q., Antinore, M. J., Wang, X. W., Carrier, F., Smith, M. L., Harris, C. C., and Fornace, A. J., Jr. (1999) *Oncogene* **18**, 2892-2900
77. Yang, Q., Manicone, A., Coursen, J. D., Linke, S. P., Nagashima, M., Forgues, M., and Wang, X. W. (2000) *J. Biol. Chem.* **275**, 36892-36898
78. Schrag, J. D., Jiralerspong, S., Banville, M., Jaramillo, M. L., and O'Connor-McCourt, M. D. (2008) *Proc. Natl. Acad. Sci. U. S. A* **105**, 6566-6571
79. Nakajima, A., Komazawa-Sakon, S., Takekawa, M., Sasazuki, T., Yeh, W. C., Yagita, H., Okumura, K., and Nakano, H. (2006) *EMBO J.* **25**, 5549-5559
80. Pelech, S. (2006) *J. Biol.* **5**, 12
81. Gao, H., Jin, S., Song, Y., Fu, M., Wang, M., Liu, Z., Wu, M., and Zhan, Q. (2005) *J. Biol. Chem.* **280**, 10988-10996
82. Bogoyevitch, M. A. and Fairlie, D. P. (2007) *Drug Discov. Today* **12**, 622-633

## 6. ABBREVIATION INDEX

**4-VP:** 4- vinyl pyridine  
**BSA:** Bovine Serum Albumin  
**CD:** Circular Dichroism  
**DMEM:** Dulbecco's Modified Eagle's Medium  
**DMF:** *N,N*-dimethylformamide  
**DTT:** 1,4-Dithiothreitol  
**ELISA:** Enzyme-Linked Immunosorbent Assay  
**ERK:** Extracellular Signal-Regulated Kinase  
**FACS:** Fluorescence-Activated Cell Sorting  
**FBS:** Fetal Bovine Serum  
**Fmoc:** 9H-Fluoren-9-ylmethoxycarbonyl  
**FPLC:** Fast Protein Liquid Chromatography  
**Gadd:** Growth Arrest DNA Damage inducible  
**GdnHCl:** Guanidine Hydrochloride  
**GFP:** Green Fluorescent Protein  
**HA tag:** Hemagglutinin (Epitope YPYDVPDYA)  
**HEK:** Human Epithelia Cells  
**HPLC:** High Performance Liquid Chromatography  
**HRP:** horseradish peroxidase  
**IPTG:** isopropyl-beta-D-thiogalactopyranoside  
**JNK:** Jun N-terminal Kinase  
**LB:** Luria-Bertani  
**LC-MS:** Liquid Chromatography-Mass Spectrometry  
**LPS:** Lipopolysaccharide  
**MAPKs:** Mitogen Activated Protein Kinase  
**MKK:** MAP Kinase Kinase  
**NF- $\kappa$ B:** Nuclear Factor- $\kappa$ B  
**NHS:** N-hydroxysuccinimide  
**OD<sub>600</sub>:** Optical Density at 600 nm  
**OPD:** orthophenyldiamine  
**P/I :** PMA/ ionomycin  
**PBS:** Phosphate Buffered Saline  
**PCR:** Polymerase Chain Reaction  
**PDA:** Photodiode Array  
**PMA:** Phorbol Myristate Acetate  
**PMSF:** Phenylmethylsulphonylfluoride (Inhibitor of Serine proteases)  
**RP-HPLC:** Reverse Phase-High Pressure Liquid Chromatography  
**SAPK:** Stress Activated Protein Kinase  
**SPPS:** Solid-Phase Peptide Synthesis  
**TFA:** Trifluoroacetic acid  
**TIS:** triisopropylsilane  
**TNF- $\alpha$ :** Tumor Necrosis Factor- $\alpha$   
**Tris:** Triisopropylsilane

## 7. SCIENTIFIC PRESENTATIONS

1. **Tornatore L**, Monti SM, Dathan N, Sandomenico A, Marasco D, Doti N, Viparelli F, Pizzulo M, Amoroso M, Benedetti E, Pedone C, Ruvo M. Expression, purification and characterization of Gadd45 $\beta$ . 10th Naples workshop on bioactive peptides, Naples (Italy), 11-14 June 2006
2. Viparelli F, Doti N, Sandomenico A, Monti SM, Nina Dathan N, **Tornatore L**, Pizzulo M, Amoroso M, Beguinot F, Miele C, Marasco D, Benedetti E, Pedone C, Ruvo M. PED binds with high affinity to the D4 domain of PLD1. 10th Naples workshop on bioactive peptides, Naples (Italy), 11-14 June 2006
3. Sandomenico A, Monti SM, **Tornatore L**, Dathan N, Doti N, Viparelli F, Marasco D, Saporito A, Sabatella M, Pedone C, DeCapua A, Saviano M, Benedetti E, Ruvo M. Peptide mimics of the IgE high affinity receptor Fc $\epsilon$ . 6 $^{\circ}$  Pharmaco-Bio-Metallics, Naples (Italy), 30 November-1 December 2006
4. **Tornatore L**, Monti SM, Dathan N, Doti N, Viparelli F, Sandomenico A, Marasco D, Saporito A, Sabatella M, Pedone C, Benedetti E, Ruvo M. Antagonists of Gadd45 $\beta$ -MKK7 interaction by screening of a synthetic peptide library. 9th International symposium on Applied Bioinorganic Chemistry, Naples (Italy), 2-5 December 2006
5. Sandomenico A, Monti SM, **Tornatore L**, Dathan N, Doti N, Viparelli F, Marasco D, Ronga L, Saporito A, Sabatella M, Pedone C, DeCapua A, Benedetti E, Ruvo M. Synthetic peptide ligands for  $\alpha$ 1AT. 6 $^{\circ}$  Pharmaco-Bio-Metallics, Naples (Italy), 30 November-1 December 2006
6. **Tornatore L**, Monti SM, Marasco D, Dathan N, Vitale RM, Benedetti E, Pedone C, Papa S, Franzoso G, Ruvo M. Gadd45 $\beta$  dimerization does not affect MKK7 binding. 2007 American Peptide Society Symposium, Montreal, Quebec, CANADA 26-30 June 2007
7. Marasco D, Cutillo F, Saporito A, **Tornatore L**, Sandomenico A, Sabatella M, Doti N, Viparelli F, Pedone C, Dathan N, Monti SM, Ruvo M. A simplified and automated perspective for the screening of universal synthetic peptide libraries. EUROCOMBI 4, Firenze, 15-18 Luglio 2007
8. **Tornatore L**, Vitale RM, Dathan N, Marasco D, Papa S, Franzoso G, Benedetti E, Ruvo M and Monti SM. Insights into the dimeric structure of Gadd45 $\beta$  and its interaction with MKK7. 11th Naples workshop on bioactive peptides, Naples (Italy), 25-27 May 2008

9. Marasco D, Sandomenico A, **Tornatore L**, Viparelli F, Doti N, Sabatella M, Monti SM, Benedetti E, Pedone C and Ruvo M. Protein-protein interactions and peptide antagonists. 11th Naples workshop on bioactive peptides, Naples (Italy), 25-27 May 2008

## **8. PUBLICATION**

**Tornatore L**, Marasco D, Dathan N, Vitale RM, Bendetti E, Papa S, Franzoso G, Ruvo M, Monti, S. "Gadd45 $\beta$  forms a homodimeric complex that binds tightly to MKK7". (2008) Journal of Molecular Biology, 378, 97-111.

**Gadd45 $\beta$  forms a homodimeric complex that binds tightly to MKK7**  
**Laura Tornatore<sup>1,2#</sup>, Daniela Marasco<sup>1#</sup>, Nina Dathan<sup>1</sup>, Rosa Maria Vitale<sup>3</sup>,**  
**Ettore Benedetti<sup>2</sup>, Salvatore Papa<sup>4</sup>, Guido Franzoso<sup>4</sup>, Menotti Ruvo<sup>1\*</sup>,**  
**Simona Maria Monti<sup>1\*</sup>**

<sup>1</sup> Istituto di Biostrutture e Bioimmagini (IBB), CNR, via Mezzocannone, 16, 80134, Napoli, Italy

<sup>2</sup> Dipartimento delle Scienze Biologiche, via Mezzocannone, 16, 80134, Napoli, Italy

<sup>3</sup> Istituto di Chimica Biomolecolare (ICB), CNR, Via Campi Flegrei, 34, 80078 Pozzuoli, (NA), Italy.

<sup>4</sup> Department of Immunology at Hammersmith, Division of Investigative Science, Imperial College, London, Du Cane Road, London W12 ONN, UK.

# These two authors equally contributed to the work

\*Corresponding authors.

Correspondence should be mailed to either:

**Simona Maria Monti**

Istituto di Biostrutture e Bioimmagini (IBB), CNR,  
via Mezzocannone, 16, 80134, Napoli, Italy

Ph.: +39-081-2534583

Fax: +39-081-2534574

Email: marmonti@unina.it

and

**Menotti Ruvo**

Istituto di Biostrutture e Bioimmagini (IBB), CNR,  
via Mezzocannone, 16, 80134, Napoli, Italy

Ph.: +39-081-2536644

Fax: +39-081-2534574

Email: menotti.ruvo@unina.it

Running title: homodimerization of Gadd45 $\beta$  and binding to MKK7

## **Abstract**

Gadd45 $\alpha$ ,  $\beta$ , and  $\gamma$  proteins, also known as growth arrest and DNA damage-inducible factors, exert a number of cellular functions, including cell cycle regulation and propagation of signals produced by a variety of cellular stimuli, maintaining genomic stability and apoptosis. Furthermore Gadd45 $\beta$  has been indicated as a major player in the endogenous NF- $\kappa$ B-mediated resistance to apoptosis in a variety of cell lines. In fibroblasts this mechanism involves the inactivation of MKK7, the upstream activator of JNK, by direct binding within the kinase ATP pocket. Based on a number of experimental data, the structures of Gadd45 $\beta$  and the Gadd45 $\beta$ -MKK7 complex have recently been predicted and data show that interactions are mediated by the acidic loop1 and 2 and helices 3 and 4 of Gadd45 $\beta$ . Here we provide further evidence that Gadd45 $\beta$  is a prevalingly  $\alpha$ -helical protein and that in solution it is able to form non covalent dimers but not higher order oligomers, contrarily to what reported for the homologous Gadd45 $\alpha$ . We also show that the contact region between the two monomers is comprised of the predicted helices 1 (residues Q17-Q33) and 5 (residues K131-R146) of the protein which appear to be antiparallel and to form a large dimerization surface not involved in MKK7 recognition. Data thus suggest the occurrence of a high molecular weight complex containing at least an MKK7-Gadd45 $\beta$ :Gadd45 $\beta$ -MKK7 tetrameric unit whose complexity could be further increased by the dimeric nature of the isolated MKK7.

## **INTRODUCTION**

The *gadd45* growth arrest and DNA damage-inducible family of genes, comprising *gadd45a*, *gadd45b* and *gadd45g*, encode for the corresponding Gadd45 $\alpha$ , Gadd45 $\beta$  and Gadd45 $\gamma$  acidic proteins of about 18 kDa. They are ubiquitously expressed and exert the primary function of growth arrest and apoptosis induction in response to several genotoxic stresses thus contributing to cellular homeostasis<sup>1; 2; 3; 4; 5; 6</sup>. They have also been implicated in a variety of other cell functions such as DNA replication and repair<sup>7</sup>, cell

cycle regulation<sup>8</sup>, and, depending on cell type and cell metabolic state, also in cell survival<sup>4; 9; 10; 11; 12; 13; 14; 15; 16</sup>. This last property is seemingly mostly exhibited by Gadd45 $\beta$  which has been described as an NF- $\kappa$ B-inducible gene and as a prominent mediator of the NF- $\kappa$ B protective response to TNF $\alpha$ - and UV-induced apoptosis<sup>4; 11; 17</sup>. However this aspect is still controversial and several reports indicate Gadd45 $\beta$  as an effective pro-apoptotic factor, too<sup>5; 6; 17</sup>. The mechanisms by which Gadd45 $\beta$  can promote cell survival have been extensively investigated and it has been found that in MEFs and other cells, upon NF- $\kappa$ B induction, it provides selective JNK inactivation by inhibition of the upstream MKK7<sup>1; 10; 18</sup>. In hematopoietic cells, instead, it blocks JNK activation by binding to MKK4<sup>4; 19</sup>, and in B cells it is a critical mediator of the pro-survival activity of CD40 elicited in response to Fas stimulation<sup>9</sup>.

Since there is no reported enzymatic activity for the Gadd45 proteins, it is believed that they exert their functions interacting with protein partners. Indeed, other than MKK7 and MKK4, highly specific interactions with PCNA<sup>6; 20; 21; 22</sup>, cdc2<sup>23</sup>, waf/p21<sup>24</sup>, cdk1/cyclinB1<sup>25</sup>, MEKK4<sup>26</sup> and CRIF1<sup>27</sup> are involved in Gadd45 regulation of the cell cycle and the response to external cell stimuli. A further interaction with the protein nucleophosmin<sup>28</sup> has been described for Gadd45 $\alpha$  and it has been shown that this protein can work as a vehicle for nuclear import. However, at present it is unknown whether Gadd45 $\beta$  and Gadd45 $\gamma$  share a similar mechanism of nuclear translocation. Importantly, it has been reported that Gadd45 proteins are also able to homo- and hetero-dimerize or oligomerize and regions involved in self-association of Gadd45 $\alpha$  have been investigated using overlapping synthetic peptides spanning the entire protein sequence<sup>29</sup>.

The primary sequences of Gadd45 proteins share an overall 70% homology (about 60% identity, See Fig. 1a) and all contain six cysteines, five of which (from the 2nd to the 6th) are located in highly conserved positions.

An unusually long stretch of glutamic and aspartic acid residues, only partially conserved within the Gadd45 $\gamma$  variant, can be found starting from position 60 of Gadd45 $\alpha$  and Gadd45 $\beta$ . These residues have been described as having a key role in both cdc2<sup>23</sup> and MKK7 inhibition<sup>1; 10</sup>. However, the 3D structure of this important class of proteins is currently unknown and so far a

predicted model has been reported<sup>1</sup> for Gadd45 $\beta$  (Fig. 1b, 1c) and its complex with MKK7. These structures, supported by various experimental evidences, present a central four-stranded  $\beta$ -sheet surrounded by 5  $\alpha$ -helices and, as expected for a nuclear protein, all cysteine residues are predicted to reside far from each other and thus in the reduced state<sup>1</sup>. The acidic stretch appears to be in a large loop interacting with several basic and polar residues within the kinase active site and it is part of the minimum region of Gadd45 $\beta$  needed to bind and block MKK7 activity (A60-D86 fragment). Other regions involving the putative helix 3 (H3), a second acidic loop and part of helix 4 (H4) harbour other key residues contacting MKK7.

Following an approach of protein enzymatic fragmentation and HPLC fractionation, here we identify the regions of Gadd45 $\beta$  implicated in self-association and confirm those involved in binding with MKK7. We also show that Gadd45 $\beta$  is unable to form higher order oligomers, as only dimers are detected using different methods. These studies extend our knowledge on Gadd45 $\beta$  properties and suggest that protein self-association can have a primary role in regulating its biological activity.

## RESULTS

### Gadd45 $\beta$ purification

Recombinant construct pGEX6P-GADD45 $\beta$  allowed expression of the protein as a GST-fusion product containing a highly specific cleavage site for PreScission Protease upstream of the Gadd45 $\beta$  protein. The applied overexpression system was quite efficient, producing more than 6 mg of highly purified protein from 1 L of induced culture under the previous reported conditions<sup>1</sup>. The recombinant protein obtained after GST removal had the sequence reported in Fig. 1b and was used only for oligomerization studies. The protein was characterized by SDS-PAGE and LC-MS analysis determining the exact MW ( $MW_{Exp/Theor}$ : 18096.6 $\pm$ 1.0/18096.1 Da). His<sub>6</sub>-Gadd45 $\beta$  used in the ELISA assays was similarly obtained with high yields and purity. The MW of 19196.5 amu as determined by LC-MS was consistent with the protein sequence ( $MW_{theoretical}$ : 19196.52 amu). The protein was efficiently derivatized with biotin as described in the Methods section. Protein derivatization was assessed by mass spectrometry showing that about 90% of the protein harboured one biotin molecule, while the remaining appeared underivatized (data not shown).

### Investigation of Gadd45 $\beta$ oligomerization by gel filtration and CD studies

Since previous studies reported on the capacity of Gadd45 proteins to oligomerize<sup>29</sup>, we investigated this point by carrying out a gel filtration analysis in the presence and/or absence of DTT and by native electrophoresis experiments. Gel filtration analysis of protein aliquots at the concentration of 5.0  $\mu$ M, showed that, in absence of DTT, two peaks were eluted at column volumes corresponding to a dimeric and tetrameric protein, that is 36 kDa and 72 kDa, respectively (Fig. 2a, 2c). Conversely, under reducing conditions, the tetramer peak disappeared (Fig. 2b), indicating that it was held together by disulfide bridges, whereas the dimer was associated also through strong non-covalent interactions. The presence of protein dimers or oligomers was also investigated by native gels, observing in this case the dimer and the monomer (Fig. 2d). According to these data Gadd45 $\beta$  seemingly exists in solution prevalently as a dimeric protein, in partial equilibrium – under certain

conditions (the non-denaturing gel) – with the monomer. Indeed, no higher order oligomers have been detected by either techniques.

The far-UV CD spectrum of Gadd45 $\beta$  ( $11 \times 10^{-6}$  M) in aqueous solution showed two negative bands at 209 and 222 nm and a positive band at 195 nm indicative of a high content of  $\alpha$ -helical conformations (Fig. 3a), as previously reported<sup>1</sup>. Importantly, also the His<sub>6</sub>-Gadd45 $\beta$ , utilized in different assays exhibited a very similar CD spectrum (not shown). The occurrence of oligomers was also investigated by this technique by comparative analysis of protein solutions at different concentrations. No differences were detectable between CD curves recorded on protein solutions at concentrations ranging between  $5.5 \times 10^{-5}$  M and  $5.5 \times 10^{-6}$  M (not shown) suggesting that dilution, at least in the range of the explored concentrations, did not affect the protein global folding nor the quaternary structure. Therefore, no indications could be obtained on the actual monomer-dimer status of the protein by this experiment. A CD analysis of the dependence on denaturant concentration was also performed to further assess the protein structure stability or the capacity to eventually dissociate into monomers. Chemical denaturation data (Fig. 3b and 3c) showed that Gadd45 $\beta$  unfolds cooperatively at about 2.0 M GdnHCl and 3.0 M urea. This may indicate that electrostatic interactions, which are more efficiently weakened by GdnHCl than urea<sup>30</sup>, play an important role in stabilization of Gadd45 $\beta$ .

Upon denaturant removal, the protein secondary structure was recovered (Fig. 3a), suggesting that denaturation, as well as the eventual dimer dissociation (assuming it occurs at high denaturant concentration) is a reversible event. Also thermal denaturation experiments were carried out to confirm these observations; a single transition was observed at about 46.5 °C, but, most importantly, after slow cooling back to 20 °C, the protein could not recover the original structure because of disulfide cross-linking (detected by SDS-PAGE under reducing and non-reducing conditions, not shown). In comparison to those of other globular proteins<sup>31</sup> the melting temperature is quite low indicating that Gadd45 $\beta$  is not a thermodynamically stable protein, according to the predicted structure that exhibits large and flexible loops<sup>1</sup>.

### **Expression and purification of MKK7**

MKK7 was produced in bacteria as a soluble GST-MKK7 fusion product. About 7 mg/L of the fusion protein were obtained in typical fermentations. The protein was initially purified by standard GSTrap and on-column PreScission protease cleavage. The material recovered was further purified by gel filtration chromatography, obtaining a product more than 95% pure. The protein was characterized by SDS-PAGE and LC-MS analysis and the experimental MW was consistent with that expected (not shown). Protein identity was further confirmed by trypsin digestion and LC-MS/MS analysis of the resulting fragments (not shown). The folding of MKK7 was assessed by CD analysis observing, as expected<sup>1</sup>, a spectrum with a mixed  $\alpha$ - $\beta$  content (Fig. 4a). In Fig. 4b the determination of the oligomeric state of the protein by gel filtration analysis is reported: the protein appears as a dimer, exhibiting an apparent MW of about 90 kDa. Importantly, also the fusion protein GST-MKK7, used in several assays in this study, eluted from the gel filtration column as a dimer.

### **Identification of regions of Gadd45 $\beta$ involved in auto-association**

In an attempt to determine the protein self association surface, we used Gadd45 $\beta$  fragments as competitors of the protein self-association in an ELISA-like assay (see below). For this purpose, protein digestion by several enzymes was considered, comparing enzyme efficacy and specificity other than the length and complexity of the obtainable peptides. Following this analysis, an extensive digestion of a protein aliquot was carried out with trypsin which resulted in complete digestion and formation of fragments of suitable length to ensure a complete coverage of the protein primary structure (See Table I). Upon RP-HPLC fractionation (13 fractions), Gadd45 $\beta$  peptides, identified by MW and MS/MS sequencing, were essentially distributed along 7 main fractions, since fractions 1-5 contained no material and fraction 11 contained only very small amounts (less than 4%) of fragment L46-R91. All identified trypsin fragments are reported in Table I along with a correspondence with the predicted Gadd45 $\beta$  secondary structure reported in <sup>1</sup>. Fractions 6, 7, 8, 9, 10, 12 and 13 contained relevant amounts of the protein fragments. Notably, fraction 6 only contained the C-terminal G147-R160 peptide (unstructured); fraction 7 contained, in a 1:1 ratio, the fragments L36-

K45 (part of  $\beta$ 1 and part of  $\alpha$ 2) and L98-R115 (part of  $\alpha$ 4; most of loop 2); fraction 8 contained (in a 85:15 ratio), a major fraction of fragments S132-R146 (87%, the central region of  $\alpha$ 5, hereafter H5 short) and the peptide D116-K131 ( $\beta$ 4); fraction 9 contained, in a 75:25 ratio, the N-terminal polyhistidine tag and a minor fraction of the peptide S132-R146 ( $\alpha$ 5); fraction 10 contained only the fragment M16-R32 (92%, the remaining being distributed along the contiguous fractions), corresponding to most of helix 1; fraction 12 and 13 contained the fragment L46-R91, corresponding to part of  $\alpha$ 2,  $\beta$ 2, loop1,  $\alpha$ 3, and part of  $\beta$ 3. The ELISA assay to monitor Gadd45 $\beta$  self-association was carried out by coating the His<sub>6</sub>-protein on the surface of microtiter wells. Protein association was followed by adding increasing amounts of biotinylated His<sub>6</sub>-Gadd45 $\beta$  and detecting the bound protein by using HRP-STRV. As shown in Figure 5a, the protein efficiently associated in a dose-dependent way, reaching signal saturation at a nearly 1:1 (mol/mol) ratio, as expected by a dimeric complex. The concentration of His<sub>6</sub>-Gadd45 $\beta$  resulting in a 50% of maximum binding was around 100 nM and it was taken as an estimation of the dissociation constant of self-association. To identify the Gadd45 $\beta$  regions involved in protein dimerization binding competition assays were then carried out using peptide fragments derived from Gadd45 $\beta$  digestion. The assays were performed using an invariable 1:0.5 (mol/mol) ratio of coated/soluble His<sub>6</sub>-Gadd45 $\beta$  and a 2:1 (mol/mol) ratio of peptide competitor/soluble protein. Initially, the synthetic peptide Gadd45 $\beta$ (A60-D86) described in reference<sup>1</sup> as the minimum Gadd45 $\beta$  region able to bind MKK7, inhibiting its kinase activity, together with the synthetic MKK7(G132-N156), described as recapitulating the full length MKK7 binding capacity<sup>10</sup>. Results are summarized in Fig. 5b, where a plot of representative data is reported. Gadd45 $\beta$  trypsin fractions from 1 to 5 and fraction 11 were not utilized. Fractions 6, 7, 12 and 13 which contained consistent amounts of protein fragments (see Table I) were essentially ineffective. In contrast, fractions 8 to 10 interfered with the association. In particular, fraction 8 exhibited a nearly 30% binding reduction, fraction 10, which virtually contained only fragment M16-R32 (see Table I) including most residues from the helix 1, decreased protein association to about 50%, whereas fraction 9, containing most residues of the tag and a minor part of fragment S132-R146, disrupted

Gadd45 $\beta$  self-association by 25%. Interestingly, the synthetic peptides Gadd45 $\beta$ (A60-D86) and MKK7(G132-N156), identified as forming the binding interface between Gadd45 $\beta$  and MKK7<sup>1:10</sup>, appeared totally ineffective in this assay (also discussed later). To refine the ELISA data, those fragments unable to disrupt Gadd45 $\beta$ -Gadd45 $\beta$  interaction were not considered; furthermore, on examination of the predicted Gadd45 $\beta$  3D model, it was decided not to further investigate the fragment D116-K131, present in fraction 8 at 15%, since it corresponds to the fourth  $\beta$ -strand which should be buried within the protein core and therefore virtually inaccessible to external interactions (Fig. 1c). Hence we decided to investigate regions M16-R32 and S132-R146 corresponding to the regions within the putative H1 and H5, respectively. Examining the protein model, (Fig. 1c) the peptides were opportunely designed by adding N- and C-terminal amino acids in order to complete the helices, hence the corresponding synthetic peptides, A12-R35 (hereafter extended Helix 1, eH1) and A129-N148 (hereafter extended Helix 5, eH5) were prepared by chemical synthesis and purified to homogeneity by RP-HPLC. The peptide R91-E104, corresponding to the extended predicted eH4, was also similarly prepared and utilized as a negative control. These peptides were then tested in the Gadd45 $\beta$ -Gadd45 $\beta$  competition assay, using the same protein-protein and protein-competitors ratios as described previously. As shown in the same Fig. 5b, eH1 and eH5 blocked the Gadd45 $\beta$  self association by 82% and 78%, respectively, supporting the hypothesis that these regions are strongly involved in the interaction. On the contrary, peptide R91-E104 (eH4), lying in the model in the close proximity of H1 (Fig. 1c), as well as peptides Gadd45 $\beta$ (A60-D86) and MKK7(G132-N156) and the full length kinase did not interfere with the protein homodimerization. A dose-dependent competition assay carried out with eH1, eH5, the short H5, eH4 and full length MKK7, further confirmed the properties of H1 and H5 and the inefficacy of H4 to abrogate dimerization (See Fig. 5c). As expected, the full length kinase (fused to GST) was unable to block the Gadd45 $\beta$  self-association even at higher concentrations. Remarkably, the IC<sub>50</sub> for these competitors were 100 nM for H1, 180 nM for the extended Helix 5 and only 600 nM for the short H5, indicating that the full H5 was more than 3 times efficient in disrupting the protein self-association. These results might account

for the relatively weak inhibition exhibited by fractions 8 (30%) and 9 (25%) which only contained the shorter variant of the H5. To further investigate this point, the synthetic peptides reproducing eH1, eH5, the short H5 and the eH4 were analyzed by CD. The analyses were carried out in both phosphate buffer and in the presence of 20% TFE to measure the relative propensity of peptides to adopt  $\alpha$ -helical conformations. As reported in Fig. 6a-d, whereas eHelices 1, 4 and 5 adopted a partially folded structure in buffer and readily folded into  $\alpha$ -helices upon TFE addition, the short H5 remained in the unfolded state even after addition of the structuring solvent, suggesting an intrinsic incapacity to form organized structures. Thus, increasing the length at the N- and C-termini of the putative H5 provided a 5-fold increase in potency that can be partially ascribed to the lack of any structure of shorter variant.

To further extend our knowledge of the interaction between the two monomers, we developed an assay to monitor the binding between MKK7 and Gadd45 $\beta$ . Indeed this interaction has been thoroughly investigated in previous works by pull-down assays utilizing several point-mutated variants of both proteins<sup>1; 10</sup>. As shown in Fig. 7a, the association between the two purified protein was very strong: a rough estimation of the  $K_D$ , deduced by the Gadd45 $\beta$  concentration at half of the saturation signal, was about 13 nM. Noticeably, signal saturation was reached at an approximate 1:1 molar ratio, suggesting that one MKK7 molecule should be sufficient to bind to one molecule of Gadd45 $\beta$ . The competition experiment carried out using 42 nM MKK7, 21 nM Gadd45 $\beta$  and a twofold excess of competitors over the soluble protein, is reported in Fig. 7b. As shown, peptides corresponding to the putative extended Helices 1, 4 and 5, MKK7(G132-N156) and Gadd45 $\beta$ (A60-D86) were utilized. Consistent with the notion that MKK7 proximity do not interfere with the Gadd45 $\beta$  dimerization, eH1 and eH5 do not affect the binding, whereas peptides Gadd45 $\beta$ (A60-D86) and MKK7(G132-N156), believed to form part of the interface between the two proteins, completely abolish the interaction. The peptide R91-E104 corresponding to the putative eH4 and containing two key residues (M95/Q96) involved in kinase recognition<sup>1</sup>, also proved ineffective to antagonize the Gadd45 $\beta$ -kinase binding, at the used concentration. Instead, soluble GST-MKK7, as expected, totally abolished the binding. Thus, these results corroborate the view that the

Gadd45 $\beta$ -MKK7 interaction is essentially mediated by residues comprised within loop 1 and H3 (region A60-D86) <sup>1</sup>, while other regions, such as H4, only partially contribute or may have only a structural role.

### **Modelling of the Gadd45 $\beta$ homodimer**

To have a more detailed depiction of interactions occurring at the interface between the two monomers, we performed manual docking of the two units. Examining the Gadd45 $\beta$  model, H1 and H5 helices form a continuous surface and constitute a putative half of a four-helix bundle motif. On this basis, a number of Gadd45 $\beta$  homo-dimer models were constructed. Several relative orientations, both parallel and antiparallel, of the two monomers were tested in order to optimize both steric and electrostatic complementarity. An accurate analysis was then carried out to assess the effective stability and consistency of the resulting complexes, therefore each starting model underwent energy minimisation and then 200ps of molecular dynamics (MD) simulations in solution. The best model in terms of specific side-chains interactions is reported in Fig. 8a, 8B. The model suggests that the dimerization region can form a four-helix bundle in which H1 and H5 helices of one monomer interact in an antiparallel fashion with the corresponding helices of the other monomer. This representation also shows how the proposed complex is stabilized by a network of intermolecular polar interactions involving Gln13, Thr14 and Glu21 on H1 and Glu140, Tyr137, Glu133 and His 129 on H5. The presence of Glu residues univocally determines the antiparallel orientation of the subunits, because in the parallel one these residues face each other, thus destabilizing the complex. Interestingly, a four-helix bundle search in the PDB reveals the occurrence of a homo-dimer stabilized by intermolecular polar interactions in which Glu residues interact with Tyr and His (PDB entry 1U7M), similarly to what observed in our Gadd45 $\beta$  dimer model.

## DISCUSSION

Protein dimerization and oligomerization have been often associated with protein function. Indeed, auto-association can be seen as a way to mask-unmask functional sites or, for example, to regulate protein degradation by making inaccessible regions otherwise marked for degradation<sup>32; 33</sup>. Protein self-association is therefore believed to be a regulative mechanism under both physiological and pathological conditions.

For Gadd45 proteins, a family of intracellular and intranuclear acidic proteins, this mechanism has also been speculated, as, reportedly, they homo- and hetero-dimerize and oligomerize under a variety of conditions<sup>29</sup>; the oligomerization properties of Gadd45 $\alpha$  have been previously investigated and it has been seen that the protein can form dimers and higher order oligomers also with Gadd45 $\beta$  and Gadd45 $\gamma$ <sup>29</sup>. Given the high number of molecular interactions they establish, a deeper knowledge of regions involved in self-association is of pre-eminent importance, as the occurrence of homo-oligomerization can impair Gadd45 functions as well as strongly influencing hetero-interactions.

To extend our knowledge on the properties of Gadd45 proteins, we have investigated whether Gadd45 $\beta$  can also dimerize-oligomerize and whether this ability can influence its interaction with MKK7, an important component of the MAP kinase cascade whose function in cellular apoptosis is regulated by Gadd45 $\beta$  itself<sup>10</sup>. As a first step, oligomerization was extensively investigated by gel filtration chromatography, CD and native gel analyses. Gel filtration experiments unequivocally showed that Gadd45 $\beta$  exists in solution as a non covalent dimer at a concentration of about 5  $\mu$ M, a concentration 50-fold higher than the estimated self-association  $K_D$  (about 100 nM). Indeed, under reducing conditions, only a single sharp peak at the elution volume of the dimer (36 kDa) was detected. Consistently, by CD analysis, no structural changes were observed for protein concentrations between  $5.5 \times 10^{-6}$  M and  $5.5 \times 10^{-5}$ , that is 55-fold and 550-fold excess over the estimated  $K_D$ , respectively. The ELISA-like assay utilized to determine the  $K_D$ , also showed that the protein self-binding is saturated for protein:protein ratios higher than 1:1 (mol/mol), suggesting, likewise, the occurrence of dimers only. In agreement with all these findings, the analysis on native gels revealed the

presence of the dimeric protein and some monomer, whereas no higher order oligomers were detected. Therefore, in contrast to previous data on Gadd45 $\alpha$ , Gadd45 $\beta$  is seemingly able to only form dimers, that, under some conditions appear to be in equilibrium with monomers. Importantly, the self-association constant, estimated to be about 100 nM, is much lower than that estimated for Gadd45 $\alpha$  (about 2.5  $\mu$ M,<sup>29</sup>) and close to the cellular concentration estimated for proteins of this family (about 100 nM)<sup>29</sup>. This discrepancy, partly due to the differences in primary structure, can also be explained by the large differences of protein concentrations utilized in the two studies. Indeed, as the self-association is concentration-dependent, we can reasonably assume that higher order oligomers occur only at very high protein concentration, a condition that is not actually reflected within the cytoplasm and nucleus. Furthermore, the high similarity between the values of  $K_D$  and cell concentration also suggest that an equilibrium between monomers and dimers can occur in the cytoplasm, where up- and down-regulation of the protein could be a way to finely modulate self-association as well as other external interactions.

Following an approach of self-interaction competition with protein fragments derived from trypsin digestion, we identified two distinct Gadd45 $\beta$  sites involved in self-association which correspond to the predicted H1 and H5 of the protein<sup>1</sup>. Remarkably, these findings partially agree with the previous report on Gadd45 $\alpha$ , for which also an N-terminal and a C-terminal region have been described as being involved in self-association. However, whilst the C-terminal site (129–165) is virtually overlapping with the predicted H5 of Gadd45 $\beta$ , the N-terminal site, identified with residues 33-61<sup>29</sup> does not match H1 (see the sequence alignments in Figure 1). Rather, it overlaps with the Gadd45 $\beta$  sequence predicted as the  $\beta$ 1- $\alpha$ 2- $\beta$ 2 region (see reference<sup>1</sup>, and Fig. 1) that is somewhat downstream in the sequence. In the cited study, a large fragment of Gadd45 $\alpha$  (residues 20-33) exactly matching the Gadd45 $\beta$  H1, has not been considered, therefore a further comparison between the two different variants is not possible. However, given the high sequence homology between the two proteins, especially in this part of the sequences, we cannot rule out an involvement of the missing fragment in Gadd45 $\alpha$  auto-association. Noticeably, by looking at the Gadd45 $\beta$  model (see Fig. 1 and 8), H1 and H5

are disposed contiguously and arranged anti-parallel to each other, therefore they seemingly form a large hydrophilic surface that also includes the adjacent H4. This observation still supports the view that the protein is unable to form higher order complexes, as it rules out the presence of a second independent site required to allow the oligomerization to propagate. Moreover, it suggests that auto-association is likely to occur through this unique surface (not involving H4) that, when engaged by a second monomer, could lead to the formation of a compact dimeric structure devoid of further self-interaction sites. The formation of a compact dimer is supported by studies of chemical denaturation with both GndHCl and urea, whereby it is seen that the protein, in the presence of up to 1M denaturants persists in the dimeric form (not shown), whereas it unfolds after reaching higher concentrations.

H4, being parallel to H1, virtually extends the interaction surface towards the protein Loop 2 (see Fig. 1), but does not contribute to protein self-association. On the contrary it is reportedly involved in the binding with MKK7<sup>1</sup>. In agreement with previous reports<sup>1</sup>, and in contrast with others<sup>4; 34</sup>, Gadd45 $\beta$  and MKK7 strongly interact *in vitro*, exhibiting a  $K_D$  of about 13 nM. This value is about 8-fold lower than that estimated for Gadd45 $\beta$  self-association, thus suggesting that the two proteins are also able to interact in the presence of monomeric Gadd45 $\beta$ . Consistently, the two proteins still strongly interact in the presence of both eH1 and eH5 (see Fig. 7b) that efficiently abrogate the Gadd45 $\beta$  dimerization. By characterizing the recombinant MKK7, we found that, in agreement with other reports<sup>35; 36</sup>, also the folded kinase is dimeric (see Fig. 4b), suggesting that the interaction between Gadd45 $\beta$  and MKK7 takes place in the context of a large complex comprising at least two Gadd45 $\beta$  and two kinase units (MKK7/Gadd45 $\beta$ :Gadd45 $\beta$ /MKK7). However, the occurrence of such a complex, opens the possibility that, under regimens of protein up-regulation, larger aggregates can originate, and indeed, preliminary attempts to detect this complex by gel filtration analysis have so far invariably shown the presence of high molecular weight non-covalent complexes (L.T., unpublished observations).

Despite their small size, Gadd45 proteins appear now to have a modular structure. In fact, these and previous findings show that distinct

protein regions are involved in interactions with different partners. While the N- and C-termini are involved in self-association, it similarly appears that a central region, spanning residues A60-A114 and comprising the large acidic patches, is committed to kinase binding and regulation<sup>1; 10; 23</sup>, and to the interaction with Core histones (region 72-124)<sup>37</sup>. The same sub-domains, however, have concomitantly a role in the recognition of other partners such as PCNA<sup>6</sup>, which binds the terminal region 27-50 and 127-150 of Gadd45 $\alpha$ , and nucleophosmin<sup>28</sup>, which interacts with the region 61-100 thereby regulating nuclear entry<sup>28</sup>. Therefore, while dissociation of Gadd45 proteins would be required for interaction with PCNA, a key player of the DNA repair mechanism primarily regulated by Gadd45 proteins, it seems dispensable for binding to kinases, Core histones and nucleophosmin. Importantly, all these proteins have a prevailing localization within cell nuclei, where protein concentration can be considerably higher than in the cytosol and thus self-association needs to be a less disruptive event. Assuming that Gadd45 $\alpha$  and Gadd45 $\beta$  have distinct capacities for self-association, this difference would also reflect different properties that could be even more evident at higher protein concentrations. In this instance, the control of protein overexpression and/or the capacity of more efficient translocation to sub-cellular compartments could be a further critical point that contributes to the different biological properties of the two protein variants.

## EXPERIMENTAL PROCEDURES

### Materials

Enzymes, TPCK-treated trypsin and other chemicals for buffer preparation were purchased from Sigma-Aldrich as well as urea and guanidinium hydrochloride (GdnHCl). pGEX-6P-1 expression vector, PreScission protease, ÅKTA FPLC and columns for affinity, size exclusion and ion exchange chromatography were from GE Healthcare, Uppsala, Sweden. pETM expression vectors were from EMBL, Heidelberg. *Pfu* DNA polymerase was purchased from Stratagene. Restriction enzymes BamHI and XhoI and *T<sub>4</sub>* DNA Ligase were from New England Biolabs, Germany. Perfect Protein Markers were from Novagen, whilst SeeBlue Prestained markers were from Invitrogen. Vivaspin 5 KDa cut-off PES vertical membrane concentrators were from Sartorius group, Milan. Non Fat Dry Milk (NFDM) was from BioRad. Solvents for RP-HPLC analysis were all from Romil, Dublin, Ireland. DNA coding for human Gadd45 $\beta$  and human MKK7 were previously described<sup>1; 10</sup>. For peptide synthesis, protected N $^{\alpha}$ -Fmoc-amino acid derivatives and coupling reagents were purchased from Inbios (Pozzuoli, Italy), Sequencing-grade Trypsin, DIEA, Rink amide MBHA resin and other chemicals were from Sigma-Aldrich (Milano, Italy). Other reagents and chemicals suppliers are indicated in the Methods section.

Solid phase peptide syntheses were performed on a fully automated peptide synthesizer AAPTECH 348 Q Advanced Chemtech (Louisville, KY). Preparative RP-HPLC were carried out on a Shimadzu LC-8A, equipped with a SPD-M10 AV detector on a Phenomenex Luna-COMBI HTS C18 column (5 $\times$ 2.12 cm ID; 10  $\mu$ m). LC-MS analysis were carried out on an LCQ DECA XP Ion Trap mass spectrometer (ThermoElectron, Milan, Italy) equipped with an OPTON ESI source, operating at 4.2 kV needle voltage and 320  $^{\circ}$ C and with a complete Surveyor HPLC system, comprising an MS pump, an autosampler and a photo diode array (PDA). Narrow bore 50 $\times$ 2 mm C18 BioBasic LC-MS columns from ThermoElectron were used for these analysis. Other chemicals, instrumentations and columns are specified in the Methods section. All ELISA assays to screen the Gadd45 $\beta$  trypsin fractions were carried out using a complete system (Hamilton Robotics, Milano, Italy)

comprising a liquid handler, an automatic arm, a washer and an automated 96-well and 384-well reader.

### **Expression and purification of GADD45 $\beta$ in *E.coli***

Human Gadd45 $\beta$ , hereafter Gadd45 $\beta$ , was expressed both as pGEX6P-GADD45 $\beta$  as reported previously<sup>1</sup>, and with an N-terminal His<sub>6</sub> tag using the vector pET28aGADD45 $\beta$ <sup>10</sup>; in the latter case recombinant protein expression was optimized in BL21(DE3) bacterial strain induced in the presence of 0.1 mM isopropyl- $\beta$ -D-thiogalactopyranoside (IPTG) for 16h at 22°C. 200 mL pellet was re-suspended in 20 mL cold lysis buffer (25mM Tris, 500mM NaCl, 10mM Imidazole, 1mM DTT, Triton 0.05%, pH 7.5) supplemented with protease inhibitor mixture A (1 mM PMSF, 1.0  $\mu$ g/mL aprotinin, 1.0  $\mu$ g/mL leupeptin, 1.0  $\mu$ g/mL pepstatin, 1.0 mg/mL lysozyme) and incubated at room temperature for 30 min. Cells were disrupted by sonication on ice with 10 seconds on/off cycles for a total sonication time of 10 min on. After centrifugation at 15000 rpm for 30 min at 4°C, the supernatant was purified on a ÅKTA FPLC chromatography system using 1 mL HisTrap HP. The column was washed with lysis buffer without triton and bound protein was eluted using an imidazole gradient from 10 to 500 mM. Protein elution was monitored at 280 nm and the resulting fractions were analyzed by 15% SDS-PAGE electrophoresis. The eluted fractions were dialyzed against buffer A (50 mM Tris, 150 mM NaCl, 1mM DTT, 1mM EDTA, pH 7.0). MonoQ step, gel filtration, as well as LC-MS analysis were carried out as previously described<sup>1</sup>. Analysis of the protein by gel filtration was compared with a calibration obtained with marker proteins run on the column under the same conditions. Comparison of chromatograms in the presence and in absence of 1 mM DTT in the running buffer was carried out to show the presence of covalent oligomers. Gel filtration analyses were carried out on a Superdex 75 10/300 GL column.

### **Cloning, expression and purification of human MKK7 (1- 400), in *E. coli*.**

Human MKK7 (1-400), hereafter only MKK7, was expressed as a recombinant protein with an N-terminal GST-tag using the vector pGEx-6P1, allowing the expression of the protein as GST-fusion product containing a highly specific

cleavage site for PreScission Protease upstream of MKK7<sup>10</sup>. The MKK7 cDNA was amplified by PCR using pGEX-2T-MKK7/JNKK2 as template. Recombinant protein expression was optimized in the bacterial strain BL21(DE3)*TrxB*, induced in the presence of 0.1 mM IPTG for 16h at 22°C. 200 mL culture were resuspended into 20 mL of cold buffer A added of a protease inhibitor mixture A and incubated for 30 min at room temperature. Cells were disrupted by sonication on ice and the total lysate was then centrifugated at 15000 rpm for 30 min at 4°C. The resulting supernatant was loaded onto a 1 mL GSTrap FF column equilibrated with 50 mM Tris, pH 8.0, 500 mM NaCl and washed extensively until the absorbance at 280 nm reached the baseline. The protein was then eluted with 10 mM GSH dissolved in 50 mM Tris, pH 8.0. Purity was assessed by SDS-PAGE and LC-MS analysis. When required GST-MKK7 was on-column digested with PreScission protease using 160U/mL resin incubating at 4°C for 5 days; gel filtration analysis was carried out on digested MKK7 using a Superose 6 10/30 (GE Healthcare) previously calibrated with Ovalbumin, 44 kDa; BSA, 66 kDa; Transferrin, 81 kDa; Catalase, 206 kDa; Ferritin, 460 kDa, using as running buffer 50 mM Tris, 150 mM NaCl, 1mM DTT, 1mM EDTA, pH 7.0.

### **Trypsin digestion and peptide fractionation**

An aliquot of Gadd45 $\beta$  (1.0 mg; 0.052  $\mu$ mol) was dissolved in 2.0 mL of 50 mM Tris, 20 mM CaCl<sub>2</sub>, pH 8.0. TPCK-treated trypsin (Sigma) was added at a final 1:100 enzyme-substrate ratio and the reaction left to stand at 37°C under gentle agitation for 16 hours. A protein sample (0.5  $\mu$ g) was then analyzed by LC-MS/MS to assess protein digestion using a BioBasic 30x2 mm ID C18 column. The column was equilibrated at 200  $\mu$ L/min with 5% CH<sub>3</sub>CN, 0.05%TFA, then a gradient from 5% to 55% over 65 minutes was applied and monitored by both PDA and MS. The MS analysis was conducted by alternatively recording full mass spectra and data dependent mass analysis (DDA) to obtain sequence information from peptide fragmentation. The remaining protein sample was finally injected on a 250x4.6 mm ID C18 column equilibrated at 1.5 mL/min flow rate with 5% CH<sub>3</sub>CN, 0.1%TFA, applying a gradient of CH<sub>3</sub>CN, 0.1% TFA from 5% to 55% over 65 minutes to elute the peptides; 13 fractions of 5 minutes each were collected from time

zero to time 65 minutes, and were subsequently analyzed as reported before (4  $\mu$ L) by LC-MS/MS. Lyophilized fractions were stored at  $-80^{\circ}\text{C}$  until use.

### **Circular Dichroism (CD)**

CD spectra were recorded on a Jasco J-810 spectropolarimeter (JASCO Corp, Milan, Italy) equipped with a Peltier type temperature control system according to a procedure previously reported<sup>1</sup> and native Gadd45 $\beta$  was diluted in water to obtain a  $5.5 \times 10^{-5}$  M final concentration. A blank run was always carried out before every experiment and subtracted from the protein CD spectra. Chemically-induced denaturation was carried out on native Gadd45 $\beta$  performing  $1^{\circ}\text{C}$  increments every 2 min from  $20^{\circ}\text{C}$  to  $80^{\circ}\text{C}$ , monitoring CD signal at 222 nm. The temperature was then returned to  $20^{\circ}\text{C}$  to investigate an eventual refolding capacity of the thermally denatured protein. CD spectra were again collected after each 2 degrees. To investigate the effects of concentration on protein oligomerization, serially diluted solutions at concentrations ranging from  $5.5 \times 10^{-5}$  M to  $5.5 \times 10^{-6}$  M were analyzed using cuvettes with increasing path lengths in order to compensate the signal loss due to dilution. Chemical denaturation experiments were carried out evaluating the effect of urea and GdnHCl on Gadd45 $\beta$  denaturation as reported recently<sup>30</sup>. Briefly, pH controlled solutions with different concentrations of urea and GdnHCl, with constant protein concentration ( $5.5 \times 10^{-5}$  M), were prepared and incubated for 16 h at  $20^{\circ}\text{C}$ . Chemical-induced denaturation was monitored by recording the CD value at 222 nm for each sample. The reversibility of the denaturation was controlled after removal of denaturants from the unfolded protein sample by overnight dialysis. The capacity of the recovered protein to recognize MKK7 was also evaluated by direct ELISA binding. Corresponding blanks were always recorded and subtracted. CD spectra were registered at  $25^{\circ}\text{C}$ . CD analysis was also carried on the synthetic peptides used in the ELISA assays. Peptides concentrations were kept at  $1.0 \times 10^{-5}$  M and analyzed in a 0.1 cm-path length quartz cuvette. Spectra were acquired in a 10 mM phosphate buffer at pH 7.0 and also in the presence of increasing concentration of TFE, up to 20% v/v.

## Non-denaturing gels analysis

Laemmli discontinuing system without SDS was used for non-denaturing gel separations. Protein mobilities of proteins were determined on gels at 8, 10, 12 and 15% of bis-acrylamide, by loading 18 µg of protein from a 1.8 mg/mL solution (100 µM). Calibration markers were from Sigma-Aldrich and calibration curves were obtained as reported in reference<sup>38</sup> and in the Sigma protocol, technical bulletin No. MKR-137.

## Peptide synthesis and purification

Peptides corresponding to different regions of Gadd45β and MKK7 were designed on the basis of a predicted model<sup>38</sup>, and prepared by solid phase peptide synthesis as C-terminally amidated and N-terminally acetylated derivatives following standard Fmoc chemistry protocols. A Rink-amide MBHA resin (substitution 1.1 mmol/g) and aminoacid derivatives with standard protections were used in all syntheses. Cleavage from the solid support, performed by treatment with a trifluoroacetic acid (TFA)/triisopropylsilane (TIS)/water (90:5:5, v/v/v) mixture for 90 min at room temperature, afforded the crude peptides that were precipitated in cold ether, dissolved in a water/acetonitrile (1:1, v/v) mixture and lyophilized. Products were purified by RP-HPLC using a C18 Jupiter column (50x22 mm) applying a linear gradient of 0.1% TFA acetonitrile in 0.1% TFA water from 5% to 70% over 30 minutes. Peptide purity and integrity were confirmed by LC-MS mass measurements using a Surveyor LC system and coupled to an LCQ Deca XP mass spectrometer equipped with an OPTON ESI source. Characterizations were conducted under standard conditions of peptide analysis. Peptides were designed on the basis of the predicted Gadd45β secondary structure described in reference 1 and corresponded to extended Helix1, Helix 4, Helix 5 short, and Helix 5, respectively (hereafter eH1: A12-R35, sequence: AAQKMQTVTAAVEELLVAAQRQDR; eH4: R91-E104, sequence: RVSGMQRLAQLLGE; H5 short, S132-R146 sequence: SHGLVEVASYCEESR; eH5, A129-N148, sequence: AWKSHGLVEVASYCEESRGN. The peptide GPVWKMRFRKTGHVIAVKQMRRSGN, corresponding to fragment G132-

N156 of MKK7<sup>10</sup> and the fragment A60-D86 of Gadd45 $\beta$  (sequence: AIDEEEEEDIALQIHFTLIQSFCND), corresponding to the shortest region of Gadd45 $\beta$  still able to bind to and block MKK7<sup>1</sup> were also prepared and purified. The highly acidic peptide Gadd45 $\beta$  (A60-D86) was purified by RP-HPLC using a C18 Jupiter column (50x22 mm) applying a linear gradient of pure acetonitrile over 10 mM phosphate buffer pH 7.0, from 5% to 70% over 30 minutes.

### **Biotinylation of Gadd45 $\beta$**

Fractions of Gadd45 $\beta$  (1mg/ml) were biotinylated using an EZ Link NHS-LC-biotin (Pierce) according to manufacturer's instructions with slight modifications: 1 volume of NHS-LC-biotin 2 mg/mL was added to 20 volumes of protein and incubated 1 hour on ice; the reaction was then stopped by addition of 1 volume of 50 mM glycine. Biotinylated samples were dialyzed against buffer B (25 mM Tris, 150 mM NaCl 1 mM EDTA, 1 mM DTT, pH 7.5) to remove excess of glycine and free biotin and stored as working aliquots at -80°C. The incorporation of 1-2 biotin per molecule of protein was recorded by LC-MS analysis.

### **Gadd45 $\beta$ self-association and competition ELISA assays**

To monitor Gadd45 $\beta$  dimerization, an ELISA-like assay was carried out. For this purpose Gadd45 $\beta$  at concentration of 0.52  $\mu$ M in buffer B was dispensed into a 96 well microtiter plate. Some wells were filled with the buffer alone and were used as blanks. After 16 h incubation at 4°C the solutions were removed and the wells filled with 350  $\mu$ L of a 1% w/v solution of NFDM in 1x PBS (Phosphate-Buffered Saline) buffer. The plate was left to incubate for 1h at 37°C in the dark. After washing with buffer T-PBS (PBS with 0.004% added Tween), wells were filled with 100 $\mu$ L of biotinylated Gadd45 $\beta$  at concentrations ranging between 16  $\mu$ M and 2.1  $\mu$ M. Each data point was performed in triplicate. Following 1h incubation in the dark at 37°C the solutions were removed and the wells again washed with T-PBS. To each well 100  $\mu$ L of 1:1000 HRP-conjugated streptavidine (HRP-STRV) dissolved in buffer were added and the plate left to incubate for 1 h at 37°C in the dark. After removal of the enzyme solution and washing, 100  $\mu$ L of the chromogenic

substrate OPD (*o*-phenylenediamine) 0.4 mg/mL in 50 mM phosphate-citrate buffer, containing 0.4 mg/mL urea-hydrogen peroxide were added and the colour was allowed to develop in the dark for 5 minutes. The reaction was stopped by adding 50  $\mu$ L of 2.5 M H<sub>2</sub>SO<sub>4</sub>. The absorbance at 490 nm was read in all wells and the values were properly averaged subtracting the corresponding blank lines. For the competition experiments, 100  $\mu$ L aliquots of His<sub>6</sub>-Gadd45 $\beta$  at 0.52  $\mu$ M were coated on the wells of a microtiter plates and 0.26  $\mu$ M biotinylated His<sub>6</sub>-Gadd45 $\beta$  (1:0.5 mol/mol ratio) was used throughout (pre-saturation condition). 0.52  $\mu$ M peptides used as competitors were utilized at a 1:1 mol/mol ratio to coated unbiotinylated protein and pre-incubated with 0.26  $\mu$ M biotinylated Gadd45 $\beta$  for 30 minutes at 4°C prior to addition to each well. Peptides derived from the trypsin digestion were used at a nominal concentration of 0.52  $\mu$ M, calculated assuming a 100% trypsin cleavage and a 100% recovery from the HPLC fractionation. GST-MKK7, Gadd45 $\beta$  eHelices 1, 4, 5 and the synthetic peptides MKK7(G132-N156) and Gadd45 $\beta$ (A60-D86), were always used at 0.52  $\mu$ M. ELISA assays were carried out at least twice. Competition results are reported as (B/B<sub>0</sub>)X100, where B means the average OD from the triplicate data points for a given analyte and B<sub>0</sub> is the average OD determined without competitor.

### **Dose dependent competition assay**

Dose dependent competition assays were carried out to monitor the Gadd45 $\beta$  region of dimerization. For this purpose, 100  $\mu$ L of 0.26  $\mu$ M Gadd45 $\beta$  in buffer B was coated over night at 4°C on microtiter wells. After 1 hour blocking with NFDM and TPBS washing, increasing concentration of competitors (Gadd45 $\beta$  (A12-R35), Gadd45 $\beta$  (R91-E104), Gadd45 $\beta$  (A129-N148), MKK7(G132-N156) and the whole kinase protein GST-MKK7 ranging from 0 to 0.52  $\mu$ M were pre-incubated with 0.13  $\mu$ M biotinylated Gadd45 $\beta$  for 30 minutes prior to addition to each well. The subsequent steps of ELISA assays were carried out as previously described.

### **Gadd45 $\beta$ -MKK7 association**

Association between Gadd45 $\beta$  and MKK7 was investigated by ELISA assays by coating the GST-fused full length kinase for 16 h at 4°C, at a concentrations of 42 nM. After extensive washing with T-PBS buffer and NFDM blocking (1h, 37°C, 350  $\mu$ L), wells were incubated with different solutions of biotinylated Gadd45 $\beta$  at concentrations ranging from 8.4 nM to 168 nM. Bound protein was then detected as described previously.  $K_D$  values were estimated as the concentration of Gadd45 $\beta$  able to give half of the saturation signal. Binding competition assays were performed by coating GST-MKK7 at 42 nM as described, a concentration of biotinylated Gadd45 $\beta$  of 21 nM (pre-saturation conditions) and using the competitors (synthetic eH1, eH5, H5 short, eH4, Gadd45 $\beta$ (A60-D86), MKK7(G132-N156) and GST-MKK7) at a 2:1 competitor:soluble protein ratio (concentration of competitors 42 nM).

### **Modelling of Gadd45 $\beta$ homo-dimers**

The model building procedure for Gadd45 $\beta$  protein was described in details in a previous work <sup>1</sup>. To build Gadd45 $\beta$  homo-dimers, the first ten residues of the unstructured N-terminal region were removed. The resulting models obtained from manual docking were completed by addition of all hydrogen atoms and underwent energy minimisation with NAMD<sup>39</sup> package using Charmm22 force field<sup>40</sup>. Molecular dynamics simulations were run in solvent by confining the minimized complexes in rectangular TIP3P water boxes, with a minimal distance from the solute to the box wall of 1.2 nm. Counterions (Na<sup>+</sup>) were added to neutralize the system. Particle mesh Ewald method was applied to calculate long-range electrostatics interactions, setting to 14 Å the non-bonded cutoff. The solvated molecules were then energy minimized through 1000 steps with solute atoms restrained to their starting positions using a force constant of 1 kcal mol<sup>-1</sup>Å<sup>-1</sup> prior to molecular dynamics (MD) simulations. After this, the molecules were submitted to 50 ps restrained MD (1 kcal mol<sup>-1</sup>Å<sup>-1</sup>) at constant volume, gradually heating to 310 K, followed by 50 ps restrained MD (1 kcal mol<sup>-1</sup>Å<sup>-1</sup>) at constant pressure to adjust system density. Production runs were carried out for 200 ps using a timestep of 1 fs.

Snapshots from production run were saved every 1000 steps and analyzed with NAMD program. Model figures were made with MOLMOL program<sup>41</sup>.

Fraction	Gadd45 $\beta$ tryptic peptides	Relative distribution of fragments within fractions (%)	Relative composition of the fraction (%)	Predicted secondary structure*
6	G147-R160	98	100	Unstructured
7	L36-K45	98	50	Part of $\beta$ 1, part of $\alpha$ 2 Part of $\alpha$ 4; most of loop 2
	L98-R115	99	50	
8	S132-R146	87	85	$\alpha$ 5 $\beta$ 4
	D116-K131	99	15	
9	-13-15	100	75	Tag $\alpha$ 5
	S132-R146	5	25	
10	M16-R32	92	95	$\alpha$ 1
12	L46-R91	10	100	Part $\alpha$ 2, $\beta$ 2, loop1, $\alpha$ 3, part $\beta$ 3
13	L46-R91	87	100	Part $\alpha$ 2, $\beta$ 2, loop1, $\alpha$ 3, part $\beta$ 3

**Table I:** Tryptic Gadd45 $\beta$  peptidic fragments as identified by LC-MS/MS analysis. Fragments less than 5% were not considered. Relative distributions of fragments in column 3 were calculated by comparing area integration of extracted ion peaks from a given fragment taken from the different fractions. The relative composition within each fraction was derived by comparing area integrations of extracted ion peaks of all the fraction components. \*As reported in reference<sup>1</sup>.



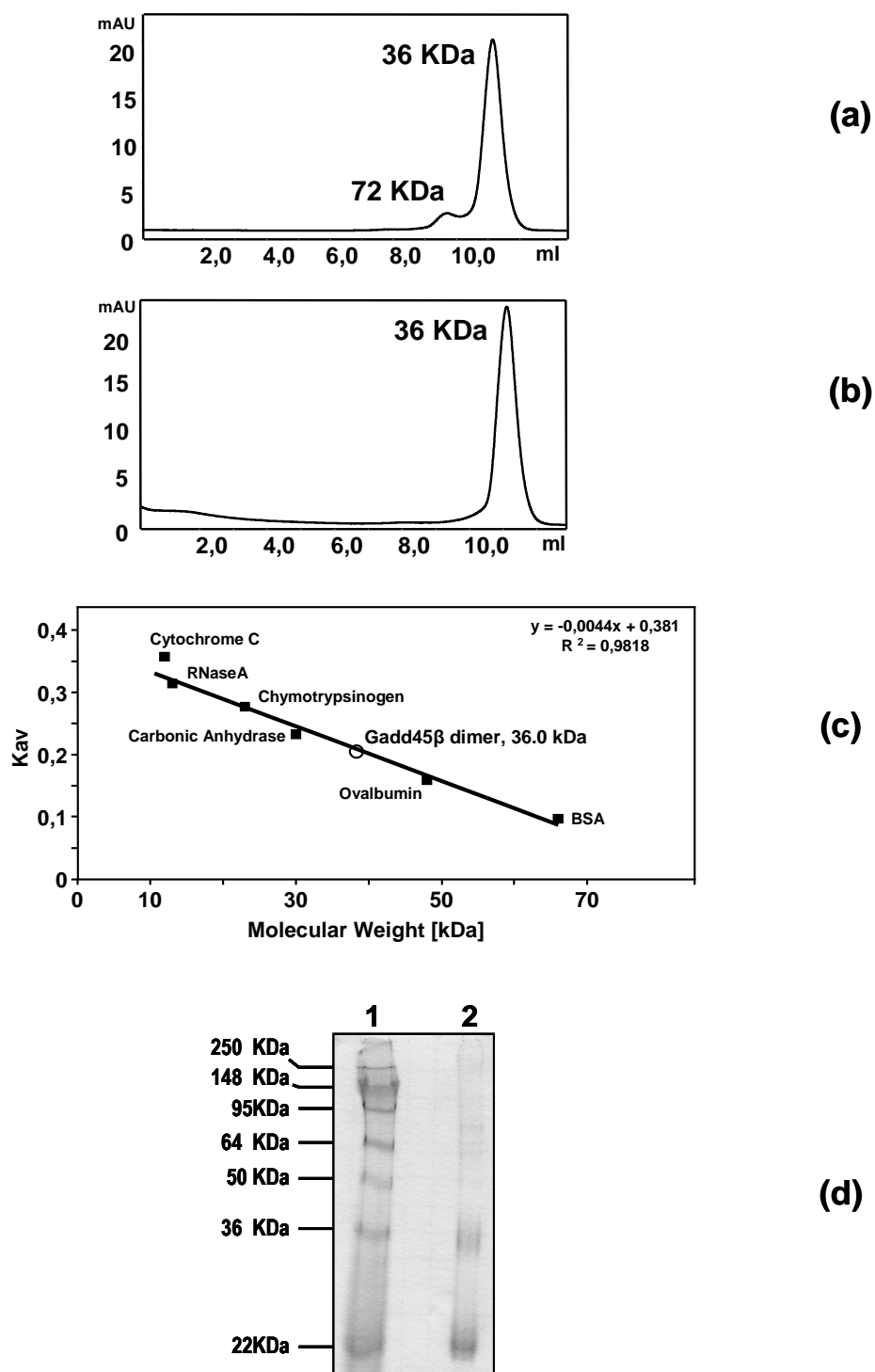
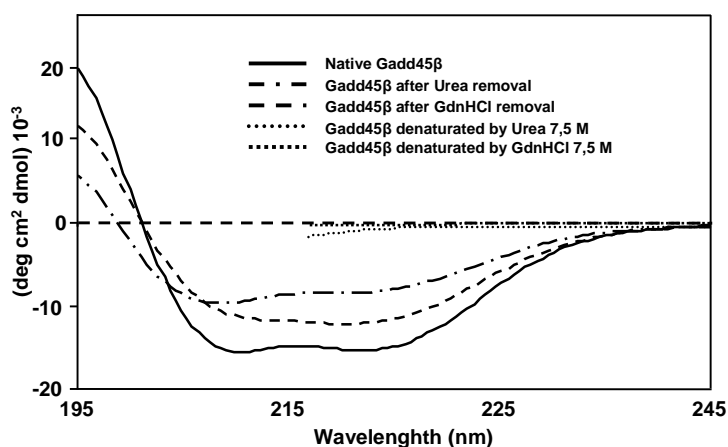
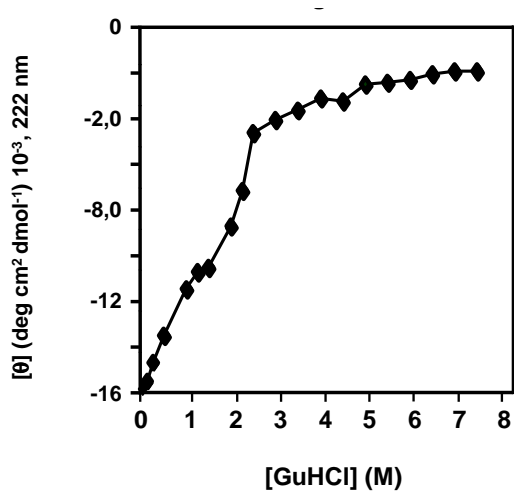


**Figure 2.** Characterization of the oligomeric state of Gadd45 $\beta$ . **a:** Gel filtration analysis on a Superdex 75 10/30 of the recombinant protein under non reducing conditions. Two peaks at elution volumes compatible with dimeric and tetrameric forms are detected. In **b**, the same analysis carried out after addition of 1 mM DTT in the running buffer. The peak at lower elution volumes disappears, suggesting that it is due to covalent disulfide bridges. In **c**, the calibration curve utilized to determine the relative MW is reported. Cytochrome C, 12.4 kDa; RNase A, 14.7 kDa; Chymotrypsinogen, 25.0 kDa; Carbonic anhydrase, 29.0 kDa; Ovalbumin, 44.0 kDa; BSA, 66.0 kDa. All determinations have been determined at least twice.

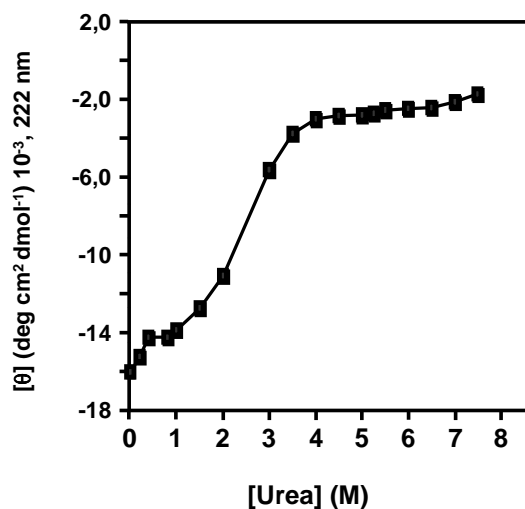
d: Non-denaturing polyacrylamide gel analysis of Gadd45 $\beta$  at a concentration of 1.8 mg/mL (100  $\mu$ M).



(a)



(b)



(c)

**Figure 3.** Circular dichroism characterization of the recombinant Gadd45 $\beta$ . **a.** CD spectra of the recombinant protein before and after denaturation with guanidinium and urea are reported. The protein appears to properly refold after the chemical treatment. Spectra at 7.5 M urea and guanidinium (dotted lines) are also reported. Curves of chemical denaturation are representative of at least two independent experiments. CD curves have been obtained by averaging at least three consecutive acquisitions. CD curves of denatured Gadd45B are missing below 215 nm since CD signals are suppressed by the high concentrations of urea and guanidinium. In **b** Chemical denaturation by GuHCl. The protein unfolds in a cooperative way at guanidinium concentrations higher than about 2.5 M (See also Figure 3a). In **c**, the chemical denaturation by urea is also reported. Also in this case the protein unfolds cooperatively. Complete denaturation occurs at concentrations higher than about 4.0 M.

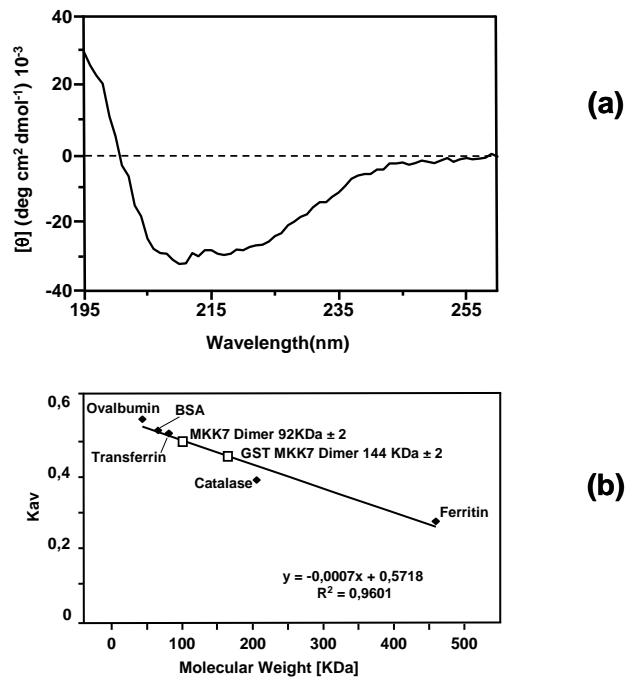


**Figure 4.** Recombinant human MKK7 is properly folded and appears to be dimeric. **a.** CD spectrum in the near UV of the protein showing that it adopts a prevalingly alpha helical conformation, as expected on the basis of the model proposed in reference 7. **b.** Calibration curve used to determine the apparent MW of the recombinant protein by gel filtration analysis. Ovalbumin, 44 kDa; BSA, 66 kDa; Transferrin, 81 kDa; Catalase, 206 kDa; Ferritin, 460 kDa. The protein appears to be dimeric as previously reported<sup>35, 36</sup>. Consistently, GST-MKK7, used in several experiments in this work, is also dimeric. All determinations were carried out under the same conditions and repeated at least twice.

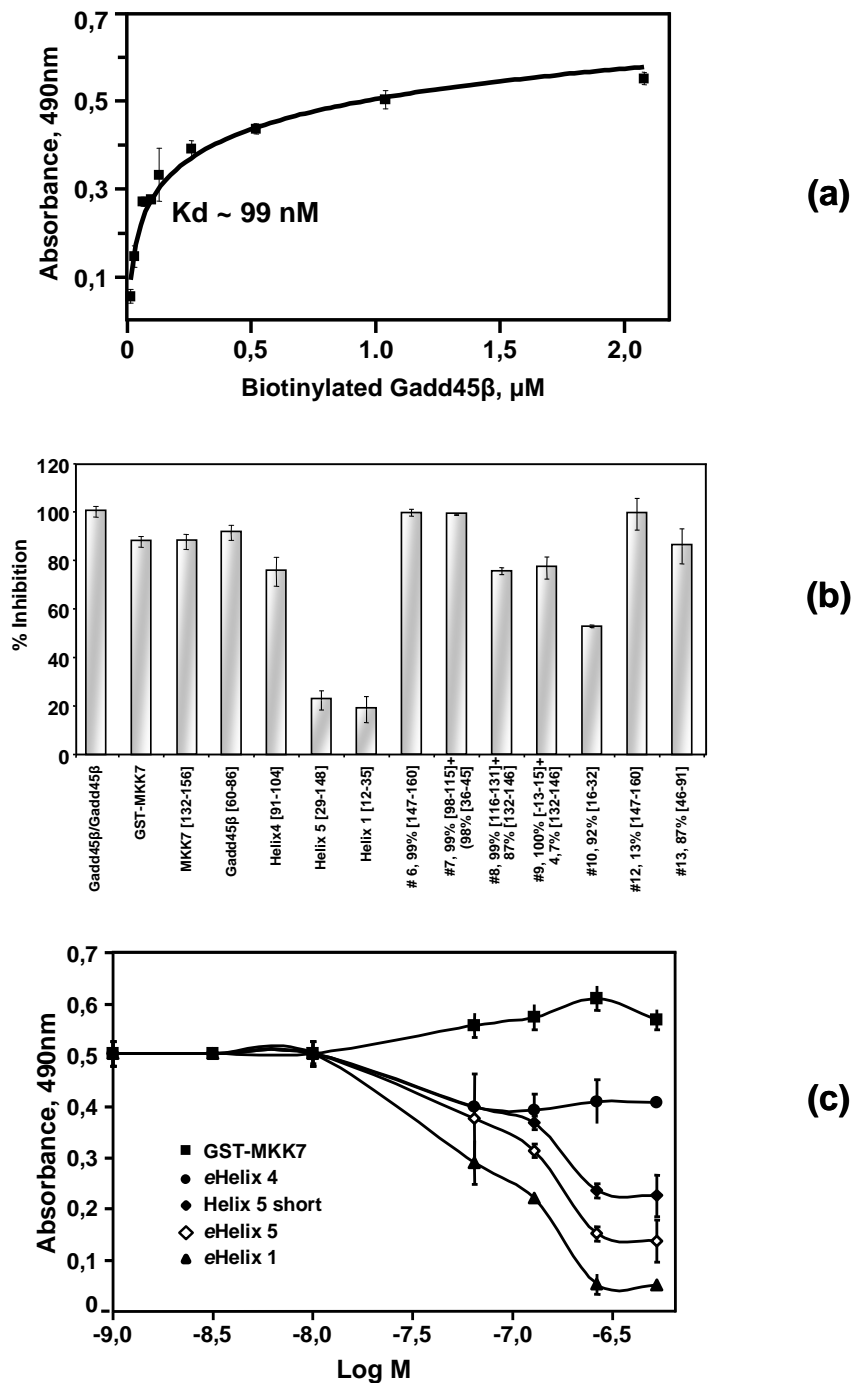


**Figure 5.** Gadd45 $\beta$  is able to self-associate, the interaction being disrupted by Gadd45 $\beta$  trypsin fragments. **a.** Dose-dependent binding of biotinylated Gadd45 $\beta$  to the plate-adsorbed protein: Gadd45 $\beta$  self associates with an estimated  $K_D$  of about 100 nM, assumed as the concentration of Gadd45 $\beta$  resulting in 50% maximum binding<sup>29</sup>. Notably, the signal reaches saturation at a 1:1 protein ratio, suggesting the formation of dimers only. **b:** Competition assay of the Gadd45 $\beta$  self-association by the trypsin-generated protein fragments and by synthetic peptides designed to reproduce helices as predicted in the protein model<sup>1</sup>. **c** Dose-dependent inhibition of Gadd45 $\beta$  self-association by GST-MKK7 full length, eHelix 4 (residues 91-104), eHelix 5 (residues 129-148), eHelix 1 (residues 12-35) and the Helix 5 short (residues 132-146). While the kinase and the eHelix 4 are not able to block the Gadd45 $\beta$  self-association, peptides corresponding to eHelix 1 and eHelix 5, potently reduce the association. The Helix 5 short, derived by trypsin cleavage, is less effective than the entire eHelix 5. Data are representative of at least 3 independent experiments.

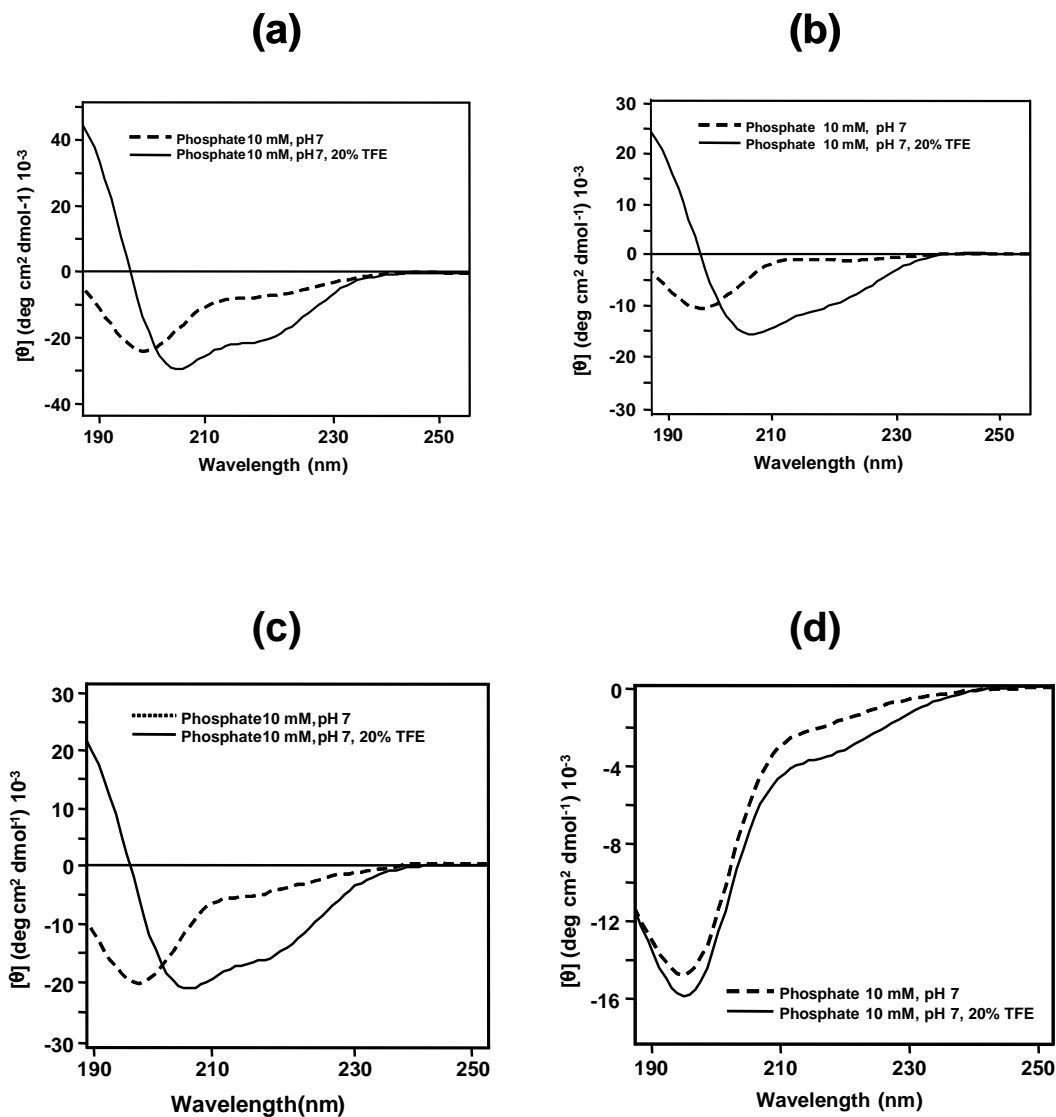


**Figure 6.** CD spectra of the synthetic peptides in neutral buffers and in the presence of 20% TFE. **a-d:** CD spectra of the synthetic eHelix 1 (**a**), eHelix 4 (**b**), eHelix 5 (**c**) and Helix 5 short (**d**) in phosphate buffer and in the presence of 20% TFE. As shown, the complete predicted helices have a good propensity to adopt an  $\alpha$ -helical conformation, whereas the short Helix 5 persists in a random conformation even after addition of the structuring agent. This different property is likely contributing to the reduced peptide capacity to block the MKK7-Gadd45 $\beta$  interaction. CD curves have been obtained by averaging at least three consecutive acquisitions.

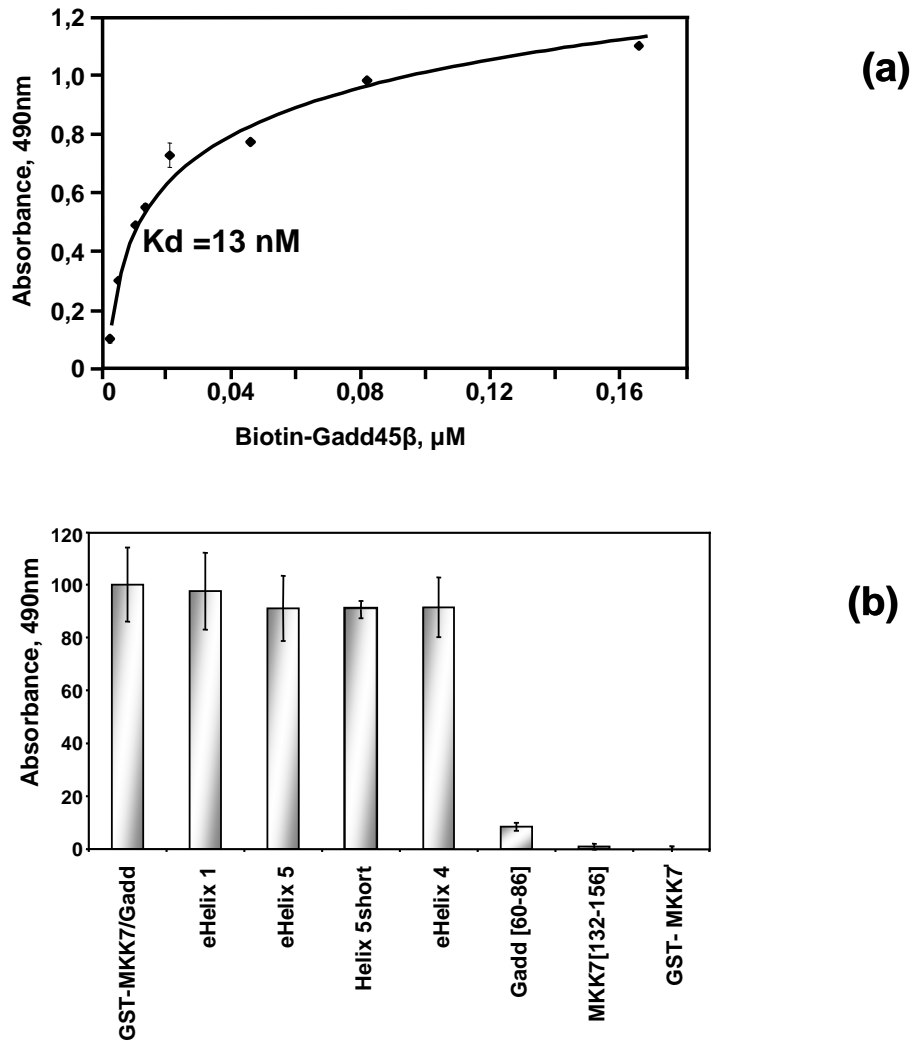


**Figure 7.** Gadd45 $\beta$  and MKK7 strongly interact and their association is not influenced by Helix 1 or Helix 5. **a:** binding curve of the association between GST-MKK7 and Gadd45 $\beta$ . The estimated  $K_D$  is 13 nM. **b:** binding competition of the MKK7- Gadd45 $\beta$  association by Gadd45 $\beta$  and MKK peptides. eHelix 1, eHelix 5, Helix 5 short and eHelix 4 cannot disrupt the binding, whereas Gadd45 $\beta$  [A60-D86] and MKK7 [G132-N156], corresponding to the interface between the two proteins, completely abolish the interaction. Also the GST-fused full length kinase abolishes the interaction as expected. Data are representative of at least 3 independent experiments.

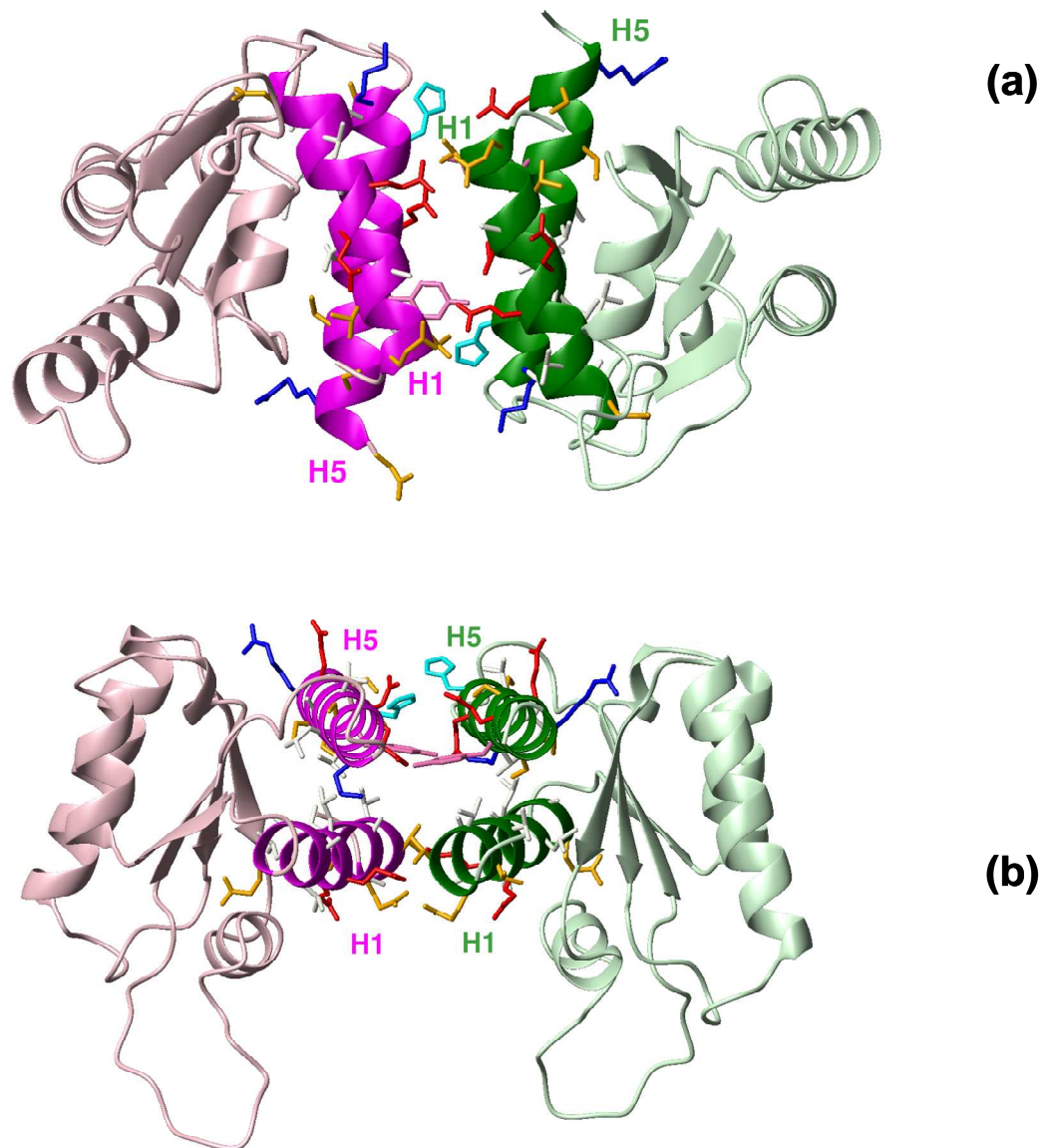


**Figure 8.** Two orthogonal views of Gadd45 $\beta$  homo-dimer three-dimensional model in ribbon representation, rotated around the horizontal axis of the figure(a, b). One monomer is colored in pink, the other in pale green. Helices H1 and H5 of each monomer are colored in magenta and dark green, respectively. Residues lying on these helices are shown in stick representation and colored according to the following scheme: hydrophobic residues in white, acidic residues in red, basic residues in blue, histidine in cyan and tyrosine in magenta.

**Acknowledgements**

This work was supported by funds from the FIRB project number RBNE03PX83\_005 to M.R. and from the Centro Regionale di Competenza in Diagnostica e Farmaceutica Molecolare (CRdC-DFM). The support of the National Research Council is also gratefully acknowledged.

## References

1. Papa, S., Monti, S. M., Vitale, R. M., Bubici, C., Jayawardena, S., Alvarez, K., De Smaele, E., Dathan, N., Pedone, C., Ruvo, M. & Franzoso, G. (2007). Insights into the structural basis of the GADD45beta -mediated inactivation of the JNK kinase, MKK7/JNKK2. *J Biol Chem* 282, 19029-19041.
2. Abdollahi, A., Lord, K. A., Hoffmann-Liebermann, B. & Liebermann, D. A. (1991). *Oncogene* 6, 165-167.
3. Amanullah, A., Azam, N., Balliet, A., Hollander, C., Hoffman, B., Fornace, A. & Liebermann, D. (2003). Cell signalling: cell survival and a Gadd45-factor deficiency. *Nature* 424, 741.
4. Gupta, M., Gupta, S. K., Hoffman, B. & Liebermann, D. A. (2006). Gadd45a and Gadd45b protect hematopoietic cells from UV-induced apoptosis via distinct signaling pathways, including p38 activation and JNK inhibition. *J Biol Chem* 281, 17552-8.
5. Takekawa, M. & Saito, H. (1998). A family of stress-inducible GADD45-like proteins mediate activation of the stress-responsive MTK1/MEKK4 MAPKKK. *Cell* 95, 521-30.
6. Vairapandi, M., Azam, N., Balliet, A. G., Hoffman, B. & Liebermann, D. A. (2000). Characterization of MyD118, Gadd45, and proliferating cell nuclear antigen (PCNA) interacting domains. PCNA impedes MyD118 AND Gadd45-mediated negative growth control. *J Biol Chem* 275, 16810-9.
7. Smith, M. L., Chen, I. T., Zhan, Q., Bae, I., Chen, C. Y., Gilmer, T. M., Kastan, M. B., O'Connor, P. M. & Fornace, A. J., Jr. (1994). *Science* 266, 1376-1380.
8. Wang, X. W., Zhan, Q., Coursen, J. D., Khan, M. A., Kontny, H. U., Yu, L., Hollander, M. C., O'Connor, P. M., Fornace, A. J., Jr. & Harris, C. C. (1999). GADD45 induction of a G2/M cell cycle checkpoint. *Proc Natl Acad Sci U S A* 96, 3706-11.
9. Zazzeroni, F., Papa, S., Algeciras-Schimnich, A., Alvarez, K., Melis, T., Bubici, C., Majewski, N., Hay, N., De Smaele, E., Peter, M. E. & Franzoso, G. (2003). Gadd45 beta mediates the protective effects of CD40 costimulation against Fas-induced apoptosis. *Blood* 102, 3270-9.
10. Papa, S., Zazzeroni, F., Bubici, C., Jayawardena, S., Alvarez, K., Matsuda, S., Nguyen, D. U., Pham, C. G., Nelsbach, A. H., Melis, T., De Smaele, E., Tang, W. J., D'Adamio, L. & Franzoso, G. (2004). Gadd45 beta mediates the NF-kappa B suppression of JNK signalling by targeting MKK7/JNKK2. *Nat Cell Biol* 6, 146-53.
11. De Smaele, E., Zazzeroni, F., Papa, S., Nguyen, D. U., Jin, R., Jones, J., Cong, R. & Franzoso, G. (2001). Induction of gadd45beta by NF-kappaB downregulates pro-apoptotic JNK signalling. *Nature* 414, 308-13.
12. Yang, Q., Manicone, A., Coursen, J. D., Linke, S. P., Nagashima, M., Forgues, M. & Wang, X. W. (2000). Identification of a functional domain in a GADD45-mediated G2/M checkpoint. *J Biol Chem* 275, 36892-8.

13. Yang, J., Zhu, H., Murphy, T. L., Ouyang, W. & Murphy, K. M. (2001). IL-18-stimulated GADD45 beta required in cytokine-induced, but not TCR-induced, IFN-gamma production. *Nat Immunol* 2, 157-64.
14. Ijiri, K., Zerbini, L. F., Peng, H., Correa, R. G., Lu, B., Walsh, N., Zhao, Y., Taniguchi, N., Huang, X. L., Otu, H., Wang, H., Wang, J. F., Komiya, S., Ducey, P., Rahman, M. U., Flavell, R. A., Gravallesse, E. M., Oettgen, P., Libermann, T. A. & Goldring, M. B. (2005). A novel role for GADD45beta as a mediator of MMP-13 gene expression during chondrocyte terminal differentiation. *J Biol Chem* 280, 38544-55.
15. Smith, G. B. & Mocarski, E. S. (2005). Contribution of GADD45 family members to cell death suppression by cellular Bcl-xL and cytomegalovirus vMIA. *J Virol* 79, 14923-32.
16. Fan, W., Richter, G., Cereseto, A., Beadling, C. & Smith, K. A. (1999). Cytokine response gene 6 induces p21 and regulates both cell growth and arrest. *Oncogene* 18, 6573-82.
17. Engelmann, A., Speidel, D., Bornkamm, G. W., Deppert, W. & Stocking, C. (2007). Gadd45beta is a pro-survival factor associated with stress-resistant tumors. *Oncogene*.
18. Papa, S., Zazzeroni, F., Pham, C. G., Bubici, C. & Franzoso, G. (2004). Linking JNK signaling to NF-kappaB: a key to survival. *J Cell Sci* 117, 5197-208.
19. Gupta, S. K., Gupta, M., Hoffman, B. & Liebermann, D. A. (2006). Hematopoietic cells from gadd45a-deficient and gadd45b-deficient mice exhibit impaired stress responses to acute stimulation with cytokines, myeloablation and inflammation. *Oncogene* 25, 5537-46.
20. Hall, P. A., Kearsley, J. M., Coates, P. J., Norman, D. G., Warbrick, E. & Cox, L. S. (1995). Characterisation of the interaction between PCNA and Gadd45. *Oncogene* 10, 2427-33.
21. Smith, M. L., Chen, I. T., Zhan, Q., Bae, I., Chen, C. Y., Gilmer, T. M., Kastan, M. B., O'Connor, P. M. & Fornace, A. J., Jr. (1994). Interaction of the p53-regulated protein Gadd45 with proliferating cell nuclear antigen. *Science* 266, 1376-80.
22. Azam, N., Vairapandi, M., Zhang, W., Hoffman, B. & Liebermann, D. A. (2001). Interaction of CR6 (GADD45gamma) with proliferating cell nuclear antigen impedes negative growth control. *J Biol Chem* 276, 2766-74.
23. Jin, S., Antinore, M. J., Lung, F. D., Dong, X., Zhao, H., Fan, F., Colchagie, A. B., Blanck, P., Roller, P. P., Fornace, A. J., Jr. & Zhan, Q. (2000). The GADD45 inhibition of Cdc2 kinase correlates with GADD45-mediated growth suppression. *J Biol Chem* 275, 16602-8.
24. Vairapandi, M., Balliet, A. G., Fornace, A. J., Jr., Hoffman, B. & Liebermann, D. A. (1996). The differentiation primary response gene MyD118, related to GADD45, encodes for a nuclear protein which interacts with PCNA and p21WAF1/CIP1. *Oncogene* 12, 2579-94.
25. Vairapandi, M., Balliet, A. G., Hoffman, B. & Liebermann, D. A. (2002). GADD45b and GADD45g are cdc2/cyclinB1 kinase inhibitors with a role in S and G2/M cell cycle checkpoints induced by genotoxic stress. *J Cell Physiol* 192, 327-38.
26. Chi, H., Lu, B., Takekawa, M., Davis, R. J. & Flavell, R. A. (2004). GADD45beta/GADD45gamma and MEKK4 comprise a genetic

- pathway mediating STAT4-independent IFN $\gamma$  production in T cells. *Embo J* 23, 1576-86.
27. Chung, H. K., Yi, Y. W., Jung, N. C., Kim, D., Suh, J. M., Kim, H., Park, K. C., Song, J. H., Kim, D. W., Hwang, E. S., Yoon, S. H., Bae, Y. S., Kim, J. M., Bae, I. & Shong, M. (2003). CR6-interacting factor 1 interacts with Gadd45 family proteins and modulates the cell cycle. *J Biol Chem* 278, 28079-88.
  28. Gao, H., Jin, S., Song, Y., Fu, M., Wang, M., Liu, Z., Wu, M. & Zhan, Q. (2005). B23 regulates GADD45a nuclear translocation and contributes to GADD45a-induced cell cycle G2-M arrest. *J Biol Chem* 280, 10988-96.
  29. Kovalsky, O., Lung, F. D., Roller, P. P. & Fornace, A. J., Jr. (2001). Oligomerization of human Gadd45a protein. *J Biol Chem* 276, 39330-9.
  30. Granata, V., Graziano, G., Ruggiero, A., Raimo, G., Masullo, M., Arcari, P., Vitagliano, L. & Zagari, A. (2006). Chemical denaturation of the elongation factor 1 $\alpha$  isolated from the hyperthermophilic archaeon *Sulfolobus solfataricus*. *Biochemistry* 45, 719-26.
  31. Wang, W. (1999). Instability, stabilization, and formulation of liquid protein pharmaceuticals. *Int J Pharm* 185, 129-88.
  32. Chung, S. H., Weiss, R. S., Frese, K. K., Prasad, B. V. & Javier, R. T. (2007). Functionally distinct monomers and trimers produced by a viral oncoprotein. *Oncogene*.
  33. D'Ambrosio, C., Talamo, F., Vitale, R. M., Amodeo, P., Tell, G., Ferrara, L. & Scaloni, A. (2003). Probing the dimeric structure of porcine aminoacylase 1 by mass spectrometric and modeling procedures. *Biochemistry* 42, 4430-43.
  34. Nakajima, A., Komazawa-Sakon, S., Takekawa, M., Sasazuki, T., Yeh, W. C., Yagita, H., Okumura, K. & Nakano, H. (2006). An antiapoptotic protein, c-FLIPL, directly binds to MKK7 and inhibits the JNK pathway. *Embo J* 25, 5549-59.
  35. Cobb, M. H. & Goldsmith, E. J. (2000). Dimerization in MAP-kinase signaling. *Trends Biochem Sci* 25, 7-9.
  36. Pelech, S. (2006). Dimerization in protein kinase signaling. *J Biol* 5, 12.
  37. Carrier, F., Georgel, P. T., Pourquier, P., Blake, M., Kontny, H. U., Antinore, M. J., Gariboldi, M., Myers, T. G., Weinstein, J. N., Pommier, Y. & Fornace, A. J., Jr. (1999). Gadd45, a p53-responsive stress protein, modifies DNA accessibility on damaged chromatin. *Mol Cell Biol* 19, 1673-85.
  38. Gallagher, S. (1999). *Current protocols in Molecular Biology* 2, 10.2.B.1-10.2.B.10.
  39. Phillips, J. C., Braun, R., Wang, W., Gumbart, J., Tajkhorshid, E., Villa, E., Chipot, C., Skeel, R. D., Kale, L. & Schulten, K. (2005). Scalable molecular dynamics with NAMD. *J. Comput. Chem.* 26, 1781-1802.
  40. MacKerell, A. D., Bashford, D., Bellott, M., Dunbrack, R. L., Evanseck, J. D., Field, M. J., Fischer, S., Gao, J., Guo, H., Ha, S., Joseph-McCarthy, D., Kuchnir, L., Kuczera, K., Lau, F. T. K., Mattos, C., Michnick, S., Ngo, T., Nguyen, D. T., Prodhom, B., Reiher, W. E., Roux, B., Schlenkrich, M., Smith, J. C., Stote, R., Straub, J., Watanabe, M., Wiorkiewicz-Kuczera, J., Yin, D. & Karplus, M. (1998).

All-Atom Empirical Potential for Molecular Modeling and Dynamics  
Studies of Proteins. *J. Phys. Chem.* 102, 3586-3616.

41. Koradi, R., Billeter, M. & Wuthrich, K. (1996). MOLMOL: a program for display and analysis of macromolecular structures. *J. Mol. Graphics.* 14, 51-55.